

UNCLASSIFIED

AD NUMBER	
AD394115	
CLASSIFICATION CHANGES	
TO:	unclassified
FROM:	confidential
LIMITATION CHANGES	
TO:	Approved for public release, distribution unlimited
FROM:	Distribution authorized to U.S. Gov't. agencies and their contractors; Administrative/Operational Use; AUG 1968. Other requests shall be referred to Air Force Rocket Propulsion Lab., Edwards AFB, CA.
AUTHORITY	
31 Aug 1980, DoDD 5200.10; AFRPL ltr, 5 Feb 1986	

THIS PAGE IS UNCLASSIFIED

SECURITY

MARKING

The classified or limited status of this report applies to each page, unless otherwise marked.

Separate page printouts MUST be marked accordingly.

THIS DOCUMENT CONTAINS INFORMATION AFFECTING THE NATIONAL DEFENSE OF THE UNITED STATES WITHIN THE MEANING OF THE ESPIONAGE LAWS, TITLE 18, U.S.C., SECTIONS 793 AND 794. THE TRANSMISSION OR THE REVELATION OF ITS CONTENTS IN ANY MANNER TO AN UNAUTHORIZED PERSON IS PROHIBITED BY LAW.

NOTICE: When government or other drawings, specifications or other data are used for any purpose other than in connection with a definitely related government procurement operation, the U. S. Government thereby incurs no responsibility, nor any obligation whatsoever; and the fact that the Government may have formulated, furnished, or in any way supplied the said drawings, specifications, or other data is not to be regarded by implication or otherwise as in any manner licensing the holder or any other person or corporation, or conveying any rights or permission to manufacture, use or sell any patented invention that may in any way be related thereto.

CONFIDENTIAL

(Title-Unclassified)

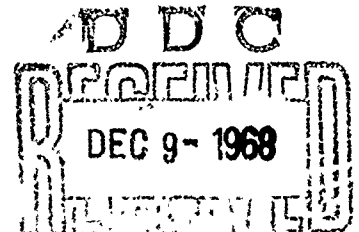
DEMONSTRATION OF BIPROPELLANT GAS GENERATOR TECHNOLOGY FOR AIR AUGMENTATION APPLICATIONS

FINAL REPORT

AUGUST 1968

D. G. PHILLIPS

W. F. HASSEL



AD 394115

THE MARQUARDT CORPORATION

GROUP 4

DOWNGRADED AT 3 YEAR INTERVALS:

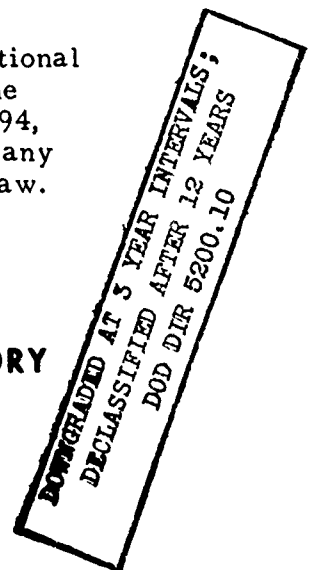
DECLASSIFIED AFTER 12 YEARS

In addition to security requirements which must be met, this document is subject to special export controls and each transmittal to foreign governments or foreign nationals may be made only with prior approval of the AFRPL (RPPR-STINFO) Edwards, Calif. 93523.

This document contains information affecting the national defense of the United States within the meaning of the Espionage Laws. Title 18 U.S.C. Sections 793 & 794, its transmission or the revelation of its contents in any manner to an unauthorized person is prohibited by law.

DEPARTMENT OF THE AIR FORCE
AIR FORCE ROCKET PROPULSION LABORATORY
AIR FORCE SYSTEMS COMMAND
EDWARDS, CALIFORNIA

CONFIDENTIAL



"When U.S. Government drawings, specifications, or other data are used for any purpose other than a definitely related Government procurement operation, the Government thereby incurs no responsibility nor any obligation whatsoever, and the fact that the Government may have formulated, furnished, or in any way supplied the said drawings, specifications, or other data, is not to be regarded by implication or otherwise, or in any manner licensing the holder or any other person or corporation, or conveying any rights or permission to manufacture, use, or sell any patented invention that may in any way be related thereto."



CORPORATION 16555 SATICOY STREET • VAN NUYS, CALIFORNIA 91409 • TELEPHONE 213-781-2121 • DTWX-910-495 1710 • CABLE MARQCOR

CONFIDENTIAL

Ref: 5428/155-22/16829
27 November 1968

Department of the Air Force
Air Force Rocket Propulsion Laboratory
Edwards Air Force Base, California 93523

Attention: FTMKR-3 (Mrs. Bernice V. Wilson/277-2625)

Subject: Final Report - Demonstration of Bipropellant Gas Generator
Technology for Air Augmentation Applications, Transmittal
of.

Enclosure: (1) Final Report AFRPL-TR-68-161, "Demonstration of
Bipropellant Gas Generator Technology for Air
Augmentation Applications". CONFIDENTIAL (Title -
Unclassified)


References: (A) Contract F04611-67-c-0110
(B) Ltr from Mary M. Racovich (undated) to The Marquardt
Corporation regarding final report review.
(C) Ltr from Mary M. Racovich dtd 24 October 1968
approving revised draft of final report.

1. (U) This final report is submitted in compliance with the
requirements of BOO4 of Reference A and Amendment P003. The report
contains the revisions and corrections called out in References B and
C.

2. (U) This report will be distributed in accordance with the
distribution list supplied in Reference B.

Very truly yours,

THE MARQUARDT CORPORATION


Howard R. Wedell
Contract Administrator

HRW:DGP:ls

Ltr only - AFFTC/FTMKR-3
DCASD/VN; DCRL/DVCD

This document contains information affecting the national
defense of the United States, within the meaning of the
Espionage Laws, Title 18, U. S. C., Sections 793 and 794,
the transmission or revelation of which in any manner to
an unauthorized person is prohibited by law. An Equal Opportunity Employer

CONFIDENTIAL

THIS LETTER MAY BE UNCLASSIFIED
IF ENCLOSURE () IS DETACHED.

CONFIDENTIAL

FOREWORD

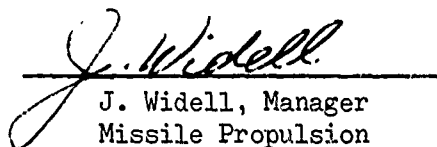
(This Foreword is Unclassified)

This final report was prepared in accordance with the requirements of Contract FO4611-67-C-0110.

Project Number:	5730
Contractor:	The Marquardt Corporation 16555 Saticoy Street Van Nuys, California 91409
Air Force Project Engineer AFRPL	1st/Lt. W. E. Spangler - RPRRT

The effort documented by this report covers the time period from 15 June 1967 to 1 July 1968. The Marquardt Corporation number for this report is Report 25,265.

APPROVED:


J. Widell, Manager
Missile Propulsion

Appendix B of this report contains classified information extracted from The Marquardt Corporation Report No. 25,256 dated April 26, 1968, Confidential, Group 4 downgrading.

This technical report has been reviewed and is approved.

1st/Lt. W. E. Spangler - RPRRT

CONFIDENTIAL

AFRPL-TR-68-161

DEMONSTRATION OF
BIPROPELLANT GAS GENERATOR
TECHNOLOGY FOR
AIR AUGMENTATION APPLICATIONS
(Title - Unclassified)

D. G. Phillips

W. F. Hassel

The information contained in this document will not be disclosed to foreign nationals or their representatives.

SPECIAL HANDLING REQUIRED
NOT RELEASABLE TO FOREIGN NATIONALS

In addition to security requirements which must be met, this document is subject to special export controls and each transmittal to foreign governments or foreign nationals may be made only with prior approval of the AFRPL (RPPR-STINFO) Edwards, California 93523

GROUP - 4
DOWNGRADED AT 3 YEAR INTERVALS
DECLASSIFIED AFTER 12 YEARS

This document contains information affecting the national defense of the United States, within the meaning of the Espionage Laws, Title 18, U. S. C., Sections 793 and 794, the transmission or revelation of which in any manner to an unauthorized person is prohibited by law.

-i-

CONFIDENTIAL

(This page is Unclassified)

DOWNGRADED AT 3 YEAR INTERVALS;
DECLASSIFIED AFTER 12 YEARS
DOD DIR 8900.10

UNCLASSIFIED

CONFIDENTIAL

UNCLASSIFIED ABSTRACT

(U) During the period from 15 June 1967 to 1 July 1968, The Marquardt Corporation conducted an experimental program to demonstrate the feasibility of a bipropellant gas generator for air augmentation applications. Efforts concerned both development of the gas generator and its evaluation during air augmentation tests. The propellants used were MARNAF 731, a boron slurry manufactured by The Marquardt Corporation, and chlorine trifluoride. Testing with bromine pentafluoride also was conducted. The final gas generator design permitted operation over the desired O/F range, demonstrated throttling capability, and permitted the attainment of high afterburner combustion efficiencies with small scale hardware. This report describes the development of a gas generator, presents an evaluation of a number of variables affecting secondary combustor performance and presents results that demonstrate that the bipropellant gas generator concept, when using MARNAF 731 and CTF (or BFF) is a very promising system for future ducted rocket applications.

CONFIDENTIAL

UNCLASSIFIED

UNCLASSIFIED

TABLE OF CONTENTS

<u>Section</u>	<u>Page</u>
I. SUMMARY	1
II. INTRODUCTION	3
III. PROGRAM OBJECTIVES	5
IV. GAS GENERATOR DEVELOPMENT	7
A. Requirements	7
B. Theoretical Studies	11
C. Test Hardware	13
1. Test Facility	13
2. Gas Generator Hardware	14
a. Turbulator	14
b. Spiral Swirl	17
c. Modified Turbulator	23
d. Dual Chamber Impinging Jet	26
e. Single Chamber Impinging Jet	28
f. Axial Injection	28
3. Exhaust Sampling	32
a. Sampling Procedure	32
b. Particle Sampling	35
c. Gas Sampling	38
d. Mass Distribution	38
e. Temperature Measurement	38
4. Instrumentation and Control	41
D. Test Demonstration	43
1. Run Summary	44
a. Runs 1 and 2	44
b. Runs 3 and 4	47
c. Runs 5 through 9	48
d. Runs 10 through 18	50
e. Runs 19 and 20	53
2. Exhaust Sampling	54
a. Analyses of Solid Samples	55
b. Analyses, Engine Deposits, Run 3 (O/F = 0.1 and Run 4 O/F = 0.5)	61
c. Gas Sample Analyses (Runs 3 and 4)	64
E. Discussion of Gas Generator Results	68

UNCLASSIFIED

TABLE OF CONTENTS (Continued)

<u>Section</u>		<u>Page</u>
V.	AIR AUGMENTED COMBUSTION DEMONSTRATION	73
	A. General Requirements	73
	B. Test Hardware	73
	1. Gas Generator	73
	2. Secondary Combustor	74
	3. Instrumentation and Control	77
	C. Experimental Testing	84
	D. Discussion of Results	88
	1. Ignition and Combustion Performance	88
	2. Hardware Durability	102
VI.	CONCLUSIONS	109
	A. Gas Generator	109
	B. Air Augmentation	110
VII.	RECOMMENDATIONS	113
VIII.	REFERENCES	115
	APPENDIX A - Data Reduction Technique	117
	B - Descriptions and Properties of MARNAF 731	125

UNCLASSIFIED

LIST OF ILLUSTRATIONS

<u>Figure</u>		<u>Page</u>
1	Heating Value of Propellant	8
2	Effect of Oxidizer/Fuel Ratio Upon Equilibrium Gas Temperature in Gas Generator	9
3	Test Summary - Phase 1	15
4	Single Point Injection Turbulator Engine	16
5	Turbulator Gas Generator Schematic, Configuration A	18
6	Turbulator Gas Generator Schematic, Configuration B	19
7	Injector Pattern Layout Schematic	20
8	Turbulator Gas Generator	21
9	Spiral Swirl Gas Generator	22
10	Spiral Swirl Gas Generator, Disassembled View	24
11	Chamber of Modified Turbulator Gas Generator	25
12	Design of Dual Chamber Gas Generator	27
13	Design of Single Chamber Gas Generator	29
14	External View of Single or Dual Chamber Gas Generator	30
15	Gas Generator Configuration with Axial Injection	31
16	Exhaust Sampling Setup in Cell M1-A	33
17	Gas Generator With Sampling Probes Installed in Cell M1-A	34
18	Particle Sampler	36
19	Particle Sampling Probe Tip Configuration	37
20	Gas Sampling Probe	39
21	Solids Mass Distribution Sampling Probe	40
22	Bipropellant Gas Generator, Plumbing and Instrumentation Schematic	42
23	Location of Deposits in Gas Generator Chambers	49
24	MARNAF 731 Fuels	57
25	Particle Sampler - Impingement Collector Sample	59
26	X-Ray Diffraction Pattern	62
27	Variation of Gas Generator Chamber Pressure Parameter	69
28	Gas Generator Flow Rate as Function of Chamber Pressure	71

UNCLASSIFIED

LIST OF ILLUSTRATIONS (Continued)

<u>Figure</u>		<u>Page</u>
29	Temperature of Gas Generator Exhaust Products	72
30	Axial Injection Gas Generator	75
31	Gas Generator and Combustor Design	76
32	Air Augmentation Configurations	78
33	Plumbing and Instrumentation Schematic, Air Augmentation Phase	79
34	Air Augmented Rocket Test Configuration	80
35	System Design for Direct-Connect Air Augmentation Tests	82
36	Air Augmentation Hardware Installed	83
37	Test Summary, Phase II	85
38	Enthalpy Temperature Characteristics	89
39	Afterburner Autoignition Results	91
40	Effect of Gas Generator Oxidizer/Fuel Ratio Upon Afterburner Combustion Efficiency	92
41	Afterburner Combustion Efficiency	94
42	Afterburner Combustion Efficiency High Altitude Conditions	95
43	Effect of Inlet Air Mach Number Upon Afterburner Combustion Efficiency	97
44	Relationship between Combustion Efficiency and Inlet Air Temperature for Configuration II	98
45	Effect of Afterburner Pressure Upon Combustion Efficiency	100
46	Dump Pressure Recovery of Air Augmentation Combustor	101
47	Gas Generator Exit After Long Duration Run	104
48	Gas Generator Hardware - Exhaust Tube and Target	105
49	Air Augmentation Test Hardware - Air Inlet Section	106
50	Air Augmentation Test Hardware - Combustor	107
51	Air Augmentation Test Hardware - Throat Section	108
52	Data Sampling Intervals in Air Augmentation Runs	118
53	Computation Flow Diagram	123
54	Viscosity - Temperature Characteristics of MARNAF 731	128

UNCLASSIFIED

LIST OF TABLES

<u>TABLE</u>		<u>Page</u>
I	Gas Generator Test Results	45 & 46
II	Spectrographic Analysis of Boron and Slurries	56
III	Spectrographic Analysis of Engine Deposits	63
IV	Composition of Products of Run 3	67
V	Data Summary for Air Augmentation Runs Using CTF	86
VI	Data Summary for Air Augmentation Runs Using BPF	87
VII	Throat Erosion in Gas Generator Chambers	103

CONFIDENTIAL

I

SUMMARY

(U) An applied research and exploratory development program was conducted to evaluate the bipropellant gas generator concept for air augmentation applications. The fuel used was MARNAF 731, a high concentration (73%) boron slurry, and the oxidizers evaluated were chlorine trifluoride and bromine pentafluoride. The program was conducted in two phases. The first phase concerned the development of the primary gas generator and the second phase consisted of a series of direct connect air augmentation tests.

(C) Although problems of deposit buildup were encountered, the successful development of a small scale gas generator was accomplished under Phase I. Secondary combustor ignition limits and combustion performance were demonstrated under Phase II. Testing was conducted over a range of altitude conditions from sea level to 40,000 feet at a nominal Mach number of 2.8 to 2.9. The results indicate that autoignition in the secondary combustor can be expected to occur at all primary O/F ratios greater than 0.20. Performance achieved with CTF and BPF was essentially the same. Under low altitude conditions, combustion efficiencies above 90% were demonstrated at O/F ratios as low as 0.06 at an air-to-propellant ratio of 40. At 40,000 feet simulated altitude, an efficiency of 80% was demonstrated at an O/F ratio of 0.20 and an air-to-propellant ratio of 20. At essentially a given O/F ratio, a throttling capability of about 6:1 was demonstrated.

(C) Hardware durability of the final design was excellent as was demonstrated by a 160 second duration run. Design criteria for the bipropellant gas generator concept for air augmentation has been established and the propellant combination MARNAF 731 and CTF (or BPF) appears to be an ideal choice for ducted rocket applications.

CONFIDENTIAL

II

INTRODUCTION

(C) In recent years, effort has been expended by various governmental agencies to investigate improved propulsion systems or combinations of propulsion systems for high speed missile applications. One area of investigation has centered around engines for volume-limited tactical missiles. Solid propellant rocketry has long dominated the tactical missile field; however, in recent years other propulsion systems such as liquid rockets and ramjets have and are being investigated. Liquid rockets readily offer more flexibility than solid motors, but both systems inherently have relatively low levels of specific impulse. This level generally falls between 250 and 325 seconds. On the other hand, airbreathers, particularly ramjets, have much higher fuel specific impulses of 1000 to 2000 seconds with storable fuels, but suffer from lower thrust-to-weight ratios, narrower flight corridors, low thrust coefficients at flight speeds below Mach 1.0, and may have limited performance at high altitude.

(U) To overcome these shortcomings, considerable interest has recently been expressed by various agencies to investigate combined rocket-ramjet powerplants, trying to combine the best features of each. One area of interest being investigated has been termed "air augmentation," using what are known as air-augmented rockets. In principle, air-augmented rockets offer the promise of significant increases in specific impulse. Some increase is the result of primary mass addition to the secondary air stream. Greatest gains are achieved, however, when significant heat addition or combustion in the secondary stream occurs. This type is generally referred to as the ducted rocket. Use of the oxygen in the air stream obviously permits a much larger overall heat release in the system. Generally, those that operate appreciably fuel-rich in the primary combustor offer the greatest specific impulse potential, because substantial further oxidation(combustion) can occur in the secondary chamber.

(C) A number of potential propellants have been considered for air-augmented rockets and recently the following have been under active investigation:

CONFIDENTIAL

1. Solid (fuel-rich) propellant system
2. Hybrid (fuel-rich solid with liquid interhalogen oxidizer) system
3. Bipropellant liquid system.

(C) A feasibility demonstration program on the latter concept is the subject of this report. Of the possible propellants for the bi-liquid system, one combination which has great merit, because of the unusually high heat of combustion of the fuel, is the boron slurry/chlorine trifluoride (CTF) system operated under very fuel-rich conditions. In the very fuel-rich mode of operation the boron slurry/CTF rocket system has more of the characteristics of a gas generator than of a thrust-producing rocket. When employed for air augmentation, it can provide the following payoffs:

- a. Extremely flexible thrust pattern capability from a single propulsion system, as obtained from a controllable fuel flow rate.
- b. Operational ranges greater than those of solid-grain sustainer systems.
- c. Inherent relight capability because of its bipropellant nature.
- d. Potentially higher combustion efficiencies at high altitudes with its preheated fuel as compared with ramjets.
- e. Minimization of ramjet burner drag.
- f. Elimination of the dependency of the solids sustainer burn rate/mass flow upon propellant bulk temperature and operating pressures.

Because of these potential payoffs, this exploratory development program was conducted.

CONFIDENTIAL

III

PROGRAM OBJECTIVES

(C) The overall objective of this exploratory development program was to demonstrate the feasibility of a fuel-rich boron slurry-in-terhalogen oxidizer gas generator for air-augmented rocket propulsion applications. This program was to be conducted in two phases. The first phase concerned the development and evaluation of the gas generator proper and the second phase consisted of direct connect air tests to evaluate the secondary air-gas generator exhaust combustion characteristics. The first phase was to be conducted with 73% boron slurry (MARNAF 731) fuel and chlorine trifluoride oxidizer. The second phase was to be conducted primarily with MARNAF 731 and chlorine trifluoride but limited testing was to be conducted using bromine pentafluoride as the oxidizer. The bulk of the second phase testing would be conducted under simulated low altitude conditions but with limited testing under high altitude conditions. These tests were intended to supply information to determine the feasibility and potential of the bipropellant gas generator concept and also to provide information for the Air Force to permit a comparison between this concept, the solid propellant, and the hybrid propellant gas generator.

(C) The specific objectives are summarized as follows:

Phase I - Demonstrate the feasibility of a fuel-rich boron slurry/CTF gas generator suitable for air-augmented rocket applications.

Phase II- Demonstrate the air augmentation performance of the fuel-rich gas generator by determining afterburner combustion efficiency and determining the minimum primary O/F ratio for afterburner autoignition.

UNCLASSIFIED

IV

GAS GENERATOR DEVELOPMENT

A. REQUIREMENTS

(U) The boron slurry/CTF gas generator can provide a high heating value per pound of propellant, when operated in the very fuel-rich mode, for combustion of the exhaust products in air. Therefore, it becomes of interest to consider its utilization for air augmented rockets. The heating value advantage of the boron slurry/CTF system, over other less energetic fuel-rich propellants, is a function of the O/F ratio within the generator. The generator must provide an exhaust stream which is of a composition suitable for efficient burning in air. The fuel under consideration is MARNAF 731, which is described in Appendix B. The theoretical heating value as a function of O/F is presented in Figure 1.* For comparison the heating value of a solid propellant air augmentation system using a 51% loaded boron propellant is 1.66×10^6 Btu/ft³ or 16,100 Btu/lb. Other factors such as packaging density, propellant flow rate controls and afterburner combustion efficiency also must be considered when comparing the several types of gas generators for air augmentation systems. The boron slurry/CTF gas generator exhaust temperature increases with O/F ratio in the manner shown in Figure 2. In application, the O/F ratio should be sufficiently high to permit spontaneous ignition of the exhaust products when mixed with air. Analytical studies predicted that the principal gaseous fuels present in the gas generator combustion products should consist of hydrogen and methane. These gases should contribute to the spontaneous initiation of combustion with air in the lower range of O/F ratios. The resultant increase in temperature of the mixture through combustion of the gases should raise the solid species, boron and carbon, to their ignition points.

(U) The oxidizer/fuel ratios under investigations ranged nominally from 0.1 to 0.5 at chamber pressures ranging from 200 psi to 1000 psi. This range could be extended below 0.1, if warranted by spontaneous ignition data. The maximum O/F ratio of interest would be that beyond which there is no appreciable improvement in combustion efficiency. Maximum performance therefore corresponds to a trade-off between minimum oxidizer utilization and maximum

*These heating values were calculated on the basis of ideal heat release of each constituent of the gas generator effluent to stoichiometric products at room temperature, the same as heating value for slurry alone.

UNCLASSIFIED

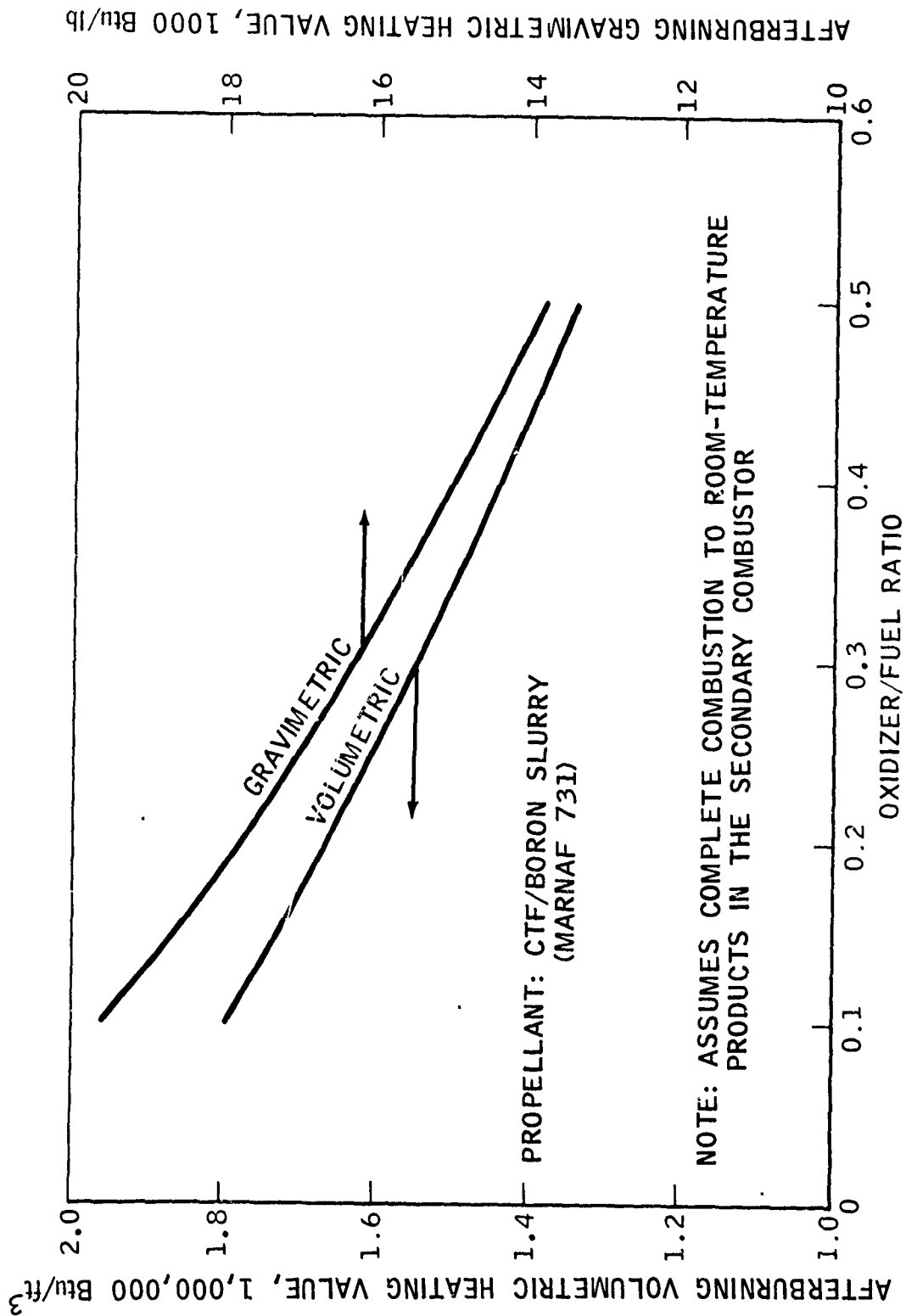


Figure 1
HEATING VALUE OF PROPELLANT

A343-4

UNCLASSIFIED

CONFIDENTIAL

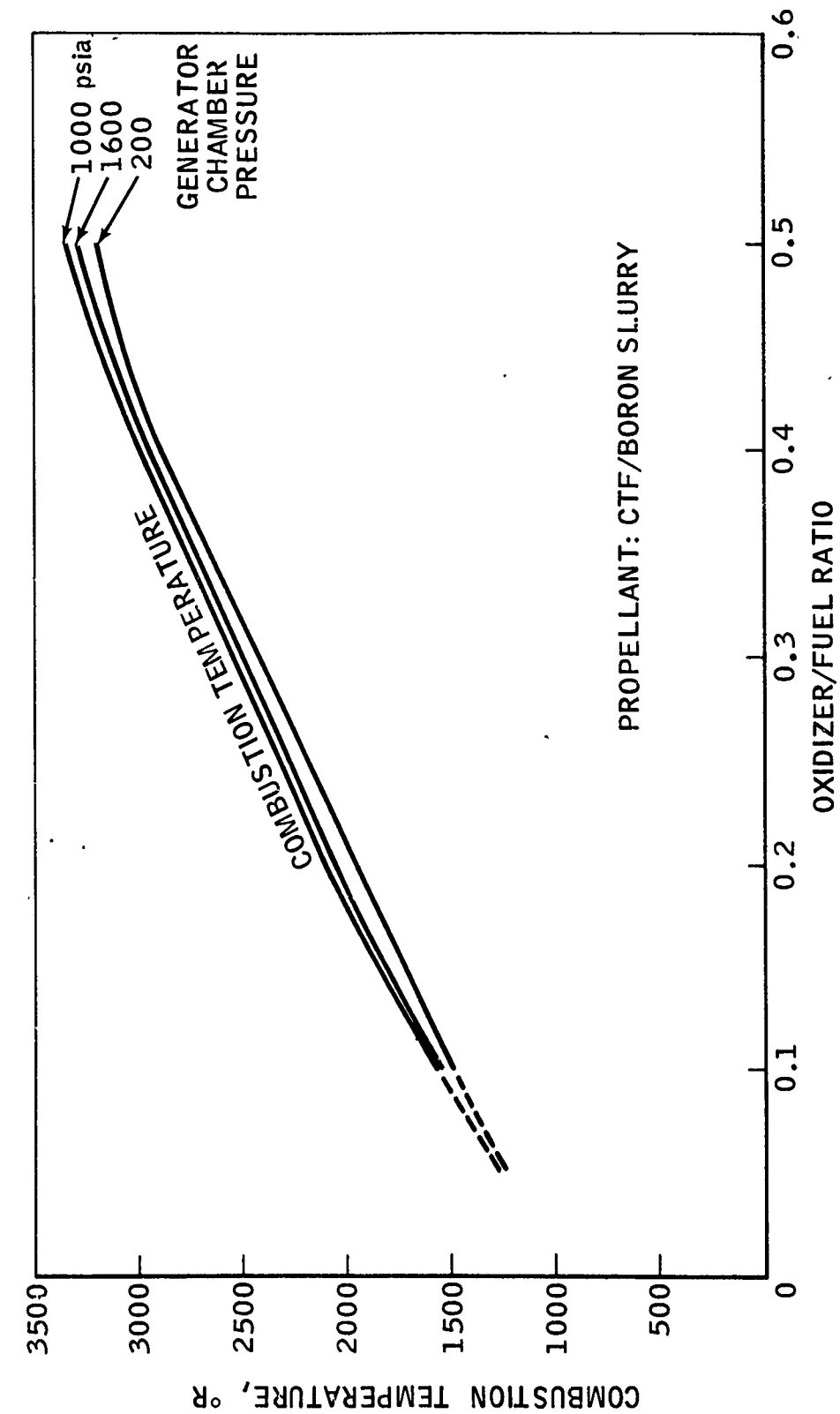


Figure 2
EFFECT OF OXIDIZER/FUEL RATIO UPON EQUILIBRIUM GAS TEMPERATURE
IN GAS GENERATOR

A407-12

-9-

CONFIDENTIAL

(This page is Unclassified)

CONFIDENTIAL

combustion efficiency. The air augmented rocket test program was oriented toward obtaining data from which the operating regime for maximum performance could be determined at each of two simulated flight conditions, corresponding to Mach 2.9 at sea level and Mach 2.8 at 40,000 ft.

(C) The most important basic requirements upon the design of a gas generator for application to air augmentation are as follows:

a. The ability to satisfy the propellant flow rate and O/F ratio requirements.

Since the operational envelope of an air augmented propulsion system ranges from sea level to high altitude, the primary combustor must be capable of throttling its propellant flow to meet specific flight requirements over this altitude range. As altitude is increased, the ability to ignite and burn the fuel-rich exhaust in the secondary air begins to deteriorate, so it may become necessary to increase the temperature of the gas generator exhaust in order to improve combustion efficiency in the afterburner. This can be accomplished by increasing the propellant O/F ratio. Since both flow rate and O/F ratio changes are accompanied by changes in chamber pressure level and propellant injection velocity, the gas generator must be designed to accommodate these changes while maintaining adequate performance.

b. The production of a primary exhaust stream containing well dispersed elementary particles of boron.

The achievement of a high combustion efficiency in the secondary combustor is dependent directly upon the state of the boron in the primary exhaust. Based upon previous ramjet experience, if the boron particles from the MARNAF 731 fuel maintain their average size of about 0.8 microns throughout the primary combustion process, then complete combustion in the secondary air flow should readily be achieved. If, however, the primary exhaust contains large agglomerates of particles, the combustion efficiency may be severely degraded because of the greater ignition delays and longer combustion times of the agglomerated particles.

c. The ability to operate continuously for relatively long durations in an uncooled, flight type configuration.

The most severe operational environment for the primary combustor would likely be that corresponding to Mach 2.9 sea level because the mass flow rate and therefore pressure and erosion rates are highest at that condition.

CONFIDENTIAL

As the boron slurry is unsatisfactory for regenerative cooling, and the chlorine trifluoride flow rate and heat capacity are too small for cooling, an uncooled gas generator appears to be necessary. An objective of this program was a 150 second run with an uncooled gas generator.

d. The ability to operate without appreciable formation of deposits in the chamber.

The gas generator should be capable of deposit-free operation for durations ranging upward to 150 seconds. The occurrence of deposits within the chamber which increase with time becomes unacceptable for flight type combustors.

B. THEORETICAL STUDIES

(U) One notable advantage of the propulsion cycle under investigation is its capability of achieving spontaneous ignition of the fuel rich exhaust of the gas generator in the afterburner. The spontaneous ignitability of the gas generator effluent is dependent upon (1), an effluent equilibrium temperature sufficiently high to result in ignition of the combustible gases when mixed with air, or (2) the presence of a sufficient concentration of free radicals in the effluent, as a result of nonequilibrium combustion in the gas generator, to initiate the combustion process in the afterburner. The latter process is the one more likely to occur, and indeed, is the preferred process, as it could result in ignition at lower effluent temperatures and therefore lower O/F ratios than would otherwise be possible. It therefore was of interest to investigate analytically the concentration of free radicals as a function of time by means of the Marquardt finite kinetic computer program, FINEK. The resulting data would be useful in guiding the direction and interpretation of the experimental effort.

(U) The free radicals in the effluent from the gas generator would result from pyrolysis of the trimethylhexane C_9H_{20} . As it was desirable to simplify the chemical system for computer analysis the boron and chlorine trifluoride constituents were deleted, for these would not contribute appreciably to the free radical concentration. Even with this simplification, there remained a total of 1138 chemical reactions which could appear in the pyrolysis of C_9H_{20} to carbon and hydrogen. Reaction rate constants were generated for these reactions by the GENCOM computer program utilizing Marquardt's IBM system 360/40 computer. These reactions were then incorporated in sets of

CONFIDENTIAL

150 into the FINEK program, which was run on the IBM 7090 computer at the Air Force Rocket Propulsion Laboratory (150 reactions comprise the limit for the FINEK program). The insignificant reactions were then discarded in a series of computer runs. This screening process resulted in an apparent basic set of 89 reactions which would be needed to describe the pyrolysis of C_9H_{20} .

(U) Carrying through the pyrolysis process with the prescribed set of reactions for an initial temperature range of 1600°F to 2500°F indicated a strong effect of initial temperature on both rate and extent of production of free radicals. The methyl radical (CH_3) was the most prominent free radical according to the computations, followed by ethyl (C_2H_5), then propyl (C_3H_7). Other free radicals were of appreciably less to trivial prominence and the three named comprised 80-90% of the total free radical mole fractions. The time incidence of peak concentration of each free radical was essentially simultaneous in any one solution, although different times were required for solutions at different initial temperatures. The peaks generally corresponded to a residual mole fraction of trimethylhexane of about 0.6, over the initial temperature range. As noted below, subsequent work showed that an important free radical was missing from the allowed set of reactions in this initial pyrolysis computation. The general trends indicated above are therefore possibly in error.

(U) Given the kinetic composition of the gas generator effluent vapors, the next step for analysis was the consideration of autoignition reactions. Approximately 1500 reactions were generated to permit oxidation of the C_1 - C_3 species which comprised the prominent free radicals generated in pyrolysis. These were reduced to about 500 by inspection for steric limitations. By computer runs comparable to those for the pyrolysis, the 500 were screened to a manageable 150 reactions.

(U) One aspect in which the calculational results were not deemed complete concerned the formation of solid carbon from hydrocarbons, with the prominent theory being that it derives from acetylene. The formation and degradation of acetylene within the pyrolysis reaction scheme was consistent with the general approach conceived, and in particular it was most consistent with the available species' thermochemical properties. Granting that the theory might be fundamentally imperfect, it was expected that at least it could serve as a suitable modus operandi to produce solid carbon and complementary hydrogen.

CONFIDENTIAL

(This page is Unclassified)

CONFIDENTIAL

150 into the FINEK program, which was run on the IBM 7090 computer at the Air Force Rocket Propulsion Laboratory (150 reactions comprise the limit for the FINEK program). The insignificant reactions were then discarded in a series of computer runs. This screening process resulted in an apparent basic set of 89 reactions which would be needed to describe the pyrolysis of C_9H_{20} .

(U) Carrying through the pyrolysis process with the prescribed set of reactions for an initial temperature range of 1600°F to 2500°F indicated a strong effect of initial temperature on both rate and extent of production of free radicals. The methyl radical (CH_3) was the most prominent free radical according to the computations, followed by ethyl (C_2H_5), then propyl (C_3H_7). Other free radicals were of appreciably less to trivial prominence and the three named comprised 80-90% of the total free radical mole fractions. The time incidence of peak concentration of each free radical was essentially simultaneous in any one solution, although different times were required for solutions at different initial temperatures. The peaks generally corresponded to a residual mole fraction of trimethylhexane of about 0.6, over the initial temperature range. As noted below, subsequent work showed that an important free radical was missing from the allowed set of reactions in this initial pyrolysis computation. The general trends indicated above are therefore possibly in error.

(U) Given the kinetic composition of the gas generator effluent vapors, the next step for analysis was the consideration of autoignition reactions. Approximately 1500 reactions were generated to permit oxidation of the C_1 - C_3 species which comprised the prominent free radicals generated in pyrolysis. These were reduced to about 500 by inspection for steric limitations. By computer runs comparable to those for the pyrolysis, the 500 were screened to a manageable 150 reactions.

(U) One aspect in which the calculational results were not deemed complete concerned the formation of solid carbon from hydrocarbons, with the prominent theory being that it derives from acetylene. The formation and degradation of acetylene within the pyrolysis reaction scheme was consistent with the general approach conceived, and in particular it was most consistent with the available species' thermochemical properties. Granting that the theory might be fundamentally imperfect, it was expected that at least it could serve as a suitable modus operandi to produce solid carbon and complementary hydrogen.

CONFIDENTIAL

(This page is Unclassified)

CONFIDENTIAL

However, the pyrolysis results indicated a "piling up" of propylene and ethylene along with methane and ethane, relatively little acetylene, and only slow degradation of acetylene to carbon and hydrogen. This was insignificant as it could influence not only the decline of free radical concentration from the peak level, but also the impedance of appearance of solid carbon as a less reactive effluent constituent.

(U) It was considered important to be able to define approximately the amount of solid carbon in the effluent as a function of gas generator operating conditions, for this could serve to impose an upper limit on O/F just as the autoignition requirement imposes some lower limit. Therefore, additional species, namely the dehydrogenated species from C_3H_6 , and all of the attendant reactions with smaller (C_2 and C_1) species and fragments, were assembled for screening calculations at the point in reaction time where "piling up" of C_3H_6 , C_2H_4 , C_2H_2 , and CH_4 has been noted. Before the screening calculations could be performed, however, the Air Force directed that the finite kinetics investigation be terminated in order to provide for shifting of contract funds allotted to it to the experimental program, which had been broadened in scope.

(U) Subsequent work performed on another program revealed that the C_3H_5 radical and species derived from it played a prominent role in the production of solid carbon by pyrolysis. As this species was not incorporated in the original basic pyrolysis scheme, the conclusions derived from the earlier computations are open to doubt. Therefore it can be concluded that the finite kinetics effort was terminated prior to the point where it could have made a significant contribution to the program.

C. TEST HARDWARE

(U) 1. Test Facility

Both Phase I, Gas Generator Development, and Phase II, Air Augmentation Demonstration tests were conducted at Marquardt's Magic Mountain test facility. The remote location in the San Gabriel Mountain Range permits testing with toxic propellants such as the interhalogen oxidizers. The test cell (M1-A) used was originally a rocket test pad where the engine fired vertically downward. In 1967, air capability was added to the test cell. Under the conditions of interest for this program, the air flowrate capacity

CONFIDENTIAL

(This page is Unclassified)

CONFIDENTIAL

is approximately 40 pps for 60 seconds or 30 pps for about 85 seconds. These flow rate conditions can be achieved at pressures up to 300 psia and temperatures up to 1200°F.

2. Gas Generator Hardware

(U) The initial designs for the gas generator were based on the requirements of a 15-inch diameter afterburner which would result in a gas generator capable of producing 500 lbs of thrust when using a convergent-divergent nozzle. These requirements resulted in the chamber dimensions used in the first three gas generator configurations. Subsequently the requirement was scaled down to match a 7-inch afterburner. In keeping with a design evolved from another Air Force air augmented rocket program, the gas generator nozzle was designed to provide two impinging sonic streams which results in a well-mixed, subsonic flow of exhaust products. The final configuration was based upon the 7-inch size requirement but deviated from the impinging sonic stream requirement.

(U) To facilitate the testing of various chamber configurations, the test item was designed as a basic stainless steel casing into which various graphite chambers could be inserted. For testing, the gas generator was attached in a downward firing position to a vertical thrust stand.

(U) During the Phase I testing several iterations on gas generator configurations were made to arrive at an acceptable one with regard to solids deposition within the chamber. The various configurations and the number of test points acquired on each are summarized in Figure 3. A brief description of each is given in the following sections.

a. Turbulator

(C) Under a Navy funded rocket-ramjet program (Reference 1), a boron slurry CTF rocket engine was tested. This engine was called the turbulator engine design. This turbulator engine consisted of a precombustion chamber into which propellants were injected from a single oxidizer-on-fuel doublet such that a vortex flow was generated. The partially reacted species then entered a conventional cylindrical combustion chamber. An engine of this type, pictured in Figure 4, was successfully operated at extreme off-design conditions down to an O/F ratio of 0.084. This engine design formed the basis for the first gas generators tested under this program.

CONFIDENTIAL

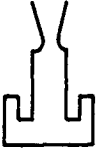

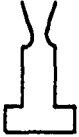
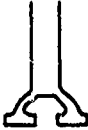


<u>DESCRIPTION</u>	<u>CONFIGURATION</u>	<u>NO. TEST POINTS</u>
TURBULATOR		4
SPIRAL SWIRL		2
MODIFIED TURBULATOR		3
DUAL CHAMBER IMPINGING JETS		7
SINGLE CHAMBER IMPINGING JETS		2
AXIAL INJECTION		2
		<u>20</u>

Figure 3
TEST SUMMARY
PHASE I

A407-28

-15-

CONFIDENTIAL

(This page is Unclassified)

CONFIDENTIAL

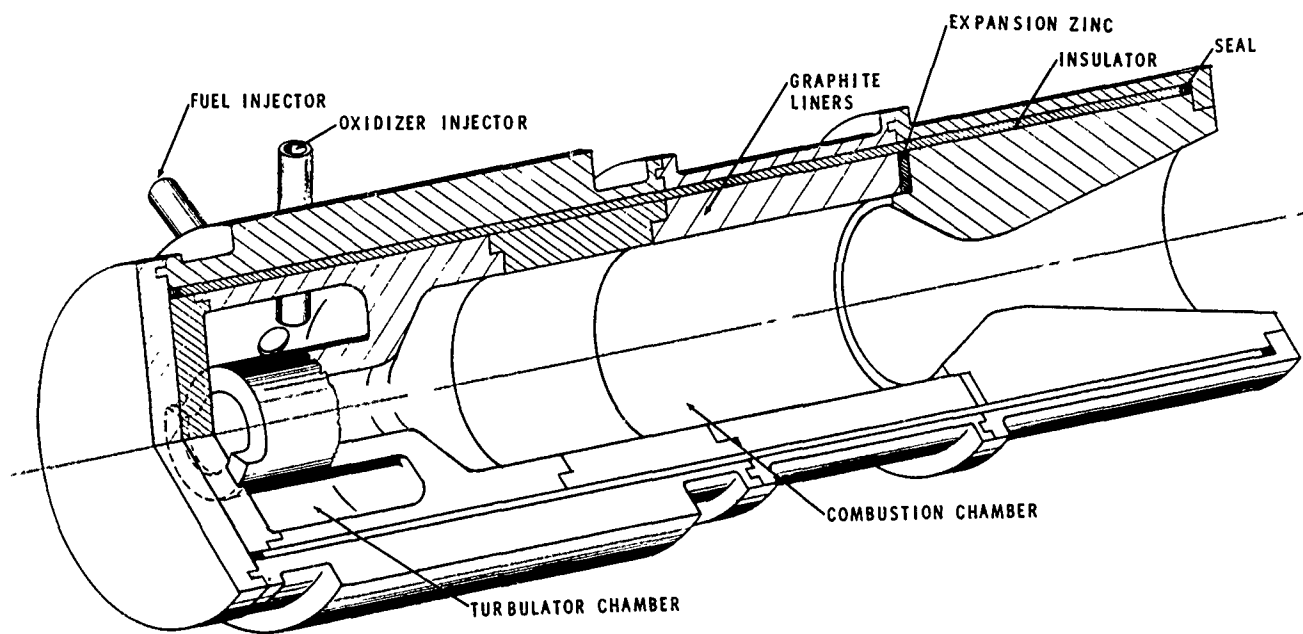


Figure 4
SINGLE POINT INJECTION TURBULATOR ENGINE (U)

R-21,391

-16-

CONFIDENTIAL

CONFIDENTIAL

(U) For air augmentation applications, a short gas generator is desirable from a packaging standpoint. Therefore, two configurations were analytically investigated for the turbulator gas generator design: Configuration A, with an L^* of 54 is a close copy of the turbulator engine operated previously. Configuration B, has the precombustion chamber integrated into the main combustion chamber and has an L^* of 66. Schematics of the two configurations are presented in Figures 5 and 6. Because of the small throat, the value of L^* has little significance.

(U) The injector pattern layout for both configurations is shown schematically in Figure 7. Three sets of injectors were required to cover the wide range of propellant flows. The injector sizes and operating conditions are tabulated below:

Injector	Fuel Injector Dia., Inches	Oxidizer Injector Dia., Inches	Chamber Press., psia	O/F Ratio
A	0.24	0.06	200	0.1-0.5
B	0.3	0.13	600 1000	0.2-0.5 0.2-0.5
C	0.4	0.11	600 1000	0.1 0.1

(U) Configuration B was the turbulator design selected for testing and is presented in Figure 8. The increased size of the precombustion chamber, as compared to turbulator engines employed in previous programs, results in an overall shortening of the engine, which is desirable from a packaging standpoint. The exhaust nozzle assembly consisted of a basic expansion section with provision for attaching two extensions of the expansion cone to meet optimum expansion requirements over a range of chamber pressures. A thermocouple located just upstream of the throat was to serve as an indicator of the completeness of combustion at that station.

(U) Subsequent testing of the turbulator design at the 200 psia level resulted in the formation of heavy deposits in the chamber for the range of O/F ratios from 0.1 to 0.5. It was therefore evident that design modifications would be necessary if the deposition problem were to be eliminated.

b. Spiral Swirl

(U) The Spiral Swirl represents the second of the two basic gas generator designs to be tested. It is shown schematically in Figure 9. This gas generator also utilizes an oxidizer-on-fuel doublet. The spiral

CONFIDENTIAL

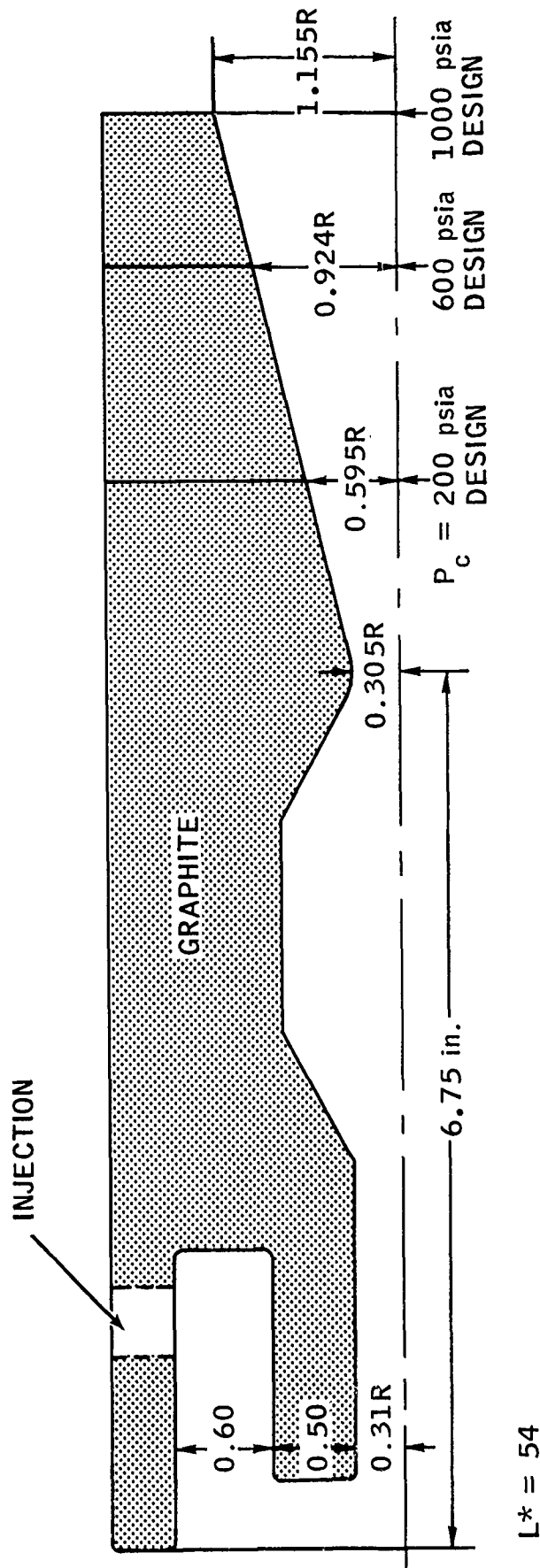


Figure 5
TURBULATOR GAS GENERATOR SCHEMATIC
CONFIGURATION A

R-23,873

-18-
CONFIDENTIAL

CONFIDENTIAL

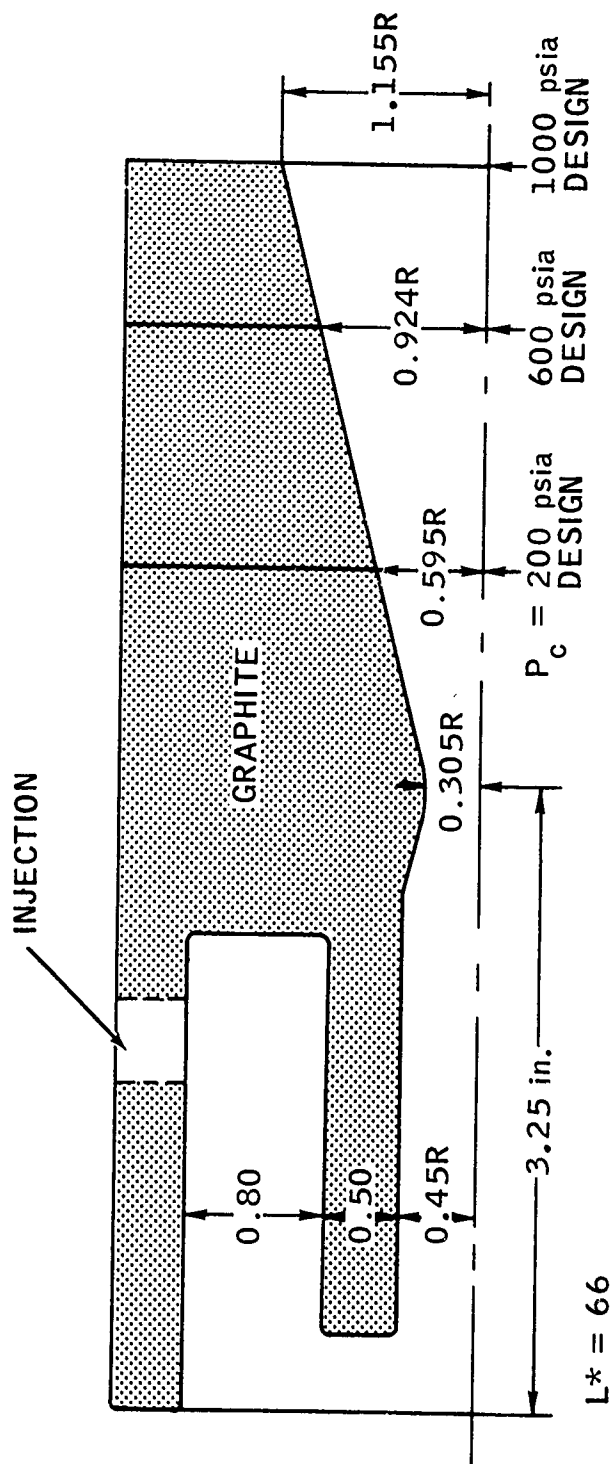
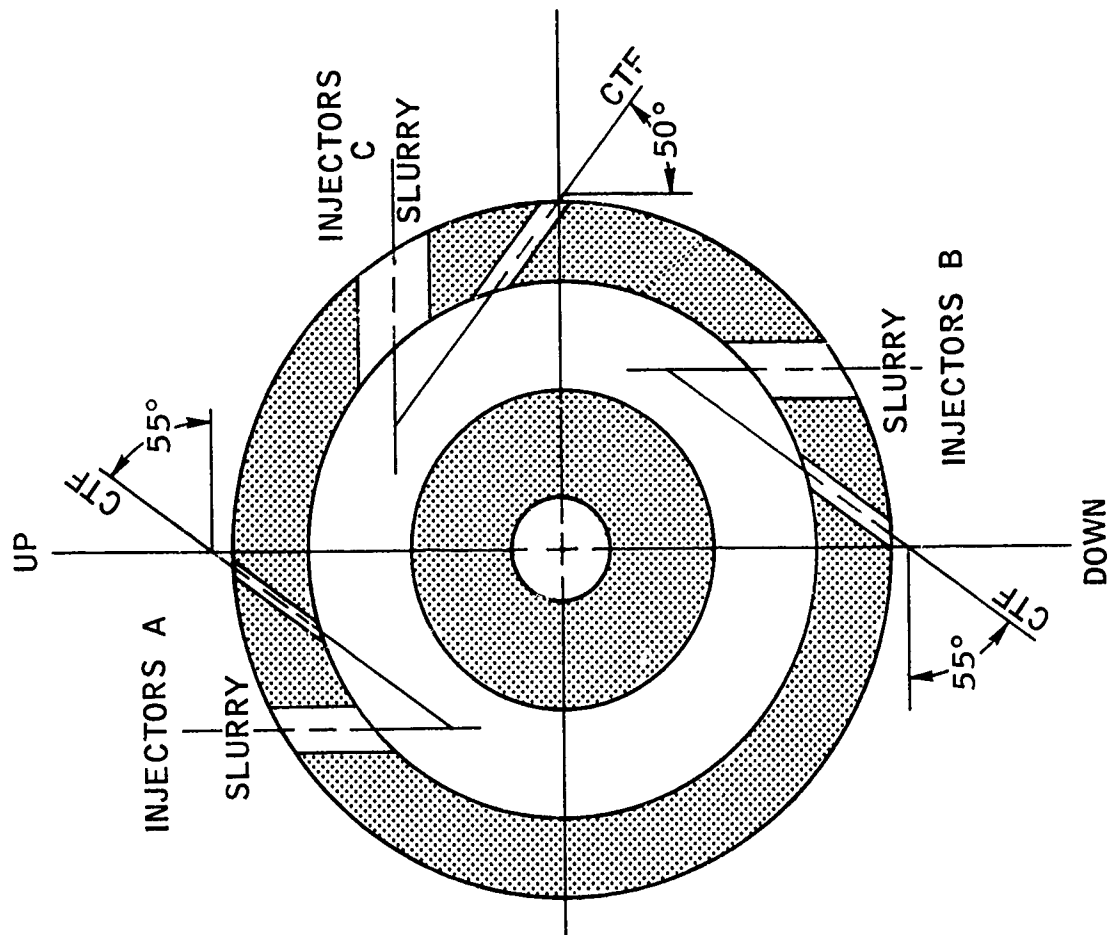


Figure 6
TURBULATOR GAS GENERATOR SCHEMATIC
CONFIGURATION B

R-23,874

CONFIDENTIAL

CONFIDENTIAL



INJECTOR A
 SLURRY = 0.24 in. DIA.
 CTF = 0.06 in. DIA.
 $P_c = 200$ psia
 $0.1 \leq O/F \leq 0.5$

INJECTOR B
 SLURRY = 0.3 in. ENTRANCE TO
 0.35 in. EXIT DIA.
 CTF = 0.13 in DIA.
 $P_c = 600$ psia
 $0.2 \leq O/F \leq 0.5$
 $P_c = 1000$ psia
 $0.2 \leq O/F \leq 0.5$

INJECTOR C
 SLURRY = 0.4 in. ENTRANCE TO
 0.45 in. EXIT DIA.
 CTF = 0.11 in. DIA.
 $P_c = 600$ psia $O/F = 0.1$
 $P_c = 1000$ psia $O/F = 0.1$

Figure 7
 INJECTOR PATTERN LAYOUT SCHEMATIC

R-23,875

CONFIDENTIAL

CONFIDENTIAL

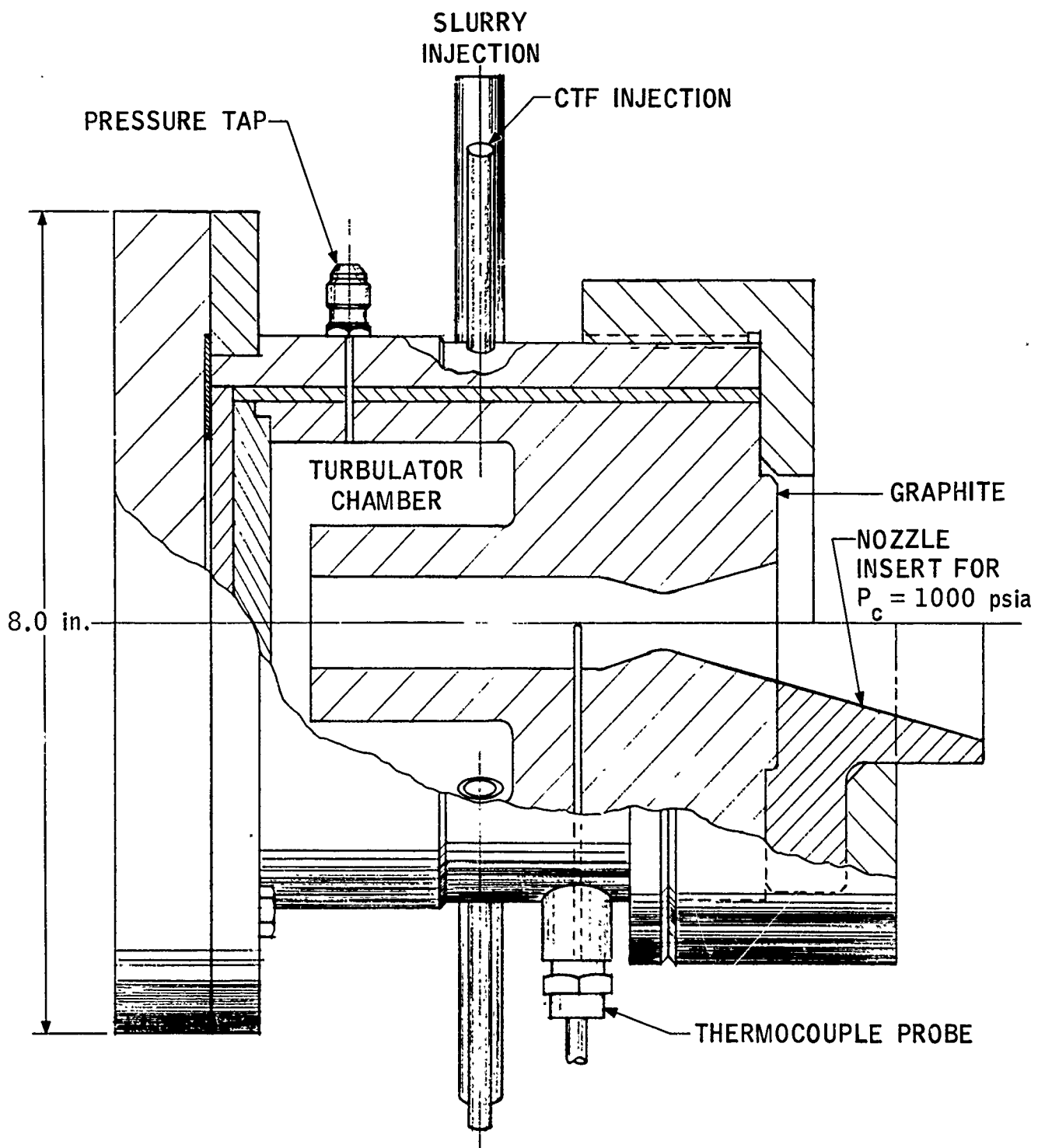


Figure 8
TURBULATOR GAS GENERATOR

R-25,141

-21-
CONFIDENTIAL

CONFIDENTIAL

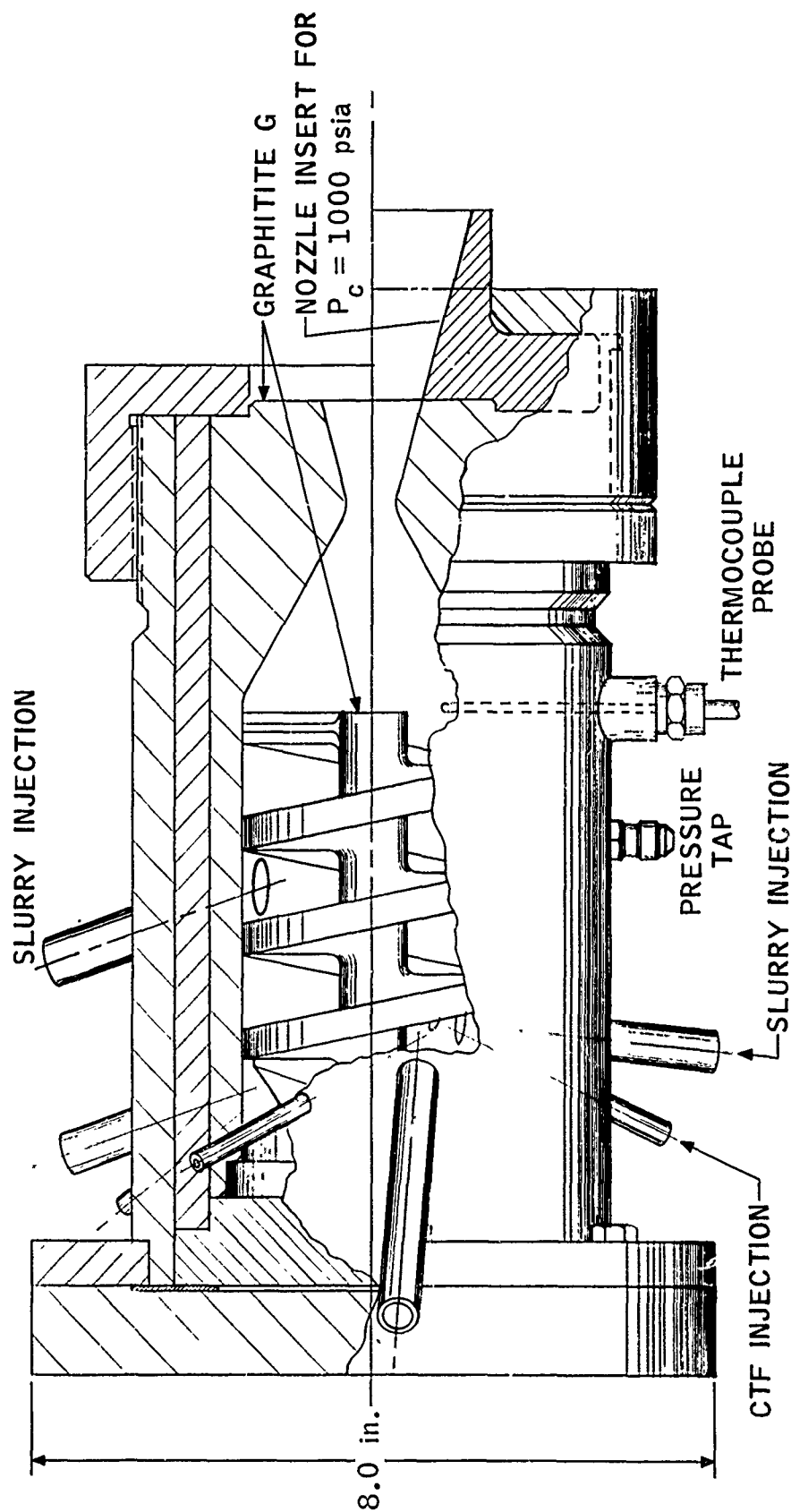


Figure 9
SPIRAL SWIRL GAS GENERATOR

R-25,142

-22-
CONFIDENTIAL

CONFIDENTIAL

flow pattern was intended to provide more thorough mixing during combustion. A possible advantage of this design was the tendency of the larger solid particles to be centrifuged away from the nozzle axis, thereby providing an opportunity for a more uniform distribution of particles in the exhaust (because normal tendency is to have larger particles in the center of the exhaust.)

(U) The Spiral Swirl engine tested is shown in Figure 10. The central spiral was made of Graphitite G. The injector configurations are very similar to that of the turbulator chamber. In addition to the primary injector, a downstream orifice, for injection of slurry only, was provided. A comparison of exhaust characteristics at low O/F ratio can thereby be made for two situations: (1) where all combustion occurs at the design O/F ratio, and (2) where upstream combustion occurs at a higher O/F (higher temperature) with additional slurry added downstream to meet design conditions. A thermocouple is located upstream of the throat to serve as an indicator of the completeness of reaction within the gas generator and to facilitate comparison of the two design approaches.

(U) Two tests were conducted in this gas generator. Both resulted in engine plugging attributable to operating sequence or spiral vane failure. Because of operational difficulties inherent in this design, principally the difficulty of disassembly for examination, no additional tests were conducted.

c. Modified Turbulator

(U) Since the initial checkout runs with the turbulator configuration indicated a severe solids deposition problem within the primary chamber, the chamber was redesigned to eliminate the 180 degree change in flow direction at the head end. The resulting chamber, shown in Figure 11, had an L^* of 25 and provided a residence time which was less than 40% of that of the initial turbulator design.

(U) Testing of the modified turbulator showed deposit-free operation over the O/F ratio range from 0.1 to 0.4 for chamber pressures less than 200 psia. A test corresponding to simultaneous high pressure and high O/F ratio demonstrated that the deposition problem was still not solved, however.

CONFIDENTIAL

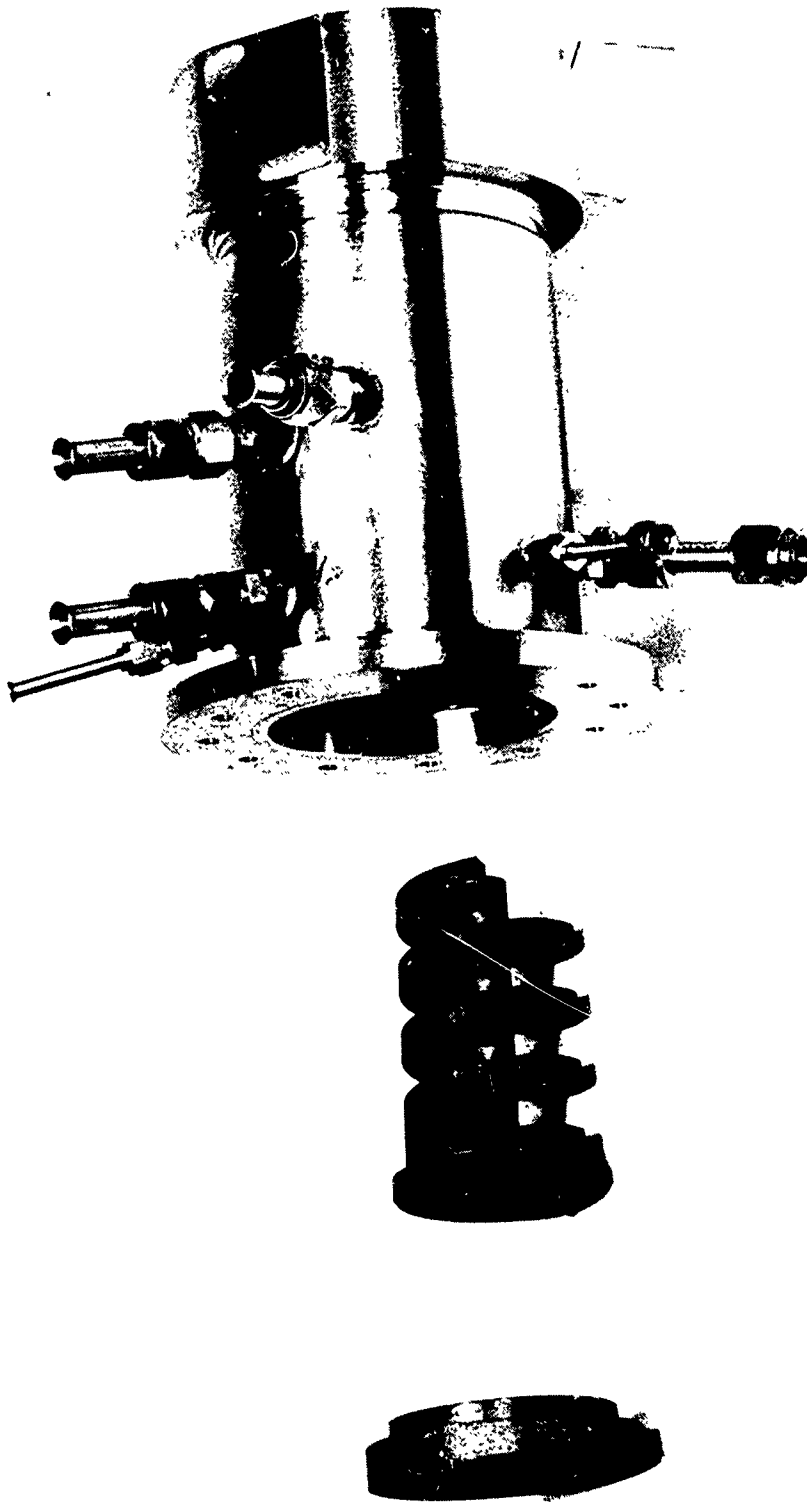


Figure 10.
SPIRAL SWIRL GAS GENERATOR
DISASSEMBLED VIEW

R-25,381
Neg. 8918-2

24

CONFIDENTIAL

(This Page is Unclassified)

CONFIDENTIAL

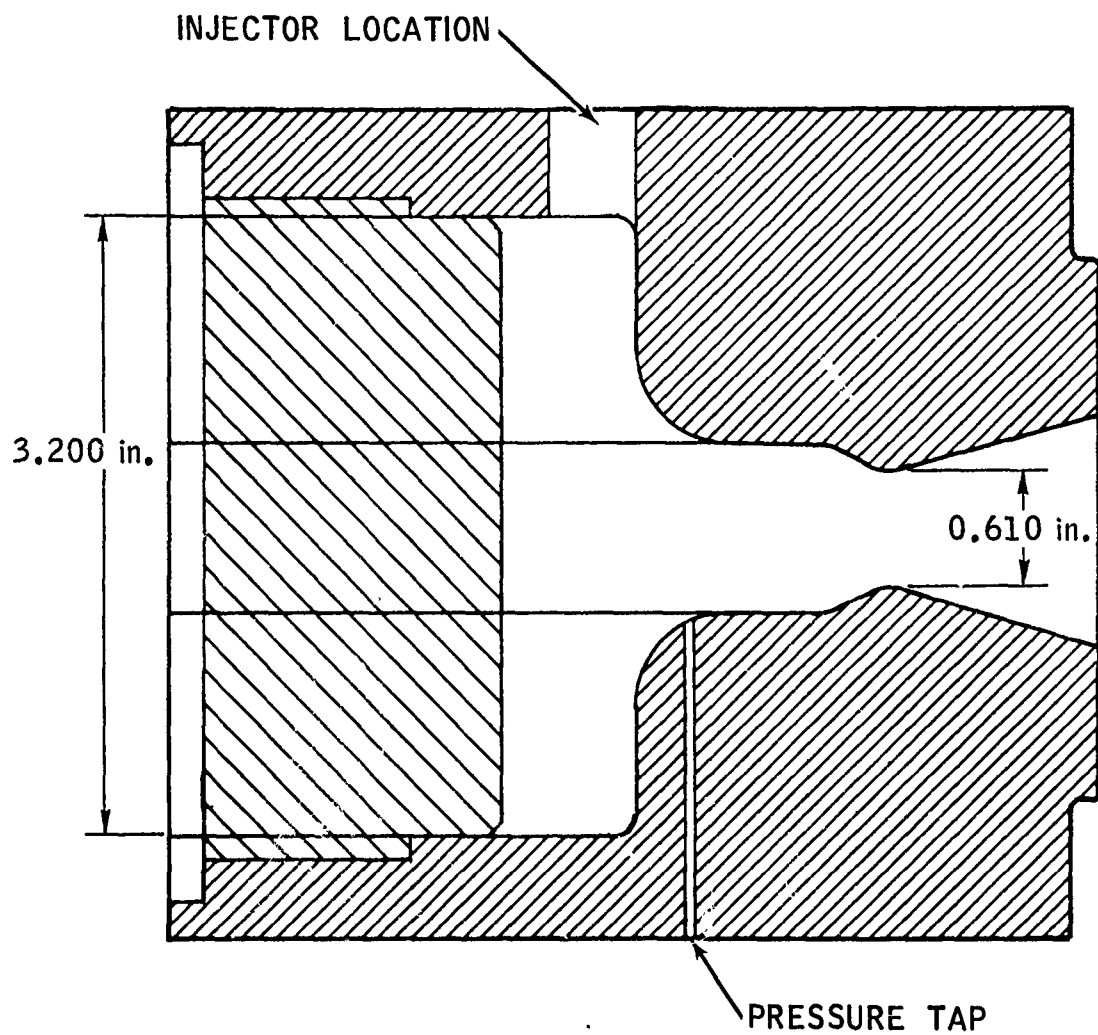


Figure 11
CHAMBER OF MODIFIED TURBULATOR GAS GENERATOR

R-25,385

-25-

CONFIDENTIAL

CONFIDENTIAL

d. Dual Chamber Impinging Jet

(U) The preceding gas generator configurations were predicated on the requirements of a 500 lb thrust and a 15-inch diameter afterburner. Coincidental with the identification of a solids deposition problem in these designs, the overall program was reviewed and it was decided that the remaining effort under Phase I should be directed towards gas generators that would be compatible with air augmentation tests of Phase II utilizing smaller scale hardware. Since the Air Force already had experimental data on a solid propellant ducted rocket with a 7-inch diameter secondary combustor, the Phase II tests under the subject program would also be conducted with 7-inch combustor hardware. Furthermore, to facilitate comparison of experimental data from the various Air Force programs, the secondary combustor hardware should be essentially identical in geometry. Since the method of injecting the exhaust products into the secondary chamber could markedly affect the afterburner performance, the Air Force requested that the gas generator exit design consist of two sonic jets impinging inside an injection tube (blast tube) which would result in subsonic flow of the primary exhaust into the secondary chamber.

(U) To comply with this requirement, two new gas generators were designed. These new designs required considerably scaling down of flow requirements. The first configuration was the dual chamber design shown in Figure 12.

(U) The dual chamber gas generator retained for its combustion chamber the general shape of that of the modified turbulator which successfully eliminated combustion chamber deposits at the lower chamber pressures. The L^* of 40 for each chamber is somewhat larger than that of the modified turbulator but the overall scale was greatly reduced. The 0.140 inch sonic jets from each chamber impinge at the axis of the injection tube resulting in a subsonic stream for mixing with the afterburner air.

(U) At an O/F ratio of 0.1 this gas generator operated without deposits to pressure levels exceeding 400 psia. Chamber deposits occurred at high O/F ratios and chamber pressures below 200 psia. Increasing the chamber pressure resulted in nozzle plugging at O/F ratios of 0.3 or above. An interaction between the chambers accelerated this plugging process. An interconnecting channel in a modified design failed to solve the plugging problem, however.

CONFIDENTIAL

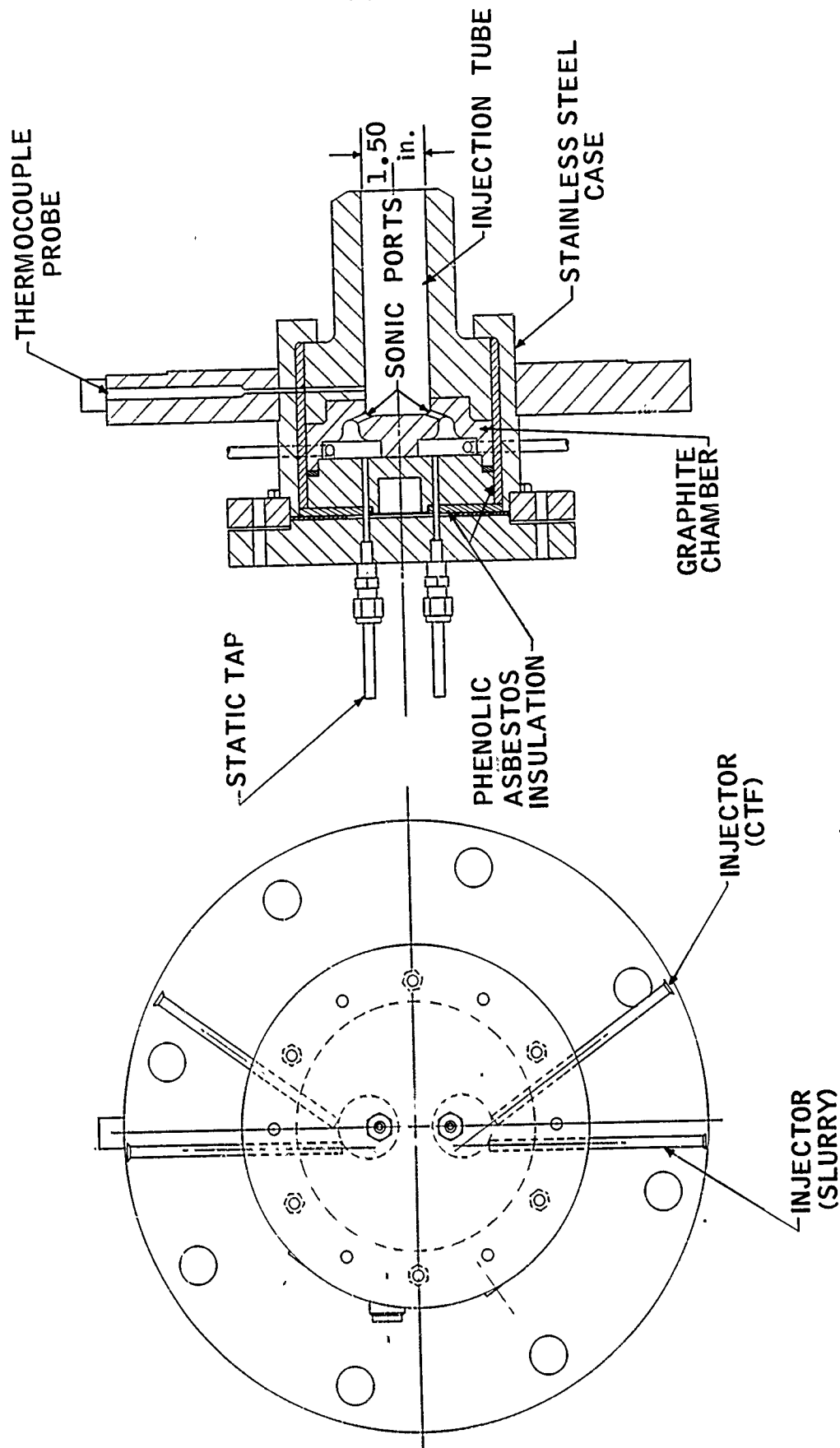


Figure 12
DESIGN OF DUAL CHAMBER GAS GENERATOR

R-25,436

CONFIDENTIAL

CONFIDENTIAL

e. Single Chamber Impinging Jet

(U) In the event that the reduced scale of the dual chambers contributed to buildup of chamber deposits and plugging of the throats, the single chamber design of Figure 13 was provided for testing. This configuration utilized identical sonic jets but had an L^* of 107 and a greatly increased volume-to-surface area. With the larger available volume a modified injection technique was incorporated into the design. In addition to the usual single point oxidizer-of-fuel injection, provisions were made for impingement of a second oxidizer stream upon the slurry stream to provide for more uniform mixing of the fuel and oxidizer. More uniform mixing will tend to eliminate the hotter regions in the combustion zone which apparently contribute to deposit formation. The assembled gas generator for either dual or single chamber is shown in Figure 14. The stainless steel shell made common to both configurations was provided with two pressure taps entering the dual chamber through the front end. The injectors mounted to the case wall comprised two sets of two each for the dual chambers and one set of three for the single chamber.

(U) When tested at intermediate O/F ratio and high pressures, nozzle plugging was experienced, but at a reduced rate compared to that of the dual chamber design. Thus the single chamber design was still inadequate for an operational gas generator.

f. Axial Injection

(U) The previous gas generators did not successfully eliminate deposition problems for all conditions and therefore a different approach was investigated.

(C) This approach, based upon a successful rocket combustion chamber design at Marquardt, employed an axial, as opposed to the previously employed circumferential, injection technique. A sketch of the configuration is shown in Figure 15. The slurry fuel is injected into the chamber as an annulus. This slurry annulus is impinged on its inner surface by a hollow conical stream of CTF. The CTF pattern is produced by first creating a swirling flow in the liquid and then injecting through a circular orifice. The injector configuration shown had been previously operated successfully at an O/F ratio of 0.04 in a rocket development program. The graphite insert was added for the gas generator tests. A zero length throat was first tested

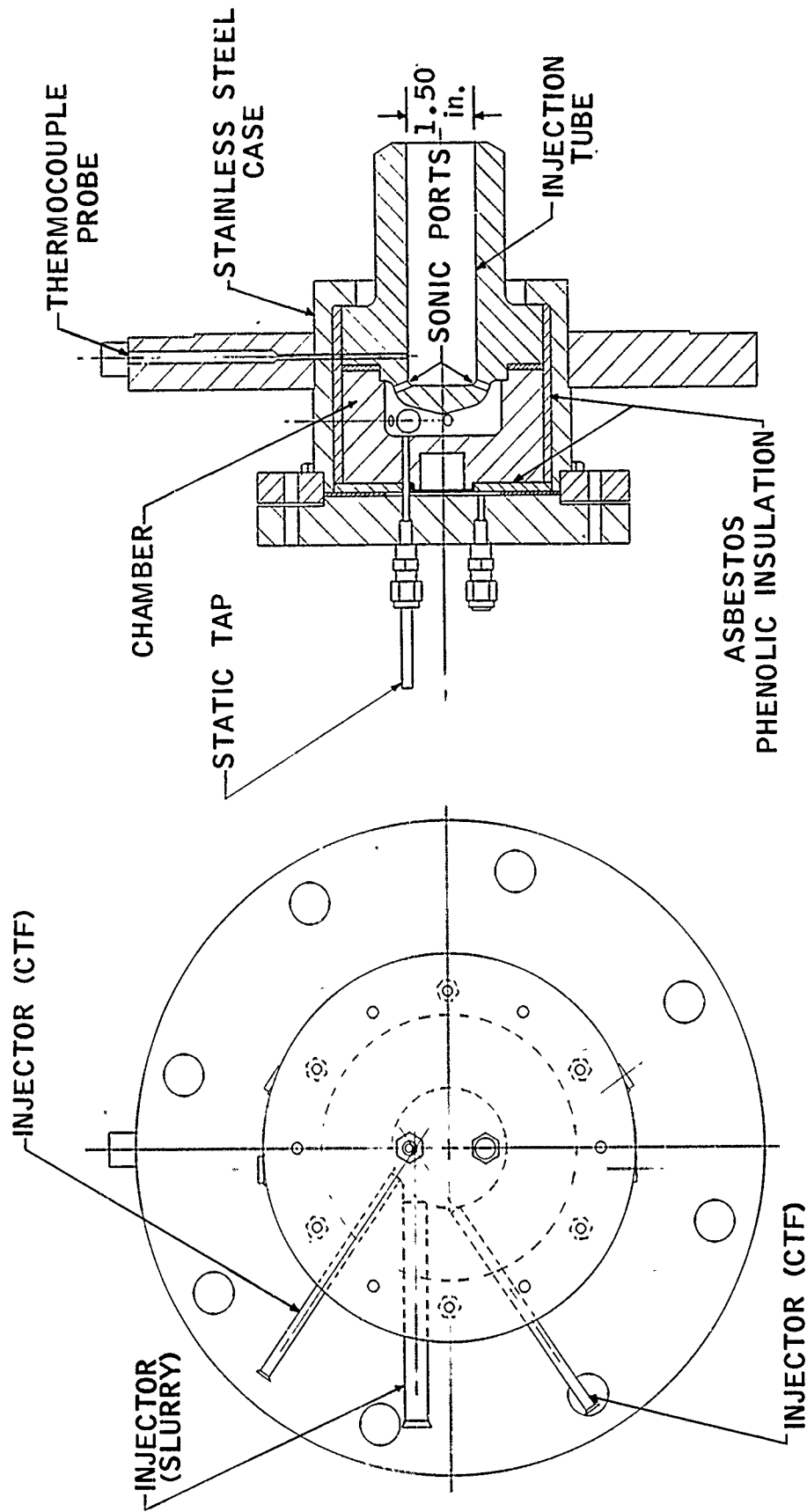


Figure 13
DESIGN OF SINGLE CHAMBER GAS GENERATOR

R-25,435

CONFIDENTIAL

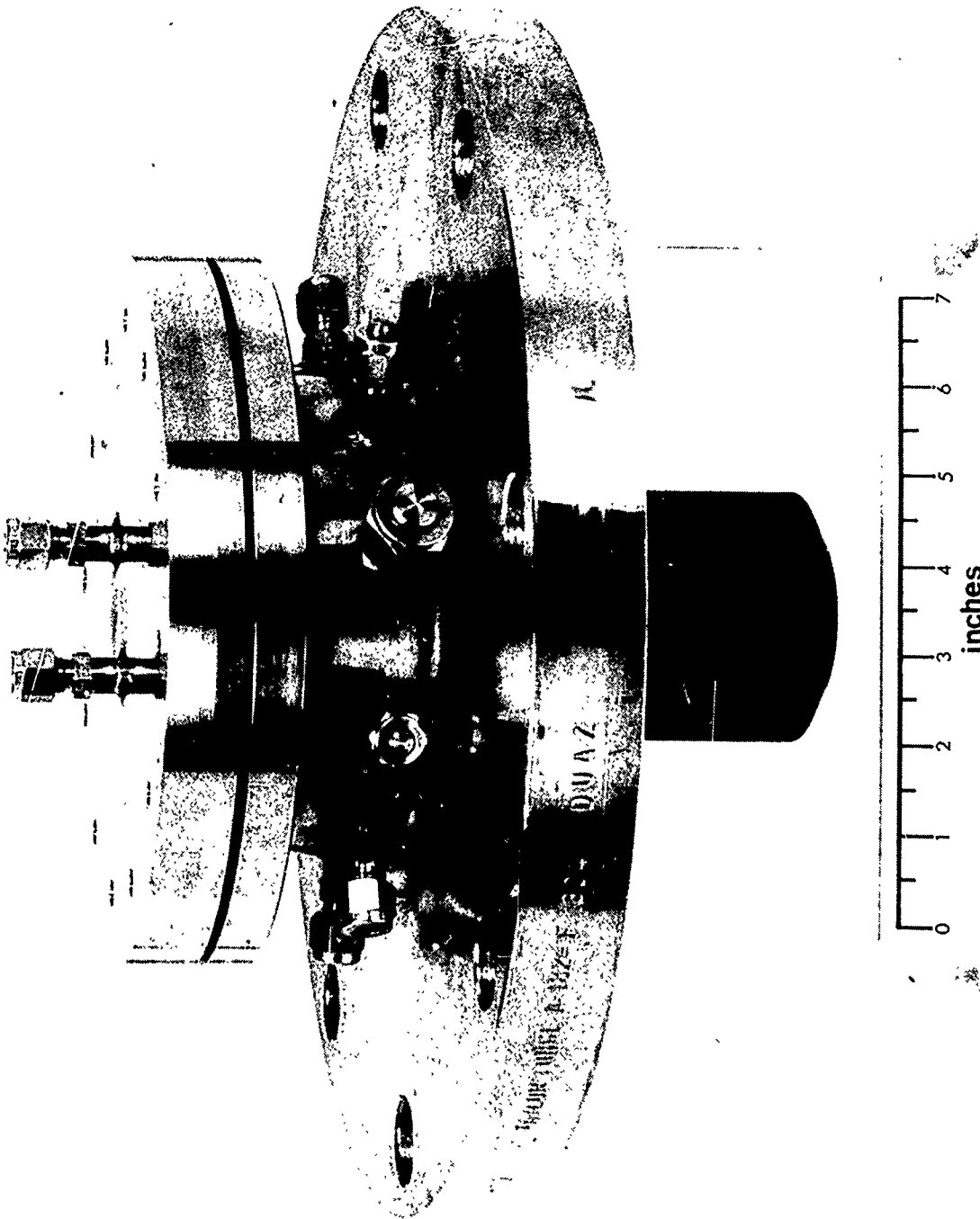


Figure 14

EXTERNAL VIEW OF SINGLE OR DUAL CHAMBER GAS GENERATOR

R-25,497
Neg. T6050-6

-30-

CONFIDENTIAL

(This Page is Unclassified)

CONFIDENTIAL

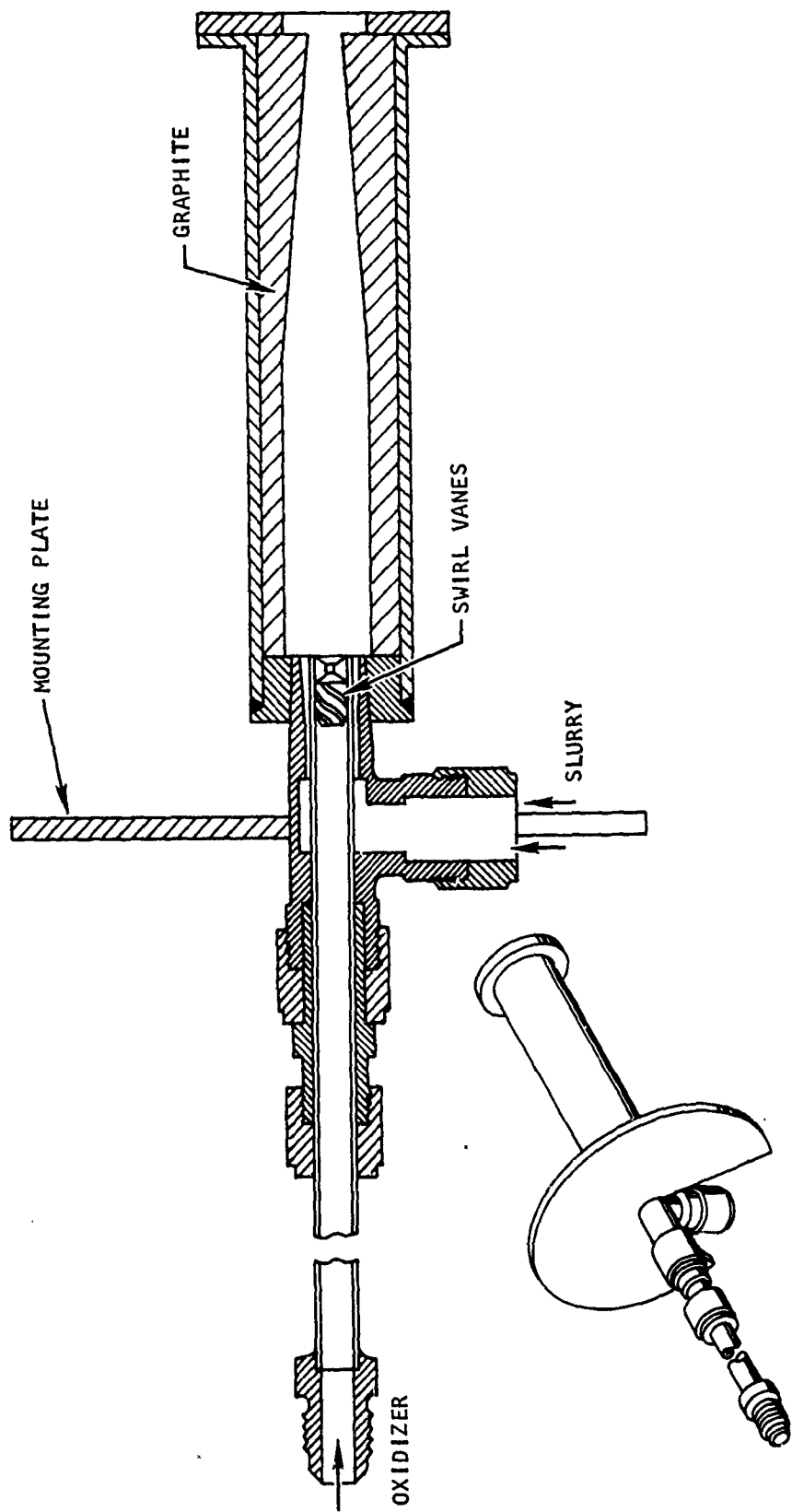


Figure 15
GAS GENERATOR CONFIGURATION WITH AXIAL INJECTION

R-26,532

CONFIDENTIAL

(This page is Unclassified)

CONFIDENTIAL

rather than a constant area throat to facilitate measurement of throat erosion.

(C) Tests conducted on the axial injection gas generator at an O/F ratio exceeding 0.3 and pressure exceeding 700 psia demonstrated that the deposit problem had been eliminated. A 30 second run at an O/F ratio of 0.1 resulted in throat erosion but no other problems. Apparently the deposition problem had been solved with the axial injection design, so no further configuration changes were made.

3. Exhaust Sampling

(U) Phase I of the experimental program was intended to characterize the exhaust products of the very fuel-rich, boron slurry/CTF gas generator. The principle characteristics of the exhaust streams which were of interest are those which would effect the combustibility of the exhaust constituents in air. The combustibility of the exhaust is a function of the exhaust gas composition and temperature, exhaust solids composition, particle size, and distribution of the combustible solids across the exhaust jet. Consequently, it was desirable that each of these quantities be measured. The exhaust sampling set up in Cell M1-A is shown in Figure 16.

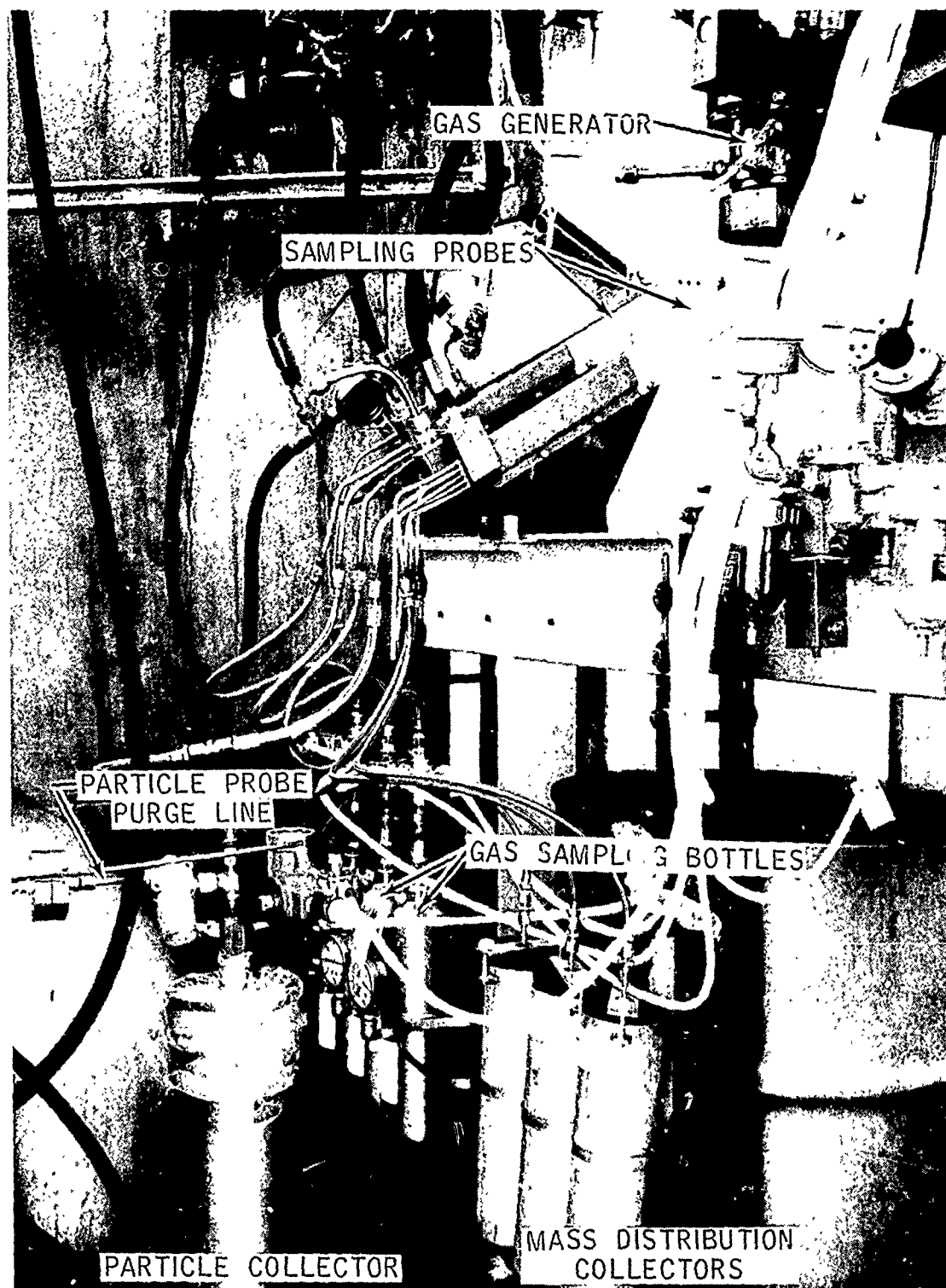
(U) Exhaust products sampling was done during some of the early gas generator runs. However, when emphasis was placed upon developing a generator for Phase II, sampling was discontinued.

a. Sampling Procedure

(U) A total of four probes, including a thermocouple probe were needed to obtain the proposed exhaust sampling data. As the dimensions of each probe preclude simultaneous sampling by two or more probes in the 1.2-inch diameter nozzle exit corresponding to a chamber pressure of 200 psia, sequential samples were taken during a run. This was accomplished by horizontal translation of the probes so as to position each in turn in the exhaust stream after the gas generator had reached steady state operation. An air-driven linear actuator (Miller Air Motor) and ratchet arrangement was employed to translate the array of probes. The sample collection probes are shown in Figure 17 for the initial position of the probes at the start of a test with the thermocouple probe located in the exhaust stream. Each stroke of the piston subsequently introduced a different probe into the exhaust stream, until at test termination, the last probe had been moved out of the exhaust.

CONFIDENTIAL

UNCLASSIFIED



EXHAUST SAMPLING SETUP IN CELL M1-A

R-25,353
Neg. T6050-4

-33-

UNCLASSIFIED

Figure 16

UNCLASSIFIED

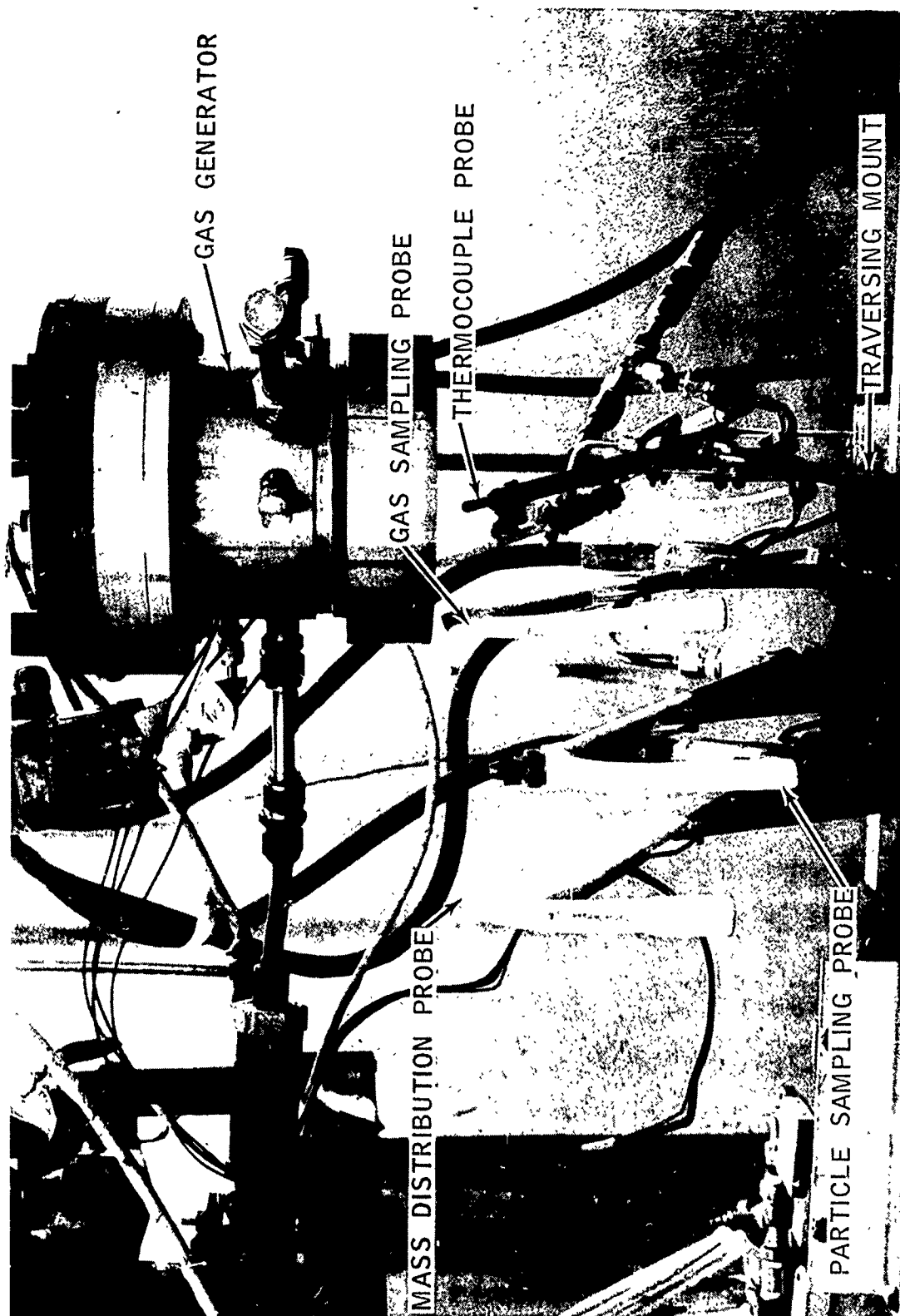


Figure 17

GAS GENERATOR WITH SAMPLING PROBES INSTALLED IN CELL M1-A

25,352
1. T6050-2

-34-

UNCLASSIFIED

UNCLASSIFIED

(U) The sampling probes were connected to the collectors by means of teflon-lined, flexible hoses. The cooling water lines for the probes were also flexible so as to permit free movement of the traversing mount. A constant period timer located on the stand initiated the air motor driving stroke at equal preset intervals. The particle probe operation governed the minimum interval which could be utilized, for it involved the sequential operation of the two valves, one of which shut off the probe purge water, while the other opened the flow passage into the collector. As the time required for valve operation was one second and for translating a probe into position was one second, the minimum interval setting for the timer for one-second samplings became 3 seconds. The run duration must therefore be in excess of 12 seconds in order to complete all samplings (temperature, particle, gas, and mass distribution). All sampling probes were coated with a protective layer of Rokide to resist the high temperature exhaust.

b. Particle Sampling

(U) A water cooled solids sampling probe, controlled by a water purge system, was employed to obtain samples of exhaust solids as schematically shown in Figure 18. This probe utilized an impingement-type collector assembly consisting of a convex-shaped impingement plate submerged beneath a quenching, damping liquid. This liquid in the collector was agitated by the exhaust sample from the probe and suppressed by damping screens to prevent splashing. The damping action of the liquid tends to protect particles from shattering. The particle collection was prepared for physical and chemical analysis by emptying and washing the contents of the impingement collector through a Millipore-type filter and drying.

(U) The probe design for particle sampling is illustrated in Figure 19. The probe tip and body were internally water cooled. Two kinds of probe tips were provided, one of 310 SS and the other of Berylco 10, to provide a backup in the event that a durability problem arose. The probe tip was designed for swallowing of the normal shock in order to provide true particle sampling, uninfluenced by flow effects tending to favor capture of the larger particles.

(U) A low flow rate of ultra clean purge water was maintained through the particle probe until initiation of the sampling interval, when the water flow was terminated and that remaining in the probe was injected into the particle collector ahead of the sample of exhaust products. The

UNCLASSIFIED

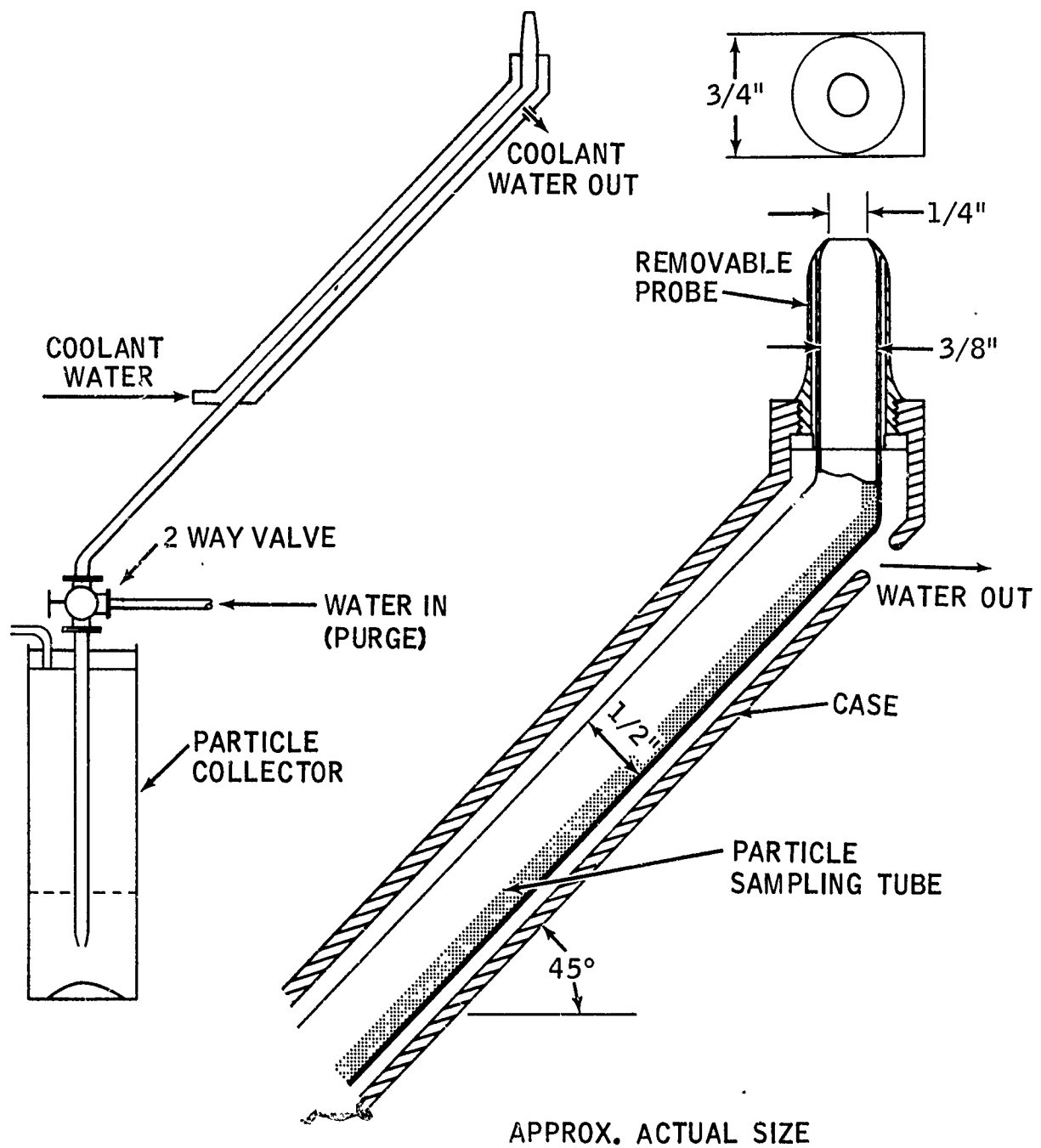


Figure 18
PARTICLE SAMPLER

R-23,562

UNCLASSIFIED

UNCLASSIFIED

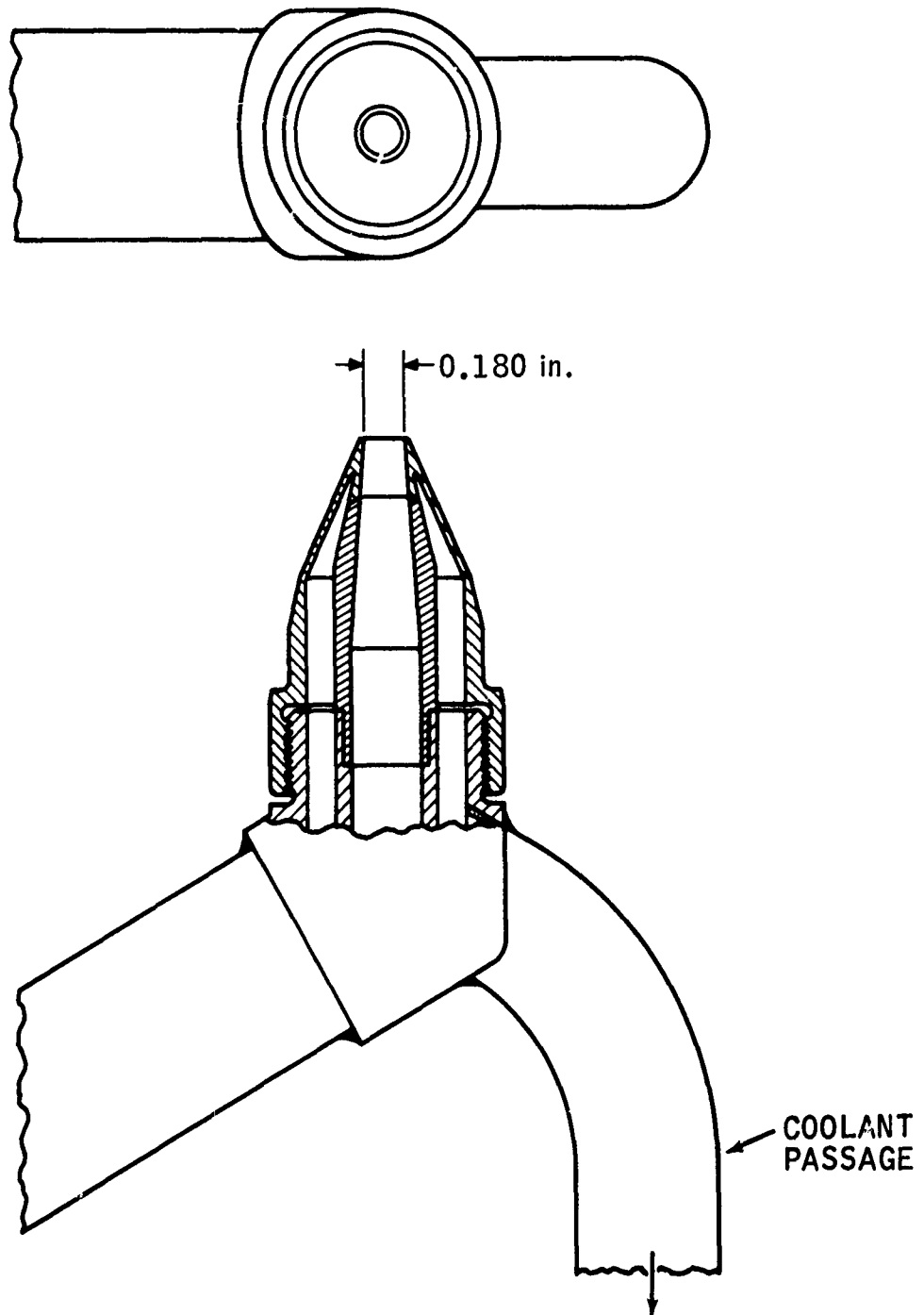


Figure 19
PARTICLE SAMPLING PROBE TIP CONFIGURATION

R-25,138

-37-

UNCLASSIFIED

UNCLASSIFIED

exhaust gases, which were not collected in the particle probe system, escaped through the Millipore filter located near the top of the collector vessel. The particles that were collected were taken to the TMC Chemistry Laboratory and analyzed by several methods. These methods and the results of the analysis are discussed later under Section IV.C.2.

c. Gas Sampling

(U) The gas sampling assembly consisted of an outer case within which were three separate gas extracting lines, all cooled by flowing water. This allowed for three individual sampling positions across the exhaust flow in a horizontal plane. The gas sampling tube inlets were positioned normal to the direction of flow to minimize particulate contamination. The design for the gas sampling probe is illustrated in Figure 20. The sample gases were captured by use of evacuated 1.6 liter stainless sampling bottles. Sample capture occurred when the solenoid valve, connecting the probe to the evacuated sample bottle was opened. Following the test the gas sampling bottles were disconnected and sent to Marquardt's Newport Beach Laboratory for gas sample analysis.

d. Mass Distribution

(U) The mass flow distribution of solids across the nozzle exhaust plane was determined by an arrangement of three sampling tubes (also two dummy tubes), each of which was attached to a collector containing water. The solid content of each bottle, after sampling, was determined by filtration and weighing. A schematic of the mass distribution probe and sample bottles is shown in Figure 21. The five water-cooled probes spanned the exhaust stream and sampled the distribution of solids from the exhaust axis to the outer edge of the plume. The outer two ports (dummy tubes) were used only to eliminate the influence of probe end effect upon sampling and were not utilized for sampling. Sampling took place for the entire period the probe was in the exhaust stream.

e. Temperature Measurement

(U) A high temperature aspirated thermocouple was located in the first position of the sampling probe array in order to determine the exhaust temperature and its rate of rise during the first three seconds of the run. The probe was oriented with its aperture facing downstream to

UNCLASSIFIED

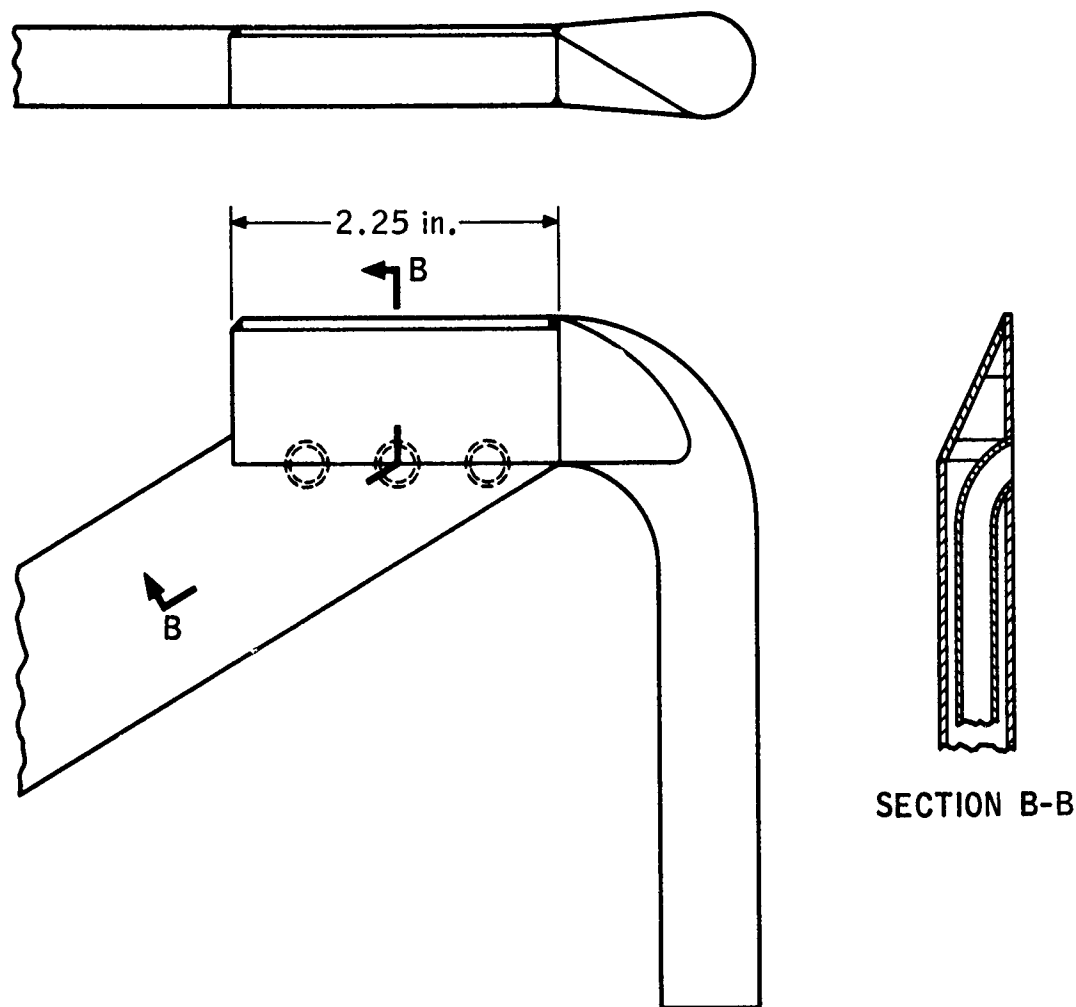


Figure 20
GAS SAMPLING PROBE

R-25,140

UNCLASSIFIED

UNCLASSIFIED

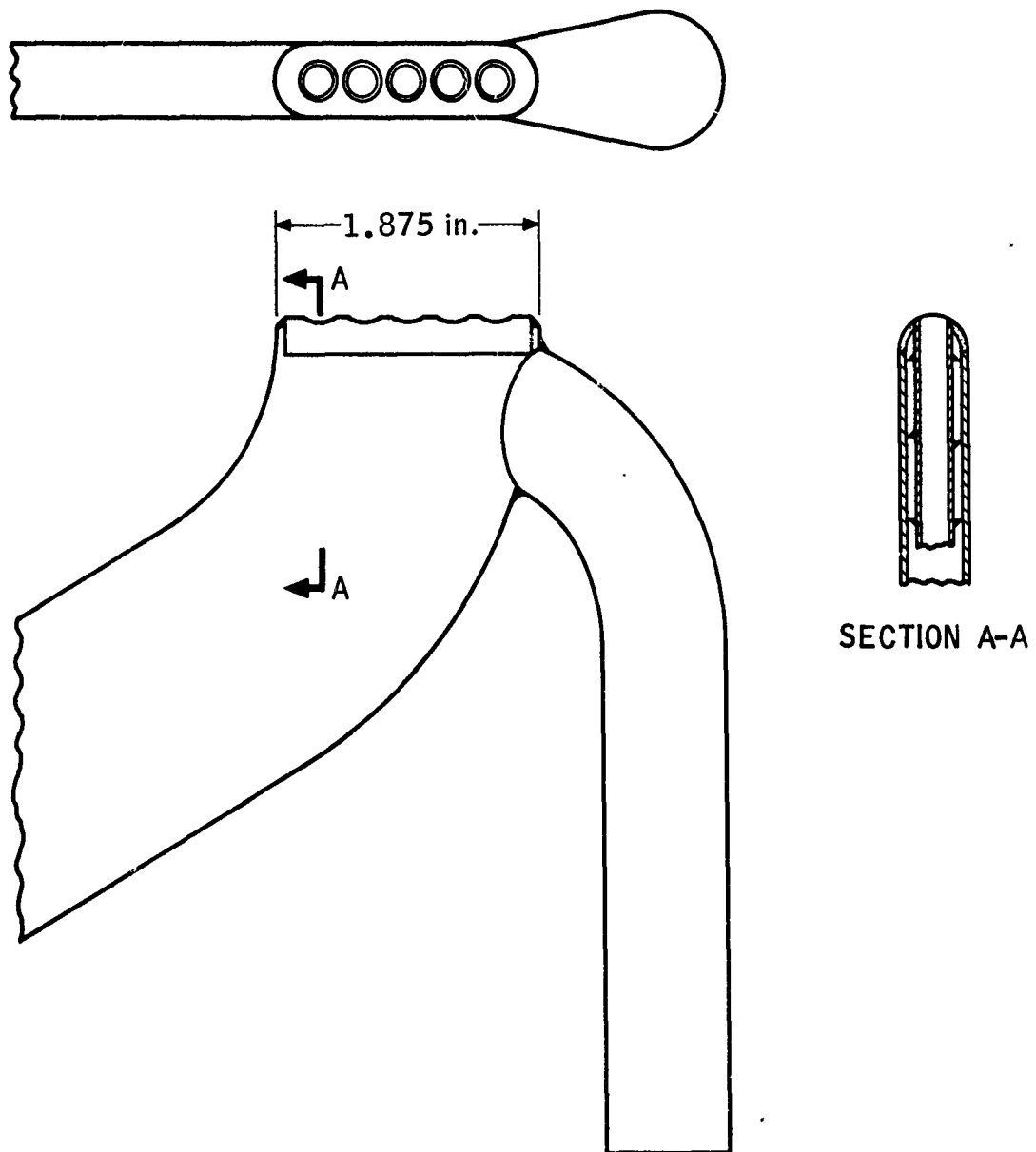


Figure 21
SOLIDS MASS DISTRIBUTION SAMPLING PROBE

R-25,139

-40-

UNCLASSIFIED

UNCLASSIFIED

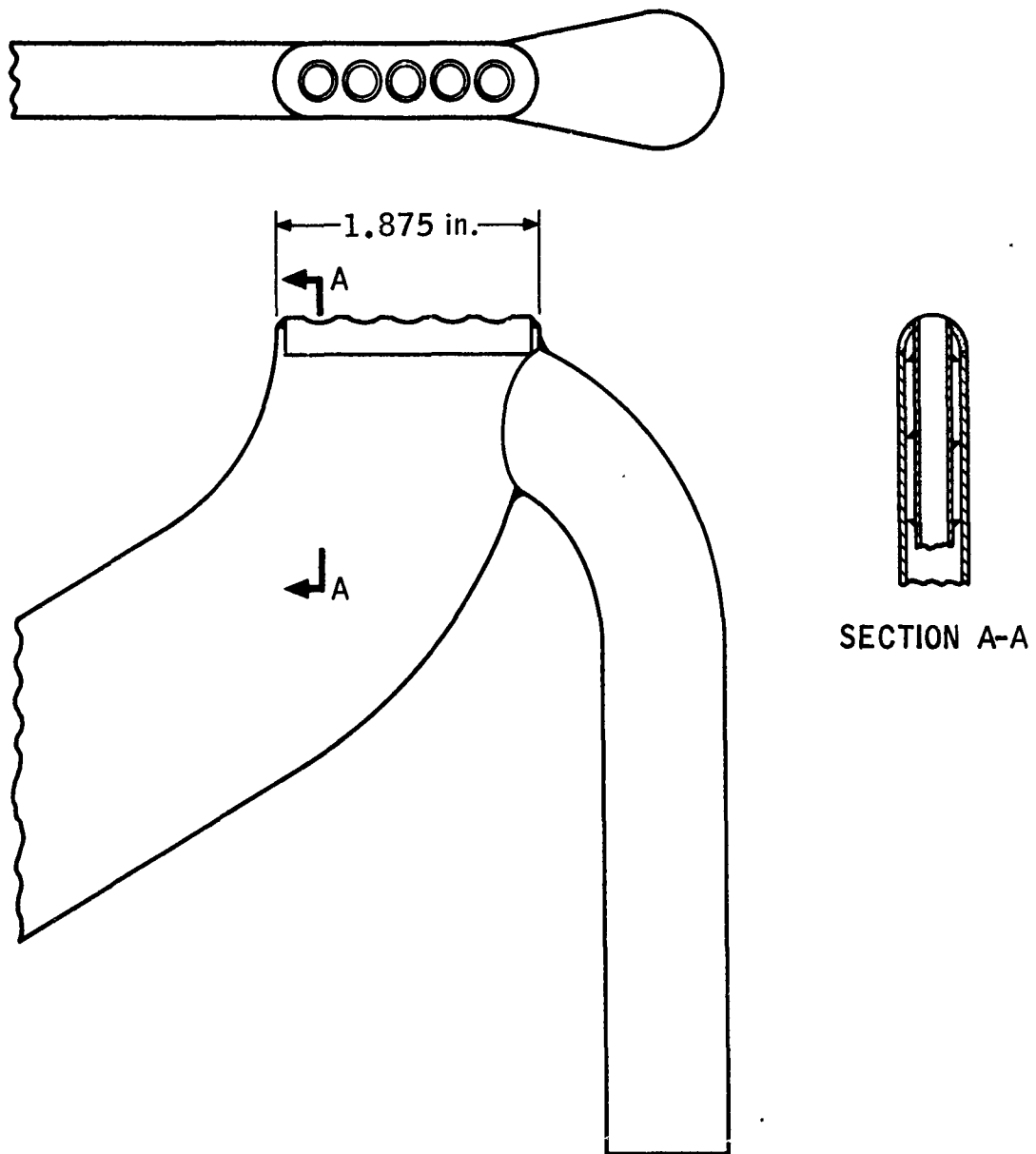


Figure 21
SOLIDS MASS DISTRIBUTION SAMPLING PROBE

R-25,139

-40-

UNCLASSIFIED

UNCLASSIFIED

minimize ingestion of exhaust particles, which could plug the internal passages. Such orientation was permissible since the manufacturer had indicated that this probe was not very sensitive to angle of orientation.

(U) Although this probe could normally withstand temperatures of 2900°F, it proved inadequate for the environment of the gas generator exhaust. During the first sampling run (No. 3) it indicated a temperature of 1500°F before burnthrough of the probe tip. A second attempt to measure exhaust temperature in the following run resulted in a break-off of the probe tip and provided no temperature data. The possible presence of quantities of CTF in the exhaust, particularly during ignition, may have contributed to these failures.

4. Instrumentation and Control

(U) A schematic diagram of the gas generator plumbing and instrumentation arrangement is shown in Figure 22. To provide the necessary data for evaluation of the performance of the gas generator, the following measurements were obtained from pressure, thrust, temperature and flow rate transducers:

<u>Parameter</u>	<u>Identification</u>	<u>Range</u>
Thrust	F - lbs	0 - 600
Combustion chamber pressure	P _c - psia	amb - 1500
Precombustion chamber pressure	P _{Pc} - psia	amb - 1500
Combustion chamber temperature	T _c - °F	amb - 3500
Oxidizer flow rate	W _{ox} - pps	0 - 1.1
Fuel flow rate	W _f - pps	0 - 8.6
Exhaust temperature	T _E - °F	amb - 3500
Oxidizer tank pressure	P _{T_O} - psia	500 - 1600
Fuel tank pressure	P _{T_F} - psia	700 - 2000

(U) The instrumentation used during the gas generator tests and the air augmentation tests was essentially the same. Pressures were measured by strain gage type pressure transducers manufactured by Taber, Inc. Simulated calibrations were provided prior to each run by using the shunt resistor technique.

UNCLASSIFIED

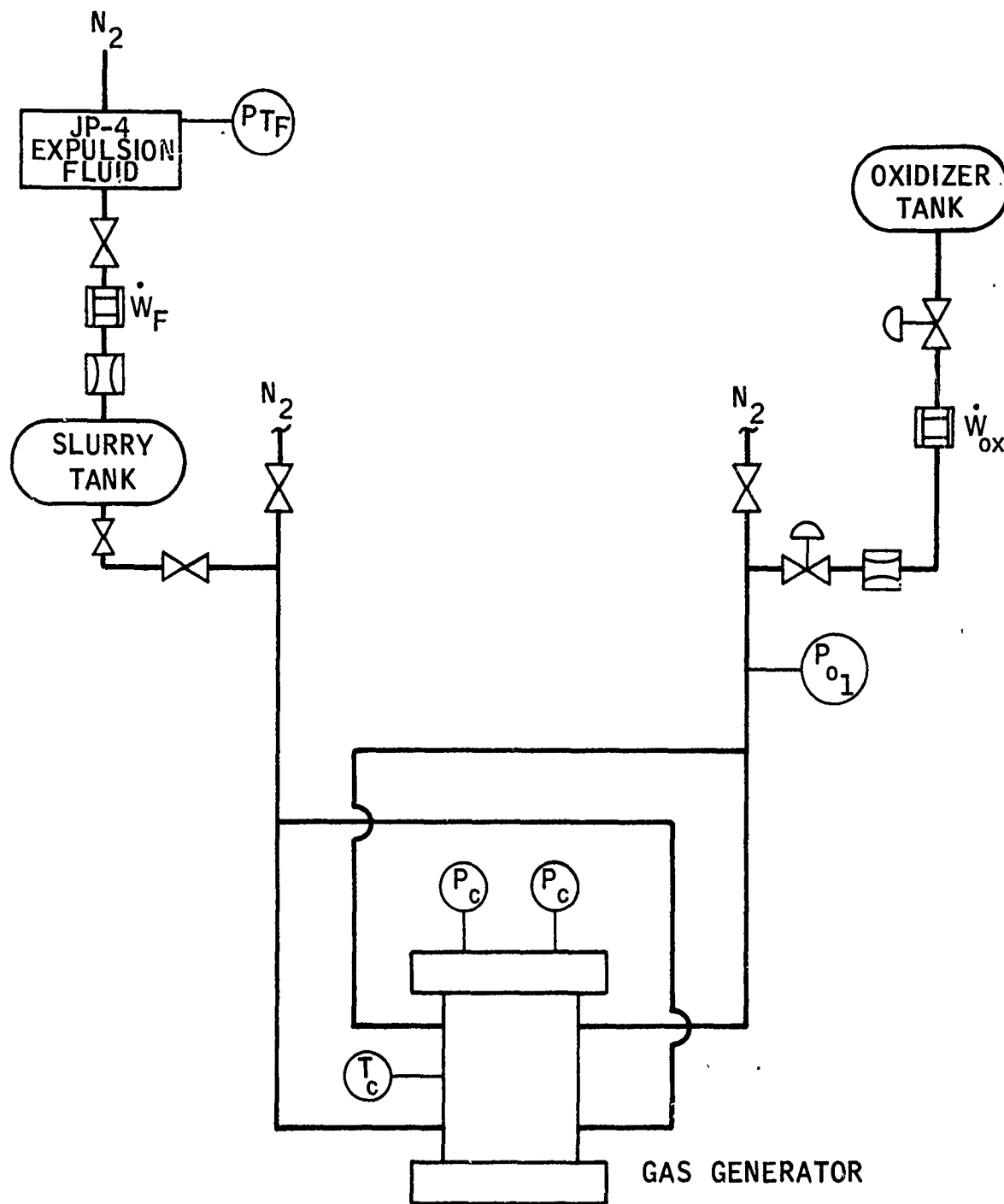


Figure 22
BIPROPELLANT GAS GENERATOR
PLUMBING AND INSTRUMENTATION SCHEMATIC

-42-

UNCLASSIFIED

UNCLASSIFIED

(U) The external exhaust-mounted thermocouple probe shown in Figure 17 was iridium-60% rhodium/iridium, positioned such that the immersed sensing head was facing downstream. The thermocouple was an aspirating type with a portion of its body water cooled. The gases were drawn over the shielded thermocouple by a facility-supplied air ejector providing a vacuum of 8 psia or lower

(U) Turbine-type flowmeters (Cox, Potter and Waugh) were used to measure liquid flow rates. A sonic venturi was used to determine air flow rates.

(U) Thrust was measured with a Kulite-Bytrex Load Cell, Model JP-20,000. Calibration was provided by using a pneumatic system to provide a compression action on the system. A Revere system was used as a transfer standard for the thrust calibration.

(U) A 36 channel Consolidated Electrodynamics Corporation (CEC) oscillograph was used for continuous recordings and for "quick-look" data. A Systems Engineering Lab (SEL) digital data recording system was used for steady state data recording. Data were sampled and digitized at a 3,750 sample/second rate and recorded on magnetic tape. The tape was processed on the TMC IBM 360 computer for raw data listings and for some data calculations.

(U) The oxidizer flow was controlled from a 30-gallon run tank pressurized with nitrogen to a maximum operating pressure of 1600 psia. A turbine flowmeter was used to manually regulate the oxidizer flow to the selected value for each run.

(U) The boron slurry fuel was controlled from a 7.5-gallon piston accumulator-type run tank using a similar tank for the JP-4 expulsion fluid. The expulsion fluid tank was pressurized with nitrogen to a maximum operating pressure of 2000 psia. Appendix B discusses the properties and handling characteristics of MARNAF 731.

(U) A turbine flowmeter was used in the JP-4 expulsion line to manually regulate the boron slurry flow for each run. All propellant lines were purged with nitrogen before and after each run.

D. TEST DEMONSTRATION

(U) The Phase I gas generator test demonstration program was designed to accomplish the following objectives: (1) Evaluate the operation of at

UNCLASSIFIED

least two configurations for a bipropellant gas generator and make measurements of the exhaust for a variety of test conditions and, subsequently, determine the exhaust stream characteristics; based upon comparative performance, select the configuration best suited for air augmentation applications; (2) Demonstrate the capability of the gas generator to operate for durations up to 150 seconds at operating conditions suitable for application to air augmentation.

(U) Initially it was believed that one of the two original configurations would permit fulfillment of these objectives. However, as the test program got underway it became necessary to deviate somewhat from the planned schedule. As a result of the first series of runs on the turbulator and spiral swirl configurations (Figures 8 and 9), it became evident that neither of these configurations would accomplish the 150 second duration requirement because of solids deposition within the combustion chamber. A modification of the turbulator configuration (Figure 11) was then evaluated and provided some promise that it would perform satisfactorily for 150 seconds under certain conditions. However, after completing eleven tests, it was mutually agreed between TMC and the Air Force monitoring agency to scale down the gas generator test item to be compatible with a 7-inch diameter afterburner. To match the scaled down flow rates a Dual Chamber Impinging Jet subsonic exhaust configuration (Figure 12) was agreed upon with a Single Chamber Impinging Jet subsonic exhaust configuration (Figure 13) as backup. These configurations were evaluated in Runs 10 through 18. A final configuration, the Axial Injection (Figure 15), was then evaluated in Runs 19 and 20 prior to commencing the Phase II Air Augmentation tests. These test runs are summarized in Table I. Discussion of each of the runs is provided in the following paragraphs.

1. Run Summary

- a. Runs 1 and 2

(U) Before installation of the sampling rig, two short 2-3 second runs of the turbulator gas generator were made to determine the mode of operation and the flow rates necessary to achieve the desired chamber pressures. These runs indicated that the thermodynamic equilibrium performance was not achieved and performance corresponded more closely to a condition where half of the TMH present in the slurry was assumed to vaporize rather than to decompose. In these preliminary runs the chamber pressure was less than 100 psia. No buildup of deposits in the chamber was observed

*Trimethylhexane (See Appendix B) -44-

UNCLASSIFIED

CONFIDENTIAL

TABLE I
GAS GENERATOR TEST RESULTS

Run	Config.	O/F	P psia	\dot{W}_p lb/sec	Duration sec	Remarks
1	Turbulator	0.039	72	2.93	1.0	Checkout run.
2	"	0.107	78	1.19	3.0	Checkout run.
3	"	0.113	205	1.84	13.0	Heavy deposits in turbulator end.
4	"	0.537	216	0.77	14.0	Heavy deposits throughout engine.
5	Modified Turbulator	0.104	179	1.93	14.0	No deposits.
6	Spiral	0.097	168	1.94	3+	Premature shutdown--loaded with slurry. 410 lb thrust achieved.
7	Modified Turbulator	0.413	156	0.90	8.0	No deposits.
8	"	0.47	800	3.48	8.0	Deposits in nozzle entrance region.
9	Spiral	0.099	-	5.61	2+	Nozzle plugged due to graphite vane failure.
10	Dual Chamber	0.103	174 202	0.204	8.6	Some deposits in one chamber. High ignition peak.
11	"	0.556	178 194	0.084	8.2	Deposits in both chamber. High ignition peak.
12	"	0.099	400 420	0.591	8.0	Pressure was low due to throat erosion during Run 11. No deposits occurred in either chamber. Pressure taps remained open during entire run without purging.
13	"	0.486	-	0.415	1.1	Oxidizer line burned through. Slurry flow continued for 7.5 seconds but no deposits built up in either chamber. (Same chamber was used for Runs 10-13).

CONFIDENTIAL

CONFIDENTIAL

TABLE I
(Continued)

Run	Config.	O/F	P _c psia	\dot{w}_p lb/sec	Duration sec	Remarks
14	Dual Chamber	0.484	>1400	0.408	2.5	Pressure rose steadily after ignition pulse. One throat plugged, filling one chamber with slurry, and resulted in a burn-through of one oxidizer line.
15	Single	0.274	1200	0.372	4.0	One throat began plugging after 2.4 seconds. Run was stopped because of rise in pressure. One pressure tap plugged at startup.
16	"	0.271	545	0.371	6.7	Gradual pressure rise occurred at 4.7 seconds due to plugging of one throat. Run was stopped because of rise in pressure. No plugging of pressure taps.
17	Dual Chamber	0.274	635	0.365	2.4	Pressure started to increase after about one second. One throat plugged.
18	Modified Dual	0.294	315 330	0.528	4.2	One throat nearly plugged. Channel between chamber plugged.
19	Axial Injection	0.333	765	0.420	4.2	No deposits. Pressure tap plugged at 0.6 sec. Throat area increased by 7%.
20	Axial Injection	0.099	~325	0.303	30.0	Slight deposits. Throat area increased by 27%.

CONFIDENTIAL

AD 394 115

AUTHORITY:

AFRPL

Ac. 5 Feb 86



CONFIDENTIAL

The results of these runs served as a guide to determine flow requirements necessary to achieve the objective chamber pressure of 200 psia.

b. Runs 3 and 4

(U) The first sampling run was conducted at a chamber pressure of 200 psia and an O/F ratio of 0.1. The run duration was 13 seconds. Sampling proceeded normally until the end of particle sampling. A correctable malfunction then occurred in the traverse system causing the particle probe to remain in the stream for the duration of the run. Consequently, no mass distribution samples were obtained.

(U) Inspection of the chamber interior at the end of the run revealed a considerable amount of deposition on the flat graphite plate at the head end of the engine, adjacent to the turbulator chamber. These deposits were hard and brittle. There was only minor deposition in the downstream cylindrical chamber.

(U) The temperature indicated by the chamber thermocouple during this run corresponded to 1500°R, which agrees with theoretical expectations. Later in the run burn-through of the thermocouple tip occurred, apparently due to a localized oxidizer concentration which attacked the sheath material. The chamber pressure lines plugged after several seconds of running, but there was sufficient time to determine the steady state pressure level. Constancy of the thrust output indicated no change in operating conditions after plugging of the pressure lines.

(U) A second sampling run was conducted at the nominal conditions of 200 psia chamber pressure and an O/F ratio of 0.5. Again high combustion efficiency was achieved. During this run the tip of the exhaust thermocouple sheath was broken off through unknown causes. Again no mass distribution samples were obtained, although the probes had traversed their full distance at the end of the run. Poor visibility due to fog prohibited visual observation of this run over closed circuit television. Consequently, the cause of the sampling failure was not evident.

(U) Examination of the chamber after the run revealed the presence of hard deposits which were more extensive than those produced at an O/F ratio of 0.1. Deposition occurred in the cylindrical chamber as well as against the head-end wall.

CONFIDENTIAL

(This page is Unclassified)

CONFIDENTIAL

The results of these runs served as a guide to determine flow requirements necessary to achieve the objective chamber pressure of 200 psia.

b. Runs 3 and 4

(U) The first sampling run was conducted at a chamber pressure of 200 psia and an O/F ratio of 0.1. The run duration was 13 seconds. Sampling proceeded normally until the end of particle sampling. A correctable malfunction then occurred in the traverse system causing the particle probe to remain in the stream for the duration of the run. Consequently, no mass distribution samples were obtained.

(U) Inspection of the chamber interior at the end of the run revealed a considerable amount of deposition on the flat graphite plate at the head end of the engine, adjacent to the turbulator chamber. These deposits were hard and brittle. There was only minor deposition in the downstream cylindrical chamber.

(U) The temperature indicated by the chamber thermocouple during this run corresponded to 1500°R, which agrees with theoretical expectations. Later in the run burn-through of the thermocouple tip occurred, apparently due to a localized oxidizer concentration which attacked the sheath material. The chamber pressure lines plugged after several seconds of running, but there was sufficient time to determine the steady state pressure level. Constancy of the thrust output indicated no change in operating conditions after plugging of the pressure lines.

(U) A second sampling run was conducted at the nominal conditions of 200 psia chamber pressure and an O/F ratio of 0.5. Again high combustion efficiency was achieved. During this run the tip of the exhaust thermocouple sheath was broken off through unknown causes. Again no mass distribution samples were obtained, although the probes had traversed their full distance at the end of the run. Poor visibility due to fog prohibited visual observation of this run over closed circuit television. Consequently, the cause of the sampling failure was not evident.

(U) Examination of the chamber after the run revealed the presence of hard deposits which were more extensive than those produced at an O/F ratio of 0.1. Deposition occurred in the cylindrical chamber as well as against the head-end wall.

CONFIDENTIAL

(This page is Unclassified)

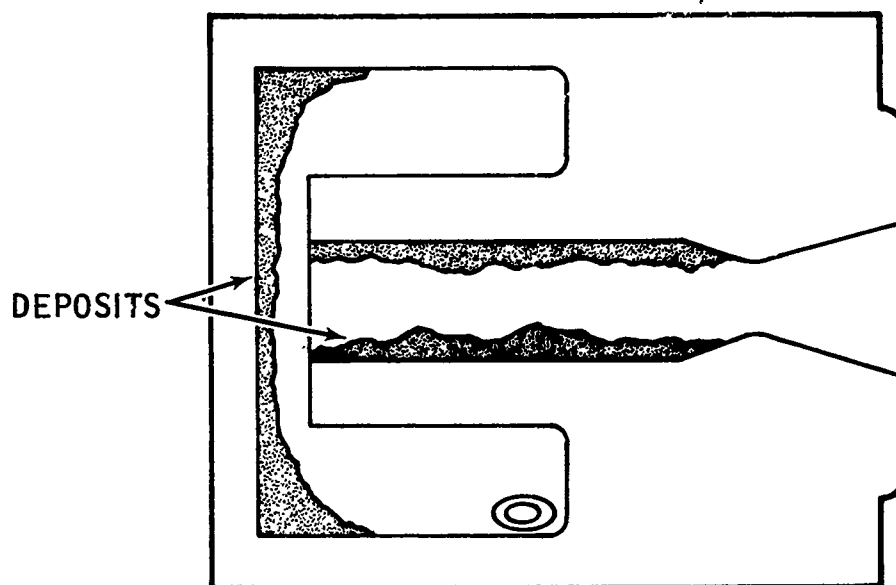
CONFIDENTIAL

c. Runs 5 through 9

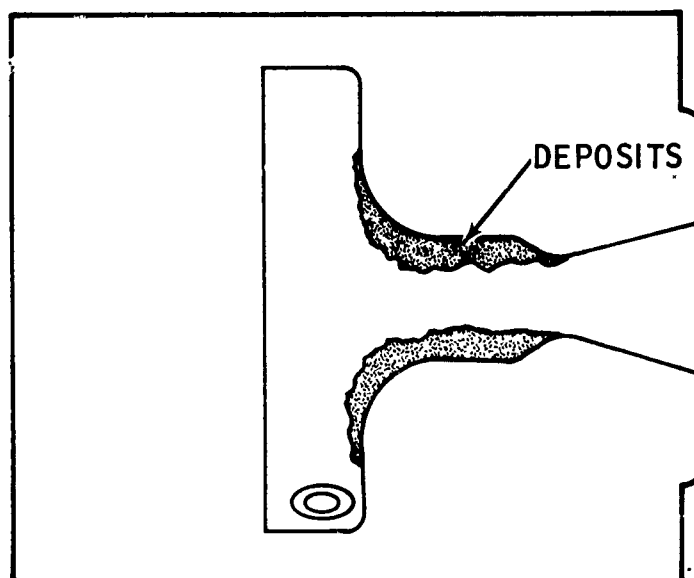
(C) Following the two runs with the turbulator chamber in which heavy chamber deposits were formed (Runs 3 and 4), the chamber was redesigned to eliminate the 180 degree change in flow direction at the head end. The resulting design, called the Modified Turbulator, is illustrated in Figure 11. The design was tested in Run 5. No deposits were found after a run of 13 seconds. The same gas generator was tested again in Run 7 at a high O/F ratio. Once again no deposits were formed. The final test of this design, Run 8, was run at a high pressure condition, where deposit buildup should be enhanced because of the greater density of solids in the chamber. Deposition did occur in the throat entrance section in this run of 8 seconds. A comparison of the deposits which occurred in Run 4, employing the Turbulator configuration with those in the Modified Turbulator is shown schematically in Figure 23. Both runs were made at an O/F ratio exceeding 0.4, but deposition occurred only at high pressure in the Modified Turbulator and not at the 200 psia level of the Turbulator test. Aside from pressure level (flow rate), Run 8 differed from Run 7 in that oxidizer injection velocity was lower. The good combustion efficiency achieved in Run 8, as evidenced by the high thrust and pressure levels, implies that the higher oxidizer injection velocity and consequent better mixing led to high temperature in the chamber with resultant deposition at the nozzle entrance. A reduction in oxidizer velocity may eliminate the deposition at the expense of a reduced combustion efficiency. A reduced efficiency was acceptable, as it would not adversely affect utilization of the gas generator for air augmentation.

(U) In the majority of runs plugging of the chamber pressure tap during the run by particles of boron and other solids resulted in loss of the pressure level beyond the time of plugging. Nevertheless, in Run No. 8 the oxidizer injection pressure provided a clear indication of the effect of deposit buildup in the throat section even though the chamber pressure tap was plugged. The oxidizer pressure exhibited a rise of several hundred lb/sq in. approximately midway through the run, indicating nozzle throat area reduction. The pressure remained at the higher level with little variation throughout the remainder of the run. One could therefore infer that deposition in the throat section had stabilized.

CONFIDENTIAL



A. TURBULATOR CONFIGURATION



B. MODIFIED TURBULATOR CONFIGURATION

Figure 23

LOCATION OF DEPOSITS IN GAS GENERATOR CHAMBERS

R-25,384

-49-

CONFIDENTIAL

CONFIDENTIAL

(C) Runs 6 and 9 were tests of the Spiral Swirl design shown in Figure 9. Run 6 was prematurely shut down by the test observer, as the dark appearance of the exhaust did not indicate that combustion was occurring. Due to a lag in slurry shut-off when the observer terminates the test, raw slurry plugged the engine passages and was forced into the oxidizer injector, causing rupture of the oxidizer injector line. After disassembly the spiral passage was found to be completely filled with dried slurry. No evidence was found of the hard deposits obtained in the turbulator design, however, the run time may not have been sufficient for deposit formation. Run 9 was intended to be a high pressure run at the 600 psia level. At initiation of the test however, the end tip of the spiral vane chipped off and partially plugged the nozzle. The resulting increase in pressure within the chamber stopped oxidizer flow and again forced slurry into the oxidizer line, which resulted in burn-through of the line at the injector and termination of the test.

(C) The tests of the Turbulator configuration had demonstrated a tendency for deposits to form, especially in the stagnant region at the head end of the chamber. The elimination of the low velocity region in the Modified Turbulator solved much of the deposition problem. Deposits were still formed in the nozzle entrance section for simultaneous high pressure and high O/F ratio. This deposition could result from the more rapid mixing of fuel and oxidizer, as implied from the higher oxidizer injection velocity compared to previous runs. Although the tendency for formation of deposits in the Spiral Swirl remained unproven due to insufficient run times, other factors, such as the difficulty of inspection for deposits and of disassembly after testing, as well as the fact that it is less compact than other designs tended to make the Spiral Swirl less desirable as the choice for future testing. Consequently, the Modified Turbulator appeared to be the most suitable candidate for use in the remainder of the test program, as it performed satisfactorily in the low pressure range and the problem of some deposition at high pressures appeared solvable.

d. Runs 10 through 18

(U) The remaining tests basically differed from those performed earlier with respect to the scale of the combustor and the type of exhaust

CONFIDENTIAL

CONFIDENTIAL

flow. The propellant flow rate through each nozzle of the dual chamber design was approximately one-twentieth the flow rate for corresponding conditions of pressure and O/F ratio in the first nine tests, and the exhaust flow was subsonic rather than supersonic. The reduction in scale could enhance any effects of nozzle plugging due to deposits or nozzle throat erosion. The time required to reach steady state conditions during a run could also be increased because of the greater surface-to-volume ratio resulting from the increased L^* of the reduced scale chamber. The advantage of subsonic exhaust flow, for a gas generator to be utilized in air augmentation, was the high static temperature of the exhaust compared to that of the supersonic streams used in some systems, with the consequent greater ease of ignition of the exhaust products in air.

(U) In order to provide simultaneous arrival in the chamber of the oxidizer and fuel streams, a long oxidizer lead was indicated, as required by the time for filling the oxidizer line after valve opening. For the very low flow rates involved in Run 10, the oxidizer lead was 2.15 sec. For Run 11 it was 1.15 sec. The commencement of slurry flow in both of these runs was accompanied by a high amplitude pressure pulse which exceeded 1000 psia. The pulse may have resulted from condensation of CTF on the interior walls of the chamber before initiation of slurry flow, thereby providing at initial injection of the slurry an instantaneous O/F ratio far in excess of the steady state value during the run. Subsequent tests indicated that the ignition pulse could be eliminated by employing a minimal CTF lead.

(U) Previous tests of the boron slurry/CTF gas generators had generally been accompanied by plugging of the chamber pressure taps by unburned boron with the attendant loss of pressure data. In an attempt to avoid such plugging a nitrogen purge system for the pressure taps was installed. The purge system provided a low flow rate of nitrogen through the tap into the chamber during firing so as to maintain an open channel from the chamber to the pressure transducer. The nitrogen flow was regulated by an orifice and a preset supply pressure so as to provide a flow rate which was a very low percentage of the propellant flow rate. In Run 10 the nitrogen purge was employed in one of the two chambers. The purged tap remained open throughout the 8.0 second run and permitted an adequate measure of chamber

CONFIDENTIAL

(This page is Unclassified)

CONFIDENTIAL

pressure. The purge flow rate was 1.3% of the propellant flow rate into that chamber. The unpurged tap on the other chamber exhibited moderate plugging during the run. The pressure taps of both chambers were purged during Run 11 at 1.8% of the propellant flow rate for each chamber. Good pressure response was obtained from both chambers until the last half-second of the run, when one tap gave evidence of plugging. Whereas, in previous tests plugging of the pressure taps was to be expected, in nearly every run with the nitrogen purge system reliable pressure data was obtained.

(U) The primary concern in conducting the series of checkout tests of the dual chamber gas generator was the occurrence of deposits within the chamber. In Run 10 a small quantity of deposits was found in the chamber incorporating the nitrogen purge. In Run 11 a considerable amount of deposition occurred in both chambers. The coincidence between deposition and nitrogen purging suggested the possibility of an influence of the nitrogen upon combustion, either by a physical process, such as cooling or disrupting the reactants, or by a chemical process, as by forming boron nitride. In regard to the latter point, it should be noted that boron nitride does not generally result from the reaction of hot boron particles with air.

(C) The temperature measured in the subsonic exhaust tube in Run 10 corresponded to 1256°R. The theoretical value of the chamber temperature for the nonequilibrium combustion situation occurring within the gas generator should be approximately 1400°R. Therefore the efficiency of combustion is seen to be adequate to provide the desired high temperature exhaust stream.

(C) The next three tests also were run with the dual chamber, having manifolded oxidizer and fuel lines. Run 12 was satisfactory in all respects, except for the reduced pressure level which was later attributable to the increased throat area resulting from erosion on the previous runs. Good pressure data was obtained without the purge of the pressure taps previously thought necessary. Run 13 was the first attempt for a pressure level of 1000 psia. Early in the run the oxidizer venturi decavitated as an apparent result of oxidizer flow stoppage to one chamber due to a large rise in the pressure of that chamber. Slurry could then enter the oxidizer

CONFIDENTIAL

CONFIDENTIAL

line and trigger a reaction within the line upon decrease of chamber pressure and resumption of oxidizer flow. The result was a burn-through of the oxidizer line. The above assumed cause of the burn-through was not evident until Run 14, when a repetition of the run conditions resulted in an identical failure. An examination of the chamber after Run 13 revealed considerable erosion of the two sonic exit ports. Whereas the initial flow angle into the injection tube was 70 degrees, the erosion resulted in an effective angle of about 45 degrees.

(C) The single chamber design was tested in Runs 15 and 16 at moderate chamber pressure (600 psia) and moderate O/F ratio (0.3). It incorporated a triplet injector system having two oxidizer streams to provide more uniform mixing. The single chamber design avoided the problem of chamber interaction which resulted in oxidizer line failure in the previous two runs. The single chamber was found to be subject to nozzle plugging to the extent that it was unsuitable for further evaluation. Another test of the dual chamber (Run 17) was conducted at the same condition of 600 psia and $O/F = 0.3$ in order to compare performance. To avoid the earlier problem of severe chamber interaction an orifice was placed in each of the oxidizer injectors to provide an injector pressure drop of 100 psi or greater. This test also resulted in throat plugging, but the oxidizer flow remained constant, indicating that the increased injector pressure drop was effective. Run 18 utilized a modification of the dual chamber. The modified design had sonic nozzles with twice the area of those of the initial design, and incorporated an open channel connecting the two chambers. This design ran for the full scheduled duration of 4.2 sec. Post-run examination revealed that one throat was nearly completely closed by deposits, and the interconnecting channel was also filled with deposits.

e. Runs 19 and 20

(U) It became evident at this point that neither the single nor the dual chamber designs resulted in a workable gas generator. An apparent contributing factor to the deposit buildups was the low flow velocity in a chamber with circumferential injection. It was believed that a chamber having axial injection and a cross-sectional area sufficiently small to provide a moderate flow velocity, while not providing the mixing turbulence of the chambers tested to date, should be effective in eliminating deposit problems.

CONFIDENTIAL

CONFIDENTIAL

A rocket engine injector of the type required was available at TMC and was suitable for low O/F ratios.

(C) It was feasible to utilize this existing hardware by fabricating a suitable graphite chamber liner and nozzle in the manner shown in Figure 15. Runs 19 and 20 were conducted with this axial injection configuration. There were no deposits in the chamber after a 4.2 sec run at a high pressure and high O/F ratio. There was a 7% throat area increase, which was not unexpected as a result of the zero length throat design. The following run (Run 20) used a new graphite liner and tested for 30 seconds duration at a low O/F and moderate pressure. Post-run examination of the chamber revealed slight deposits in the nozzle entrance section. For this run the throat area had increased by 27 percent. The throat erosion could be diminished considerably by use of a half-inch long cylindrical throat and most likely eliminated with a silicon carbide coated throat. The performance of the axial injection design appeared to be satisfactory at the two extremes of the operating range. It was therefore concluded that no further gas generator testing was necessary and the axial injection design would be utilized in the air augmentation tests with a cylindrical throat section.

2. Exhaust Sampling

(U) Sampling of the exhaust products was attempted in Runs 3 and 4. Photographic coverage indicated that the momentum of the exhaust stream was sufficient to deflect the gas sampling probe to the periphery of the stream, which resulted in considerable ingestion of air into the sampling bottles. The weather conditions at the time of Run 4 were such that considerable moisture was present in the ingested air, making the gas sample questionable for extensive analysis.

(U) Particle sampling was successfully achieved in Run 3 but not in Run 4 because of a failure of the traversing mount to move the probe into position on the second cycle of the air motor.

(U) Mass distribution sampling was unsuccessful in Run 3 because of a traversing mount malfunction after particle sampling and in Run 4 because of the one cycle delay mentioned above which resulted in movement of the probe into position after engine shutdown.

CONFIDENTIAL

a. Analyses of Solid Samples

(C) To analyze and interpret the solid particles that were sampled or to interpret analysis of solid deposits in the engine, it was necessary to determine the character of the solids in the MARNAF 731 fuel that was being used. Two batches were used during the test runs of interest. The two batches designated -71 and -72 were certified as having the following measured values of boron content, density and viscosity:

	<u>TMH-71-73</u>	<u>TMH-72-73</u>
Boron Content	72.6%	72.7%
Density	1.466 g/cc	1.469 g/cc
Viscosity at 1000 sec ⁻¹	12 poise	13.5 poise

(U) The boron content of the total fuel is composed of the below-listed lots of The American Potash and Chemical Company (Trona) 90-92% pure, commercial amorphous boron in the following weight percentages:

Lot #199	12.32%	(made 8/7/67)
Lot #203	46.32	(made 8/9/67)
Lot #206	27.60	(made 8/11/67)
Lot #207	11.58	(made 8/14/67)
Lot #208	2.18	(made 8/14/67)

(U) As an expedient, a sample of boron was made up of the above lots of boron in their stated proportions for reference and for analysis as required; and this sample is referred to as "5-Combo boron". An analysis of the "5-Combo boron" sample is given below, on the basis of values as listed in certificates of analysis (furnished by Ampot for each lot of boron), weighted in the proportions of use in the said sample.

Amorphous Boron, Net	91.0% (by weight)
Water-Soluble Boron	0.25
Magnesium	5.1
Insoluble in H ₂ O ₂	0.35
Moisture and Volatile	0.21
Average Particle Size	0.8 microns

(U) The assay values for the five lots of boron show little variation, one from the other. For instance, the net boron content varied from 90.7% for Lots 206 and 207 to 91.3% for Lot 208. After slurry fuel

CONFIDENTIAL

preparation, check values of the " H_2O_2 -insoluble" and "water soluble boron" contents of "5-Combo boron" were 0.4% and 0.3%, respectively. Amounts of these impurities are known to increase sensitivity-with-handling of boron.

(U) Spectrographic analysis results for "5-Combo boron" and for boron slurries, TMH-71-73 and TMH-72-73, are listed in Table II. The increase in aluminum content of the fuels, in comparison to that of the boron, is due to the slurry fuel processing.

TABLE II
SPECTROGRAPHIC ANALYSIS OF BORON AND SLURRIES

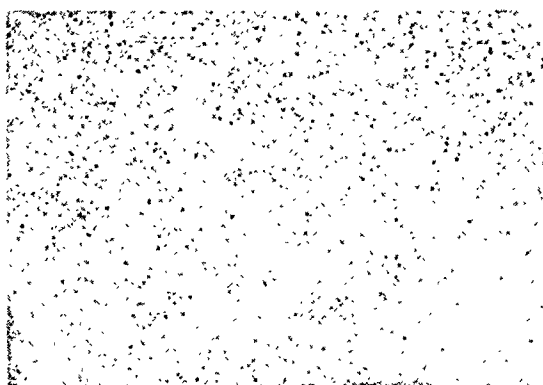
Element	5-Combo Boron	TMH-71-73	TMH-72-73
B	Matrix	Matrix	Matrix
Si	0.17	0.15	0.17
Mn	0.09	0.17	0.09
Fe	0.35	0.30	0.20
Cr	0.04	0.03	0.02
Ni	0.04	0.03	0.03
Al	0.04	0.55	0.50
Ca	0.35	0.30	0.30
Ba	<0.01	0.02	0.02
Cu	0.10	0.07	0.10
Mg	5	5	5
Na	<0.03	<0.03	<0.03

Values above are in weight percent.

(U) Photomicrographs of TMH-71-73 and TMH-72-73 are shown at 600X magnification in Figure 24. The particle sizes and distributions in the photomicrographs are characteristically representative of Trona 90 to 92% pure amorphous boron.

(C) From Run 3, at $O/F = 0.1$, a sample of particles was collected by means of the particle sampler-impingement collector apparatus. After filtration of the total (impinger) aqueous suspension and after drying over P_2O_5 , the particle sample amounted to 1.24 grams of finely divided particles.

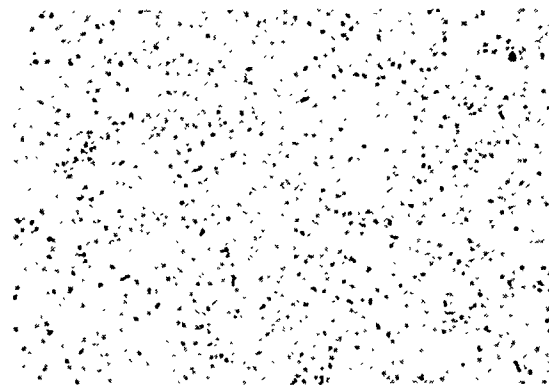
CONFIDENTIAL



Neg. 8964-2

90 X

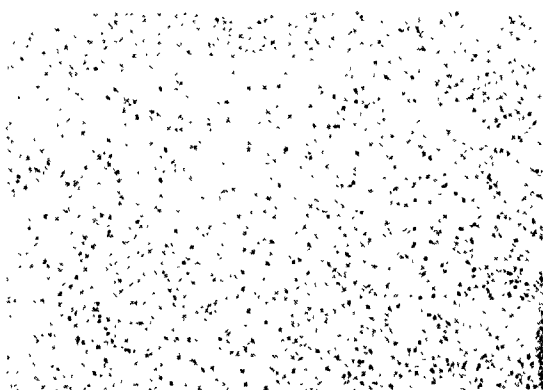
BATCH TMH-71-73



Neg. 8964-3

600 X

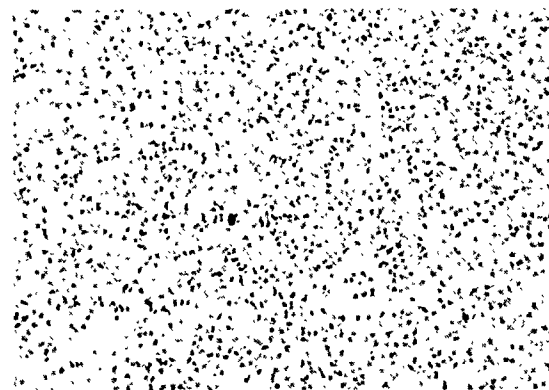
BATCH TMH-71-73



Neg. 8964-4

90 X

BATCH TMH-72-73



Neg. 8964-5

600 X

BATCH TMH-72-73

MARNAF 731 FUELS
FOR FUEL RICH LIQUID BI-PROPELLANT TESTS
RUNS #3 AND #4

(NOMINAL AVERAGE PARTICLE SIZE = 0.8 microns)

R-25,383

Figure 24

-57-

CONFIDENTIAL

(This Page is Unclassified)

CONFIDENTIAL

The (impinger) aqueous filtrate was found to have a pH of 2.65, probably due to HF and/or HCl absorption during the run. Because of the small size of the sample of particles, only a few analyses, in duplicate, were carried out, with the following results:

Total boron: 87.0 weight %
Water-soluble boron: 0.1 "
"H₂O₂-insolubles": 11.2 "
Total magnesium: 3.8 "

(C) X-ray diffraction analysis of the "H₂O₂-insoluble" residue showed a small amount of B₄C in a characteristic amorphous boron matrix. Hence, it is doubtful that the H₂O₂-insoluble residue, in the main, could be accounted for as B₄C. Spectrographic analysis of the exhaust particle sample collected from Run 3 is given below:

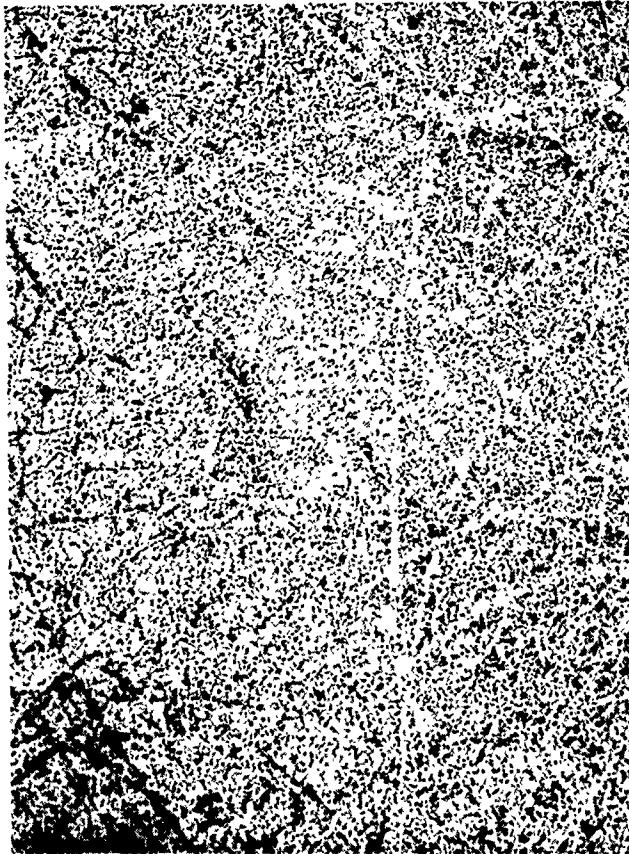
<u>Elements</u>	<u>Weight %</u>	<u>Elements</u>	<u>Weight %</u>
B	Matrix	Ba	0.01
Si	0.1	Mn	0.05
Fe	0.3	Cr	0.02
Mg	5.0	Ni	0.02
Al	0.6	Cu	0.1
Ca	0.03	Ag	0.003

(U) This analysis is typical of analyses of MARNAF 731 fuels, as is evident from comparison with analysis of the fuel (TMH-73-71 and TMH-73-72) shown in Table II.

(C) In optical microscopy examination (see Figure 25), the exhaust particles, while able to be dispersed similarly to the original boron in slide preparation, exhibited an amount of abrasiveness beyond that usually found with amorphous boron. This abrasiveness, as shown by the exceptionally large amount of scratching of the glass slide (in Figure 25) is probably due to the extremely hard and abrasive material, B₄C, in the sample. There was no evidence of crystallinity in the sample, beyond small indications usually found with amorphous boron.

(C) From the foregoing analysis (on a small particle sample), the net elemental boron content of the sample cannot be ascertained for reason of the unusually large amount of H₂O₂-insolubles -- 11.2% as compared

CONFIDENTIAL



90 X

PARTICLE SAMPLER - IMPINGEMENT COLLECTOR SAMPLE
OF EXHAUST SOLIDS, RUN #3 ($O/F = 0.1$)

R-25,382
Neg. 8964-1

Figure 25

-59-

CONFIDENTIAL

(This Page is Unclassified)

CONFIDENTIAL

to 0.2% in amorphous boron, as received. There is no established method for determining net elemental boron in the circumstance of high " H_2O_2 -insolubles". (In the American Potash and Chemical Company scheme of analyses, "water soluble boron", or boron as higher oxides, is subtracted from "total boron" to obtain elemental (net) boron. It is evident that at least one material found in the " H_2O_2 -insolubles", namely B_4C , would be digested in the total boron analysis method and could erroneously be accounted for as elemental boron.)

(C) The composition of the 11.2% H_2O_2 -insoluble content of the exhaust particle sample is also unresolved. X-ray diffraction patterns of this residue material (from H_2O_2 and HNO_3 digestion) indicate only a small amount of B_4C and no other crystalline material. Moreover, spectrographic analysis of the H_2O_2 -insolubles indicates a close similarity to boron slurry. It is possible that, in the main, this residue material is amorphous carbon or carbon in solution or chemical combination with boron. This carbon would be undetected by carbon-electrode emission spectrography and would be expected to be insoluble in H_2O_2 -insoluble assays. Unfortunately, there was insufficient sample to permit a total carbon assay. Briefly stated, carbon in solution in boron and/or in combination with boron (as "subcarbides" such as $B_{13}C_2$) might account for a large part of the H_2O_2 -insolubles in the exhaust particle sample of Run 3.

(C) The total magnesium content of the exhaust particle sample, in ratio to the total magnesium content of the boron as received, is an indicator of the degree of exposure of boron to temperatures above $2100^\circ F$. (In explanation of the above statement, magnesium in Moissan-process 90-92% pure, commercial boron, is believed to occur mostly as magnesium boride species, with minor amount of oxide present. The lower magnesium borides, MgB_2 , MgB_4 , decompose below $2100^\circ F$ to give B and Mg, and elemental magnesium is boiled off at $2100^\circ F$ and above.) In the case of the exhaust particle sample of Run 3, the spectrographic analysis (accurate to $\pm 1\%$ magnesium) indicated 5% magnesium; the wet-chemistry assay (on very small samples in duplicate) indicated 3.8% magnesium--for comparison with a 5.1% magnesium content of the elemental boron as received. The probability of error in both types of assay of magnesium in the exhaust product sample, leaves unresolved whether or not magnesium was vaporized out of the boron, and corre-

CONFIDENTIAL

latively, whether or not the boron was heated to above 2100°F for a significant period.

(C) In summary, analytical evidence from the exhaust particle sample of Run 3 indicates some unaccountability of boron (as much as 4%) and some conversion of elemental boron to B_4C and perhaps to other carbides. There is no evidence for increased boron oxide formation; nor is there direct evidence of significant loss of heating value (assuming significant amounts of carbon and carbides present and assuming the subsequent burning of carbon and boron carbides in ramjet modes of combustion).

b. Analyses, Engine Deposits, Run 3 (O/F = 0.1 and Run 4 O/F = 0.5)

(U) Samples of engine deposit materials from Run 3 and Run 4 were characterized as follows, prior to assay:

1. Run 3, E.D. (engine deposit) Sample 1: A black solid with obvious fine, grayish material fairly uniform peppered throughout, except at top and bottom surfaces; contoured to internal engine wall geometry; $3/8$ " in thickness; a hard cohesive mass showing granular, rough fracture; difficulty crushable to powder in steel dies; extremely abrasive.

2. Run 3, E.D. Sample 2: A brown-black material, more easily crushable than E.D. Sample 1 and containing much less gray inclusion; contoured; about $1/8$ " thick.

3. Run 4, E.D. Sample 1: Description identical to Run 3, E.D. Sample 1.

4. Run 4, E.D. Sample 2: Description identical to Run 3, E.D. Sample 2.

E.D. Sample 1-type material is in much greater abundance than E.D. Sample 2-type material. Spectrographic analysis results for the four samples are listed in Table III.

(U) X-ray diffraction patterns show B_4C to be present in moderate-to-large amounts in each of the four samples. The patterns give no other evidence of crystalline material. The B_4C appears to be most prominent in Run 4, E.D., S-1 and, secondly, in Run 3, E.D., S-2. Figure 26 is an X-ray diffraction pattern of Sample Run 4, E.D., S-1. Each metallic compound gives an X-ray diffraction pattern characteristic of that particular material. Boron carbide has several predominant spectral lines such as at 1.44\AA , 2.38\AA , 2.56\AA , 3.82\AA and 4.03\AA . Since these lines appear on Figure 26, it can readily be concluded that that sample was predominantly B_4C .

CONFIDENTIAL

R-25,389

-62-

CONFIDENTIAL

(This page is Unclassified)

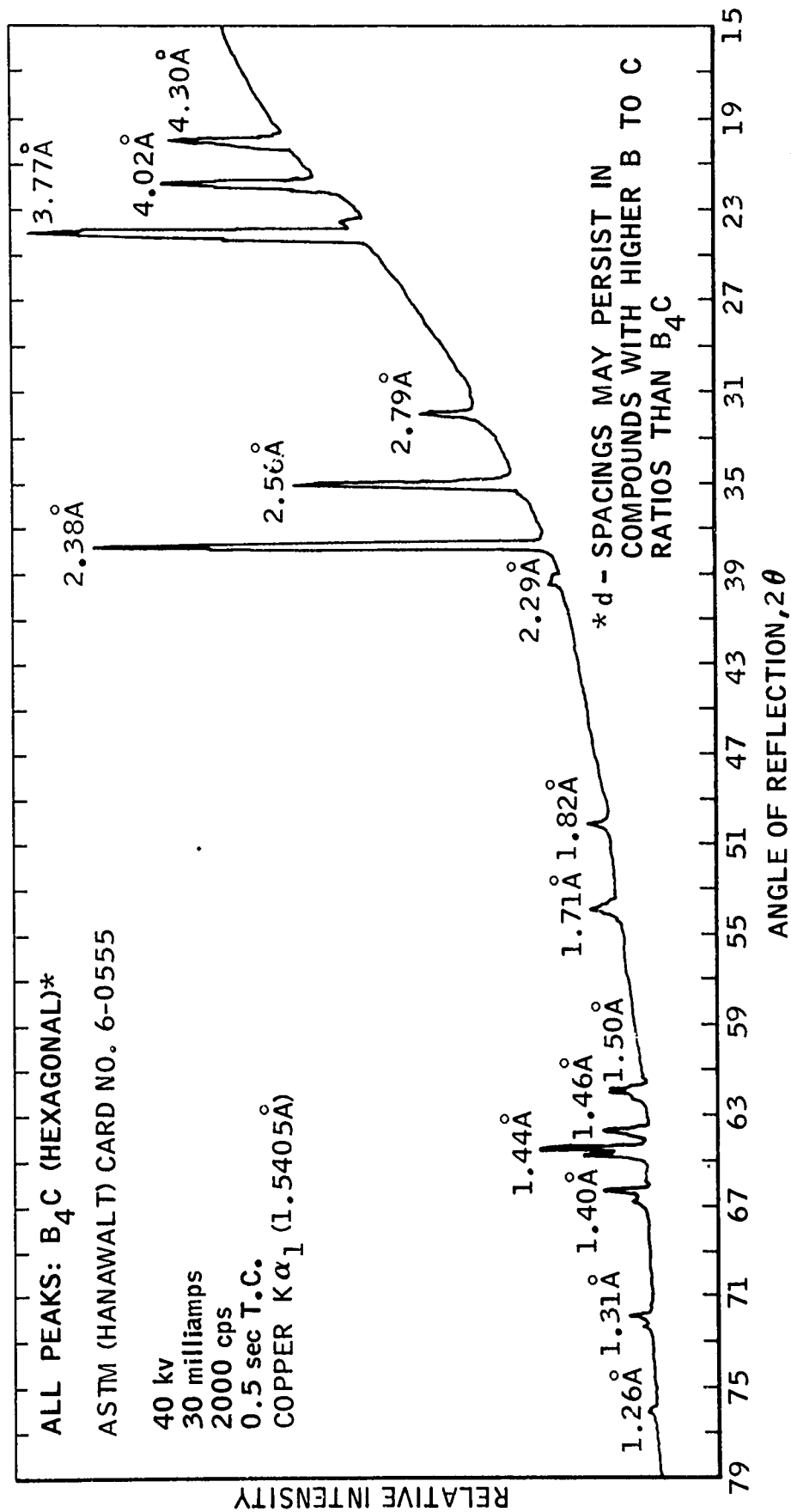


Figure 26

X-RAY DIFFRACTION PATTERN

RUN NO. 4 (O/F = 0.5), ENGINE DEPOSIT SAMPLE 1

CONFIDENTIAL

TABLE III
SPECTROGRAPHIC ANALYSIS OF ENGINE DEPOSITS

Element	Run #3 E.D., S-1	Run #3 E.D., S-2	Run #4 E.D., S-1	Run #4 E.D., S-2
B	Matrix	Matrix	Matrix	Matrix
Si	0.12	0.15	0.11	0.08
Mn	0.17	0.13	0.12	0.13
Fe	0.30	0.25	0.37	0.20
Cr	0.03	0.02	0.03	0.02
Ni	0.03	0.03	0.17	0.03
Al	0.40	0.40	0.40	0.50
Ca	0.20	0.30	0.15	0.30
Ba	<0.01	0.02	<0.01	0.01
Cu	0.06	0.05	0.05	0.05
Mg	3	4	2	5
Na	<0.03	<0.03	<0.03	<0.03

Values above are in weight percent.

(U) Chemical assays on additional engine deposit samples (which were similar in description to samples E.D., S-1 of both runs) gave the following results:

Item	Run 3 E.D., S-1A	Run 4 E.D., S-1A
Water-Soluble Boron	0.14%	1.5%
H ₂ O ₂ -Insolubles	86.8	80.8
Carbon	13.3	15.9

(U) X-ray diffraction patterns of residues of the above samples after H₂O₂-insolubles assay again revealed moderate-to-large concentrations of material identified as B₄C and no other crystalline materials.

(C) Comparisons of Tables II and III of spectrographic data show no large changes in aluminum and in trace elements in the transition from boron slurry fuel to engine deposits. However, significant decreases in the magnesium contents of E.D., S-1 types of engine deposits imply that these deposits were exposed to heating above 2100°F. The "water-soluble boron" content of sample Run 3, E.D., S-1 is consistent with the water-soluble contents of the original boron in the slurry fuels and with the exhaust

CONFIDENTIAL

particle sample of Run 3 and indicates essentially no air oxidation. The "water-soluble boron" content of Run 4, E.D., S-1, however, gave an unexpectedly high value of 1.5%.

(U) The high values of H_2O_2 -insolubles and carbon content of the engine deposits of Run 3 and Run 4 connote that these deposits are composed largely of materials in the categories of B_4C , other boron-carbon chemical combinations, boron-carbon solutions, and admixtures of boron and carbon. (If the boron and carbon were in combination entirely as B_4C , this latter material would comprise 61.6% and 73.9% of sample Run #3, E.D., S-1 and Run 4, E.D., S-1, respectively.)

(U) Inference of moderate-to-large amounts of B_4C , as shown by the X-ray diffraction patterns, may be rather misleading for the reason that the formation of B_4C is favored only within a narrow range of temperatures, approximately 3900 to 4100°F⁽²⁾. Reactions to form B_4C are slow at temperatures less than 3900°F; B_4C reverts to lower carbides and to its elements at temperatures above 4100°F. Also, the X-ray diffraction pattern, i.e., d-spacings and intensities that are presently attributed to B_4C , may be stable over a whole range of composition, perhaps from carbides of lower composition than $B_{15}C_2$ to $B_{13}C_3$ ⁽³⁾.

(U) In summary, the analyses of engine deposits of Run 3 and Run 4 are broadly explanatory of deposition occurrences associated with particular engine designs and conditions of operation. These analyses were not carried to a further degree of completeness for the reason that later engine designs produced little or no deposits and further emphasis was not warranted.

c. Gas Sample Analysis (Runs 3 and 4)

(U) Three gas samples were obtained in each run, one for each of the sampling ports on the probe. The samples were received in ~1.2 liter steel pressure cylinders equipped with toggle valves and pressure indicators. The pressures under which the samples were obtained varied from ~5.8" Hg to ~21.1" Hg. The cylinders were attached one by one to a high vacuum line via a 1/4" Swagelok fitting and the volume above the toggle valve was evacuated to better than 10^{-5} mm Hg. Then the contents of the cylinder were expanded through a 7 mm O.D. liquid nitrogen cooled glass spiral into an ~1.0 liter expansion volume, which was also cooled with liquid

UNCLASSIFIED

nitrogen. This expansion was necessary due to the relatively high cylinder pressures caused by the large quantities of air present. Without expansion the removal of condensible materials from the noncondensable gases would not have been quantitative.

(U) Following the expansion, the noncondensable gases were collected in a Sprengel pump, after being passed through two liquid nitrogen-cooled U-traps, measured, and transferred into an ampoule for mass spectroscopic analysis. The condensible materials, after removal of the noncondensable components, were collected by distillation into a U-trap and were separated into a liquid nitrogen, -78°C , and if necessary a -47°C fraction by passing the materials from a warming trap through traps kept at -47° , -78° , and -196°C . The individual fractions then were measured (the -196°C fraction by volume, the -78° and -74°C fractions by weighing) and analyzed by infrared and mass spectroscopy and by gas chromatography.

(U) The noncondensable materials were analyzed by conventional quantitative mass spectroscopic techniques. The instrument was calibrated immediately prior to analysis for all the components of the samples.

(U) The liquid nitrogen fractions were analyzed by a combination of quantitative mass (CO_2) and infrared (SiF_4) spectroscopy and gas chromatography (remainder of components). The infrared spectrometer was calibrated with a sample of silicon tetrafluoride of known purity ($\text{VP}_{-111.8^{\circ}} = 125.0 \text{ mm}$; lit.⁽⁴⁾ 118 mm). In the gas chromatographic analysis a double column technique was employed⁽⁵⁾ which makes the separation, identification, and determination of saturated as well as unsaturated hydrocarbons possible. The gas chromatograph was calibrated prior to performing the analyses with standard samples.

(U) The -78°C fractions were analyzed by combination of gas chromatography and infrared spectroscopy. In view of the relative low vapor pressure of these fractions, gas chromatography had to be done on pentane solutions. Infrared spectroscopy was performed on liquid samples using 0.1 mm liquid cells. Inasmuch as trimethylhexane was the main component, both the gas chromatograph and infrared spectrometer were calibrated using pure trimethylhexane. In addition to the -78°C fractions, the condensible materials from Run 4 also contained relatively large amounts of water (19.5 mg from

UNCLASSIFIED

position 1, 263.6 mg from position 3) as determined by vapor pressure measurements and infrared spectroscopy.

(U) The presence of large quantities of air interfered somewhat with the analyses insofar as only small amounts of products were available. In addition there were indications that a portion of the oxygen in the air reacted with the original reaction products since the ratios of $N_2:O_2$ in the analyzed samples were somewhat higher than in air.

(U) In Run 4, both samples contained such large concentrations of acetone that the condensible fractions could not be analyzed. The acetone was a residual of the cleaning process prior to sampling. In addition, it was impossible to analyze the liquid nitrogen fractions of Run 3 completely. In positions 2 and 3 the total analyzed for amounted to only 53% and 63%, respectively. The technique employed for analysis has been proven consistently to give results of better than 95%⁽⁵⁾. This discrepancy is at present unexplainable. It may, however, be connected with the fact that in none of the analyses conducted to date was it possible to detect any boron containing species. From thermodynamical calculations it is to be expected that BF_3 and BCl_3 are the main boron containing species under the conditions of the experiment. Both should be easily detected by either infrared or mass spectroscopy, provided no hydrolysis occurred. However, the detection of SiF_4 in the liquid nitrogen fractions of Run 3 strongly points to the fact that hydrolysis has occurred. Under the conditions employed for sample transfer any HF formed by hydrolysis of BF_3 would react with the pyrex glass of the high vacuum line forming SiF_4 .

(U) The quantities of SiF_4 determined in the samples from positions 2 and 3 of Run 3, however, are too small to account for the quantities of ClF_3 employed. In addition, no HCl could be detected, which should be formed concurrently with HF through hydrolysis of BCl_3 or mixed boron chlorofluorides. Based on the fact that some hydrolysis has occurred (presence of SiF_4) it can be suspected that in the presence of water the boron containing products have reacted inside the pressure cylinders resulting in involatile products.

(U) To make the results of the analyses of the different fractions (noncondensibles, -196° and $-78^\circ C$ fractions) easier to compare, the quantities of the compounds analyzed in Run 3 are given in mmoles in Table IV and are

CONFIDENTIAL

TABLE IV
COMPOSITION OF PRODUCTS OF RUN 3

	Position					
	1	2	3			
	mmoles [*]	%	mmoles	%	mmoles	%
CH ₄	0.0279	4.37	0.5390	13.34	0.5480	13.08
H ₂	0.2002	31.34	1.8407	45.55	2.0085	47.93
C ₂ H ₆	0.0022	0.34	0.0171	0.42	0.0234	0.56
C ₂ H ₄	0.0197	3.08	0.1876	4.64	0.2513	6.00
C ₂ H ₂	0.0210	3.29	0.2040	5.05	0.2393	5.71
C ₃ H ₈	0.0005	0.08	0.0053	0.13	0.0057	0.14
C ₃ H ₆	0.0077	1.21	0.0984	2.43	0.0923	2.20
C ₄ H ₁₀	0.0001	0.01	0.0136	0.34	0.0131	0.31
C ₅ H ₁₂	d)	-	0.0007	0.02	0.0011	0.03
SiF ₄	c)	-	0.0140	0.35	0.0151	0.36
CO ₂	0.0898	14.06	0.0409	1.01	0.1419	3.39
Unsaturates a)	0.0046	0.72	0.0238	0.59	0.0137	0.33
Not analyzed -196°C	0.0118	1.85	0.5065	12.53	0.3905	9.32
Not analyzed -78°C b)	0.0626	9.80	0.0543	1.34	0.0884	2.11
Trimethyl hexane	0.1906	29.84	0.4954	12.26	0.3586	8.56
Total	0.6387	99.99	4.0413	100.00	4.1909	100.03

*mmoles = moles x 10⁻³

a) Average assumed molecular weight = 81.3

b) Average assumed molecular weight = 130

c) Not detected

d) < 10⁻⁴ mmole

CONFIDENTIAL

in the same table recalculated as percents of the total gas volume of the reaction products. From the tabulation, it is evident that there is considerable methane, hydrogen and vaporized TMH in the exhaust. These gaseous species should readily combust in the afterburner and raise the local temperature sufficiently to burn the solid boron particles.

E. DISCUSSION OF GAS GENERATOR RESULTS

(U) Following Phase I, the gas generator design employed in Runs 19 and 20 was incorporated into the air augmentation hardware and testing was resumed. The gas generator design remained essentially unchanged during the remainder of the program, which included testing with both CTF and BPF oxidizers. During many of the air augmentation tests, performance measurements (pressure and temperature) were made on the gas generator, and these results along with those made during Runs 19 and 20 are included and discussed in this section.

(C) Figure 27 shows the relationship between gas generator chamber pressure (normalized) and O/F ratio. Shown are both theoretical and experimental data. The CTF nonequilibrium curve corresponds to the condition that the TMH vaporizes rather than degrading into simpler hydrocarbons. Only a small portion reacts with the CTF. Although this does not represent the true combustion process, wherein hydrocarbons are formed, it does illustrate the magnitude of deviations from equilibrium performance that could be encountered in an actual gas generator operating at very low O/F ratios.

(C) The data for the axial injection gas generator using CTF are seen to fall along the dotted line slightly below the presented nonequilibrium line. Although not shown, the data for the low L^* ($L^* = 25$) full scale gas generator (Configuration I-A) would also fall on this dotted line.

(C) The bromine pentafluoride data would be expected to lie below that of CTF, based upon the position of the equilibrium curve. However, the data are found to coincide with that of CTF in the O/F ratio region of interest. If the experimental data are parallel to the theoretical curves, the experimental data lines for CTF and BPF would cross as shown in Figure 27.

CONFIDENTIAL

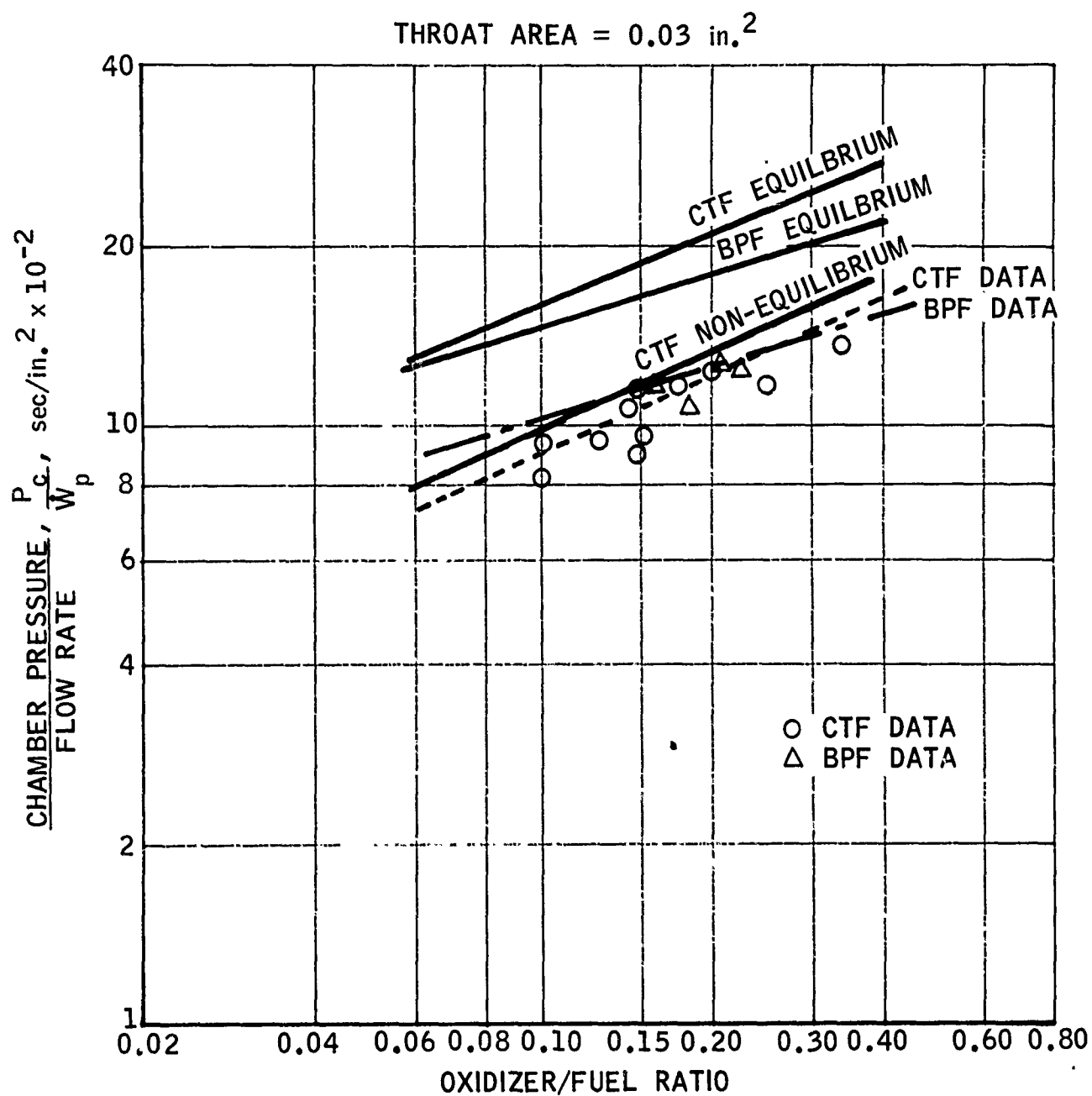


Figure 27
VARIATION OF GAS GENERATOR CHAMBER PRESSURE PARAMETER

CONFIDENTIAL

CONFIDENTIAL

(C) Figure 28 is a cross plot of Figure 27 and shows the expected flow rates required to achieve a given chamber pressure with either CTF or BPF for the axial injection gas generator used during Runs 19 and 20 and the air augmentation tests.

(C) Figure 29 shows the gas generator exhaust temperature as a function of O/F ratio. The theoretical curve for CTF at an $O/F > 0.15$ is based upon equilibrium chemistry. At $O/F < 0.10$, the prediction is based upon the non-equilibrium case incorporating enforced vaporization of the TMH. The theoretical curve for BPF corresponds to full equilibrium chemistry.

(C) As the gas generator exhaust stream is caused to impinge upon a blunt target, it would be expected that the temperature of the resulting, near stagnant stream could be approximated as nearly equivalent to the total temperature of the exhaust stream, and therefore to the expected chamber temperature at the exhaust pressure. The reference pressure for the theoretical curves has been selected as 200 psia since this approximates the gas generator exhaust pressure for sea level afterburner testing.

(C) At low altitude conditions the CTF and BPF systems appear to be equivalent in exhaust product temperature at the same O/F ratio, if the extrapolations can be considered valid. At high altitude conditions, where the afterburner pressure is 40-50 psia, a greater deviation from the theoretical curves would be expected. Such is evident from the data. At the low pressure conditions there is a decided difference in the temperatures achieved with CTF and BPF, which is approximated by the difference in the theoretical curves. The lower heat transfer rate to the measuring thermocouple, at the low pressure conditions, may account in part for the lower indicated temperatures. The thermocouples protruded only 1/4 inch out of the surface of the graphite wall, and therefore the wall could serve as a heat sink which would further lower the indicated temperature.

CONFIDENTIAL

THROAT AREA = 0.03 in.²

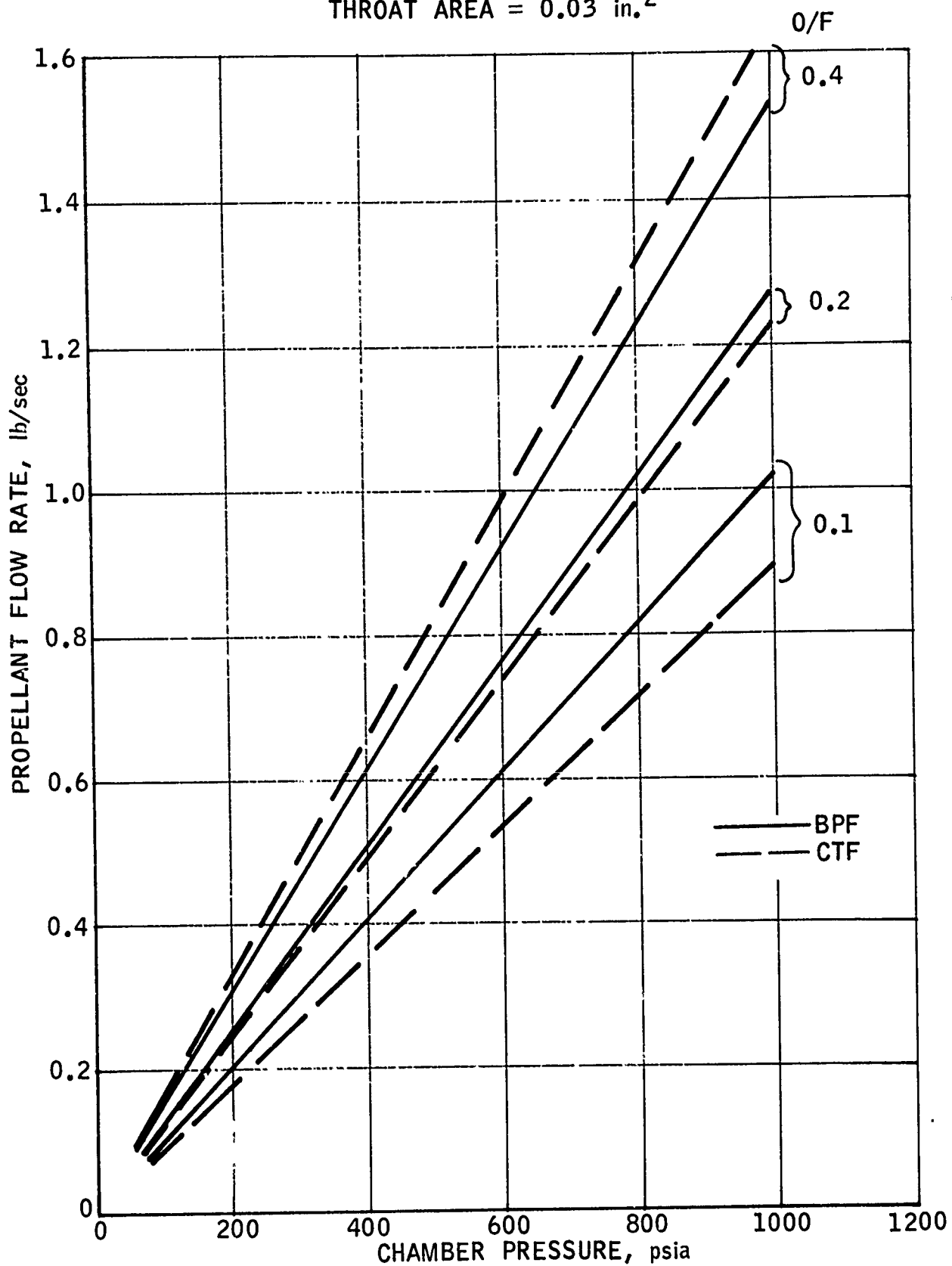


Figure 28

GAS GENERATOR FLOW RATE AS FUNCTION OF CHAMBER PRESSURE

-71-

CONFIDENTIAL

CONFIDENTIAL

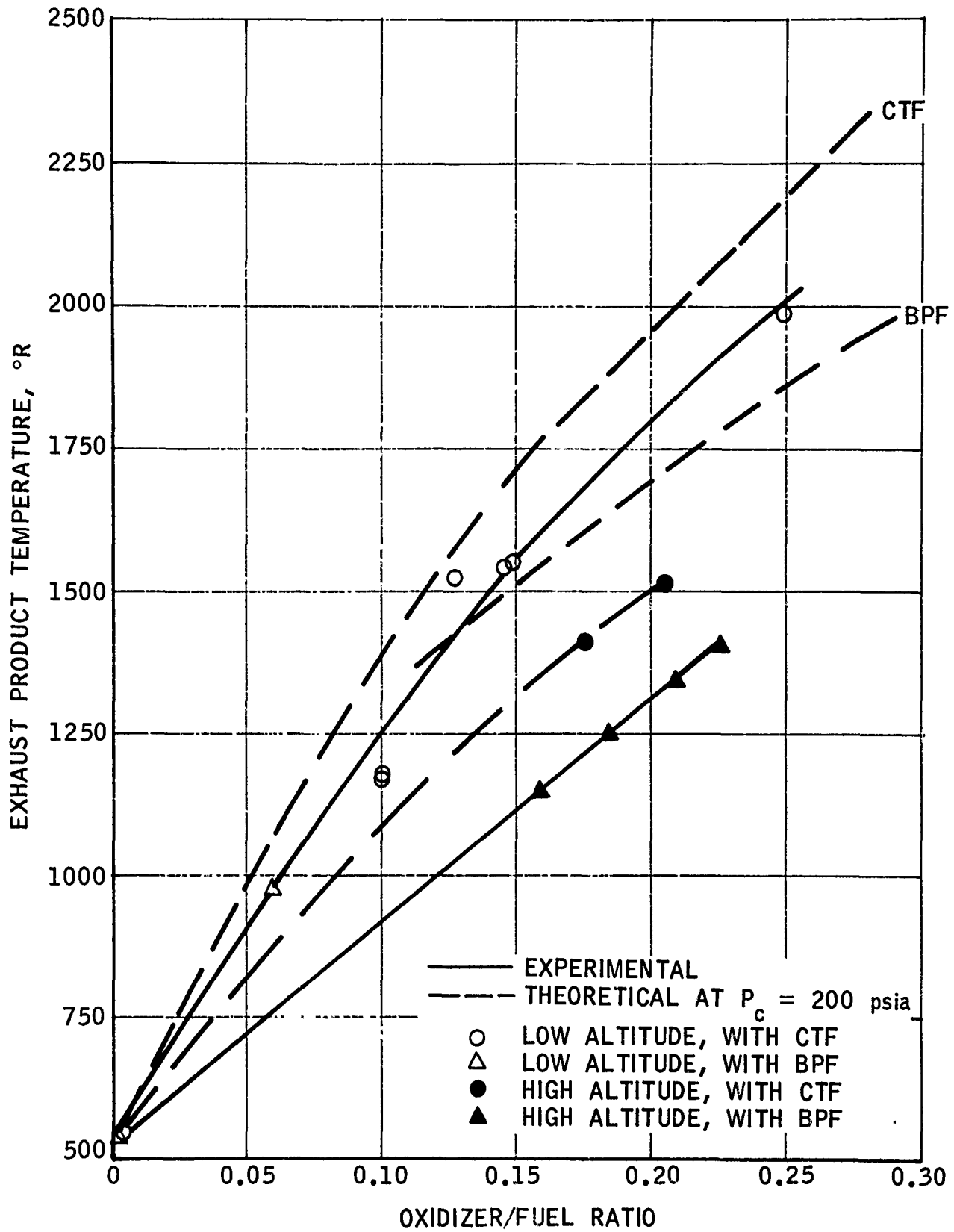


Figure 29
TEMPERATURE OF CAS GENERATOR EXHAUST PRODUCTS

-72-
CONFIDENTIAL

CONFIDENTIAL

V

AIR AUGMENTED COMBUSTION DEMONSTRATION

A. GENERAL REQUIREMENTS

(U) The purpose of a secondary combustor system is to react the exhaust products from the primary gas generator with air in the secondary combustor and produce thrust. To accomplish this task in an efficient manner, certain geometrical constraints consistent with the requirements of the ultimate application of the propulsion system are required. In addition to the production of efficient afterburner combustion efficiency, the afterburner design should permit operation over a wide O/F ratio band, wide air-to-propellant ratio, wide Mach number and altitude range, possess good afterburner autoignition characteristics, preclude significant deposit buildup and be durable enough to permit experimental testing.

(C) Under the subject program, testing was to be conducted primarily under low altitude conditions that corresponded to Mach 2.9 at 500 foot altitude. Limited tests would be conducted at altitudes up to 40,000 feet. The afterburner air-to-propellant ratio was to vary from 20 to 1 to 40 to 1 with emphasis being placed on the 40 to 1 case. The primary O/F ratio range was to be selected from the Phase I tests but, in general, the low O/F ratio range where afterburner autoignition could be assured was to be emphasized.

(U) The fuel used in all tests was MARNAF 731. Most tests used chlorine trifluoride as the gas generator oxidizer but some comparative testing was done using bromine pentafluoride as the oxidizer. Bromine pentafluoride was used because of its high density which, under some cases, offers system advantages.

B. TEST HARDWARE

(U) 1. Gas Generator

The gas generator employed during the air augmentation tests had the same internal geometry as that employed during Runs 19 and 20 of Phase I. Even though the performance of the gas generator was not documented

CONFIDENTIAL

CONFIDENTIAL

over a wide range of conditions during Phase I, its performance was sufficiently encouraging during Runs 19 and 20 to warrant initiation of the Phase II tests. Figure 30 shows how the axial injection gas generator was incorporated in the earlier gas generator housing that permitted attachment to the afterburner ducting. It had initially been planned to use two impinging jets in a blast tube similar to that shown in Figure 12. This approach would require two small gas generators and it was believed that an effect similar to impinging jets could be achieved with a "target" located downstream of a single gas generator, the exhaust of which impinged upon the target. A flight weight gas generator would be much smaller in outside diameter than that used during this test program. One minor modification that was made to the gas generator lines after the Phase I tests was the addition of a straight section of throat at the gas generator exit to minimize throat erosion.

(U) 2. Secondary Combustor

On the subject program, the afterburner geometry was specified with respect to scale and relative dimensions in order to permit an Air Force comparison of the experimental results with those of other Air Force sponsored programs utilizing solid and hybrid propellant technology. These geometrical constraints are summarized below.

<u>Component</u>	<u>Description</u>
Inlets	Two, 180° apart
Dump Mach Number	0.4
Air Injection Angle	60°
Afterburner L/D	3.2
Afterburner Diameter	7.0 inches
Afterburner Nozzle Contraction Ratio	4.05
Nozzle Expansion Ratio	2.6

(U) The exhaust products from the gas generator were to enter subsonically from the center of the afterburner. The resultant hardware, employing the above constraints, is shown in Figure 31. The hardware was cooled by spraying water on its exterior and also was lined with a modified aluminum oxide refractory material for thermal protection. The Marquardt developed refractory coating is designated as P-150. The convex surface at the forward end of the combustor also was lined. The afterburner exhaust nozzle was fabricated from

CONFIDENTIAL

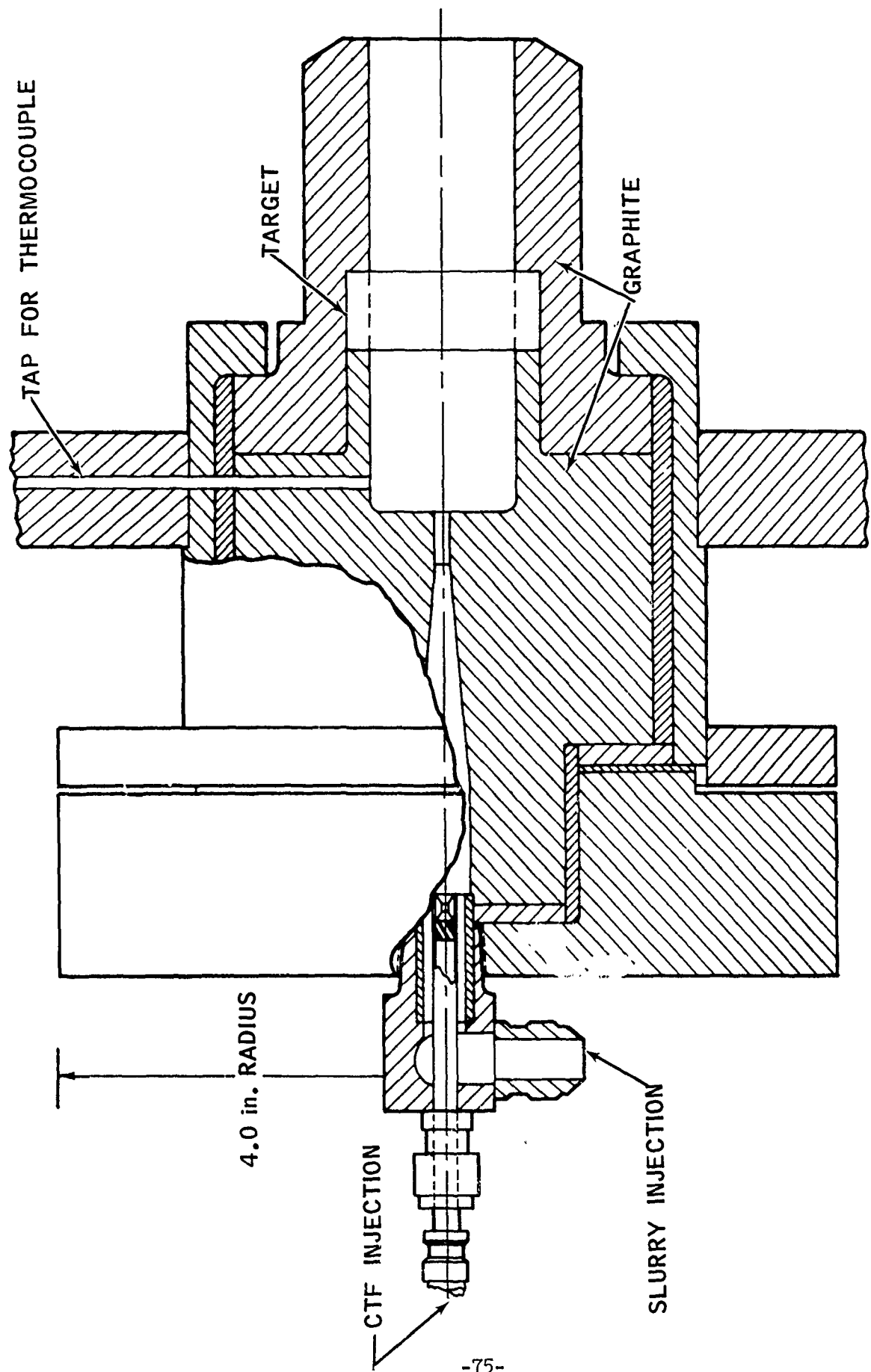


Figure 30
AXIAL INJECTION GAS GENERATOR

CONFIDENTIAL

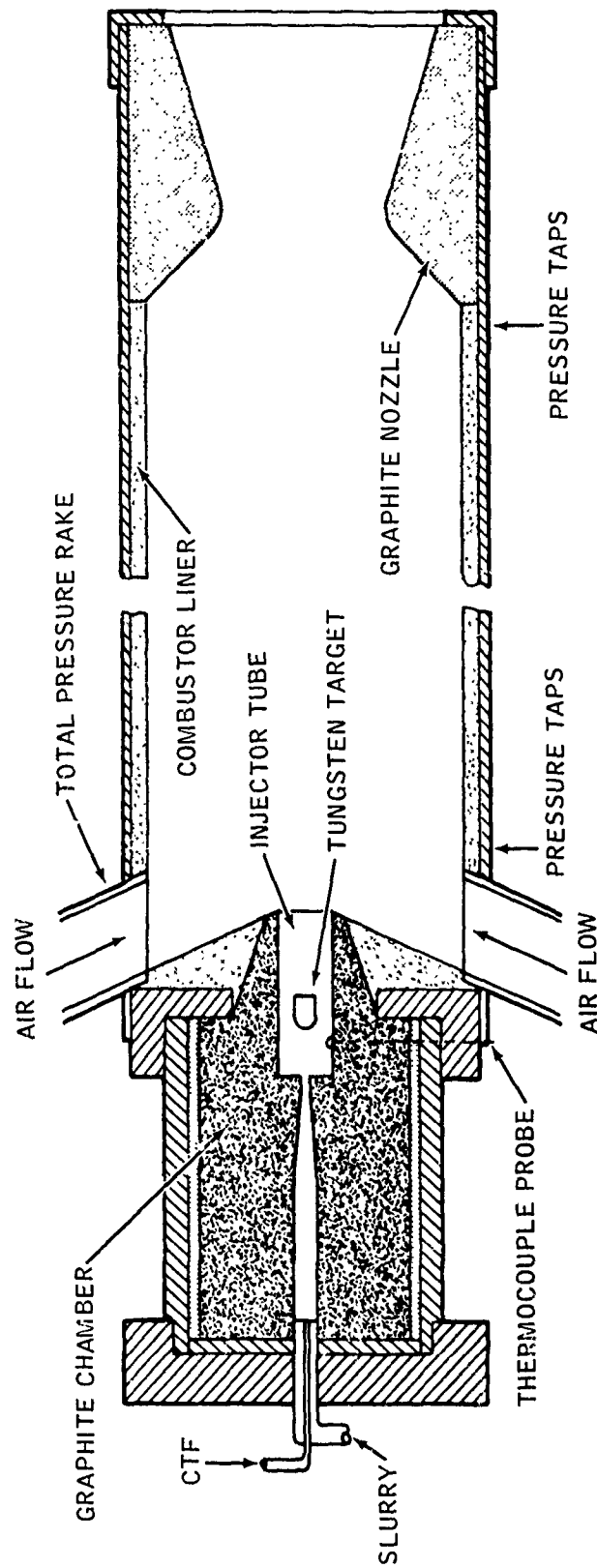


Figure 31
GAS GENERATOR AND COMBUSTOR DESIGN

A404-5

-76-

CONFIDENTIAL

UNCLASSIFIED

graphite and was coated with a thin layer of a Marquardt silicon carbide coating known as RM 005. This silicon carbide layer effectively prevented erosion of the graphite for the full series of afterburner tests.

(U) In keeping with the program objective of obtaining good afterburner autoignition and combustion efficiency at minimum primary O/F ratios, the afterburner geometry shown in Figure 31 was reviewed. System studies showed that the overall specific impulse of a ducted rocket would increase as the O/F ratio of the primary decreased. However, it was recognized that decreasing the primary O/F ratio would decrease the primary exhaust temperature, which would limit the minimum O/F ratio of operation. This limit may be higher than desired for the geometry of Figure 31 owing to the combustion quenching efforts associated with very rapid mixing. Previous experience with ramjet burners indicated that improved performance might be obtainable if a recirculation zone were provided near the forward end of the combustor. This recirculation zone would act as a "piloting" zone of relatively low air velocity which would promote ignition of the incoming fuel.

(U) As a result of this analysis, flexibility was designed into the hardware to permit the incorporation of a recirculation zone at the forward end of the afterburner. This flexibility and the design with the recirculating zone at the forward end of the combustor are shown in Figure 32. The initial geometry was designed with a short spool section, as part of the combustor, located just upstream of the afterburner exit nozzle. For the backup design, this short spool could be removed and located just ahead of the inlets. This in effect moved the inlets downstream $3\frac{1}{2}$ inches, and by making the forward dome concave instead of convex, a stable piloting region could be created. This modification did not change the overall length of the system and therefore would not violate overall missile constraints. Both designs were experimentally evaluated.

(U) 3. Instrumentation and Control

Instrumentation of the primary combustor remained essentially the same as that described previously in this report. The additional instrumentation for the augmentation tests concerned the air facility, air heater and the secondary combustor proper. A schematic diagram of the facility installation showing the significant systems and control valves is presented in Figure 33. Figure 34 shows how the combustor was mounted direct-connect to the facility air heater. The combustor was mounted vertically under the

UNCLASSIFIED

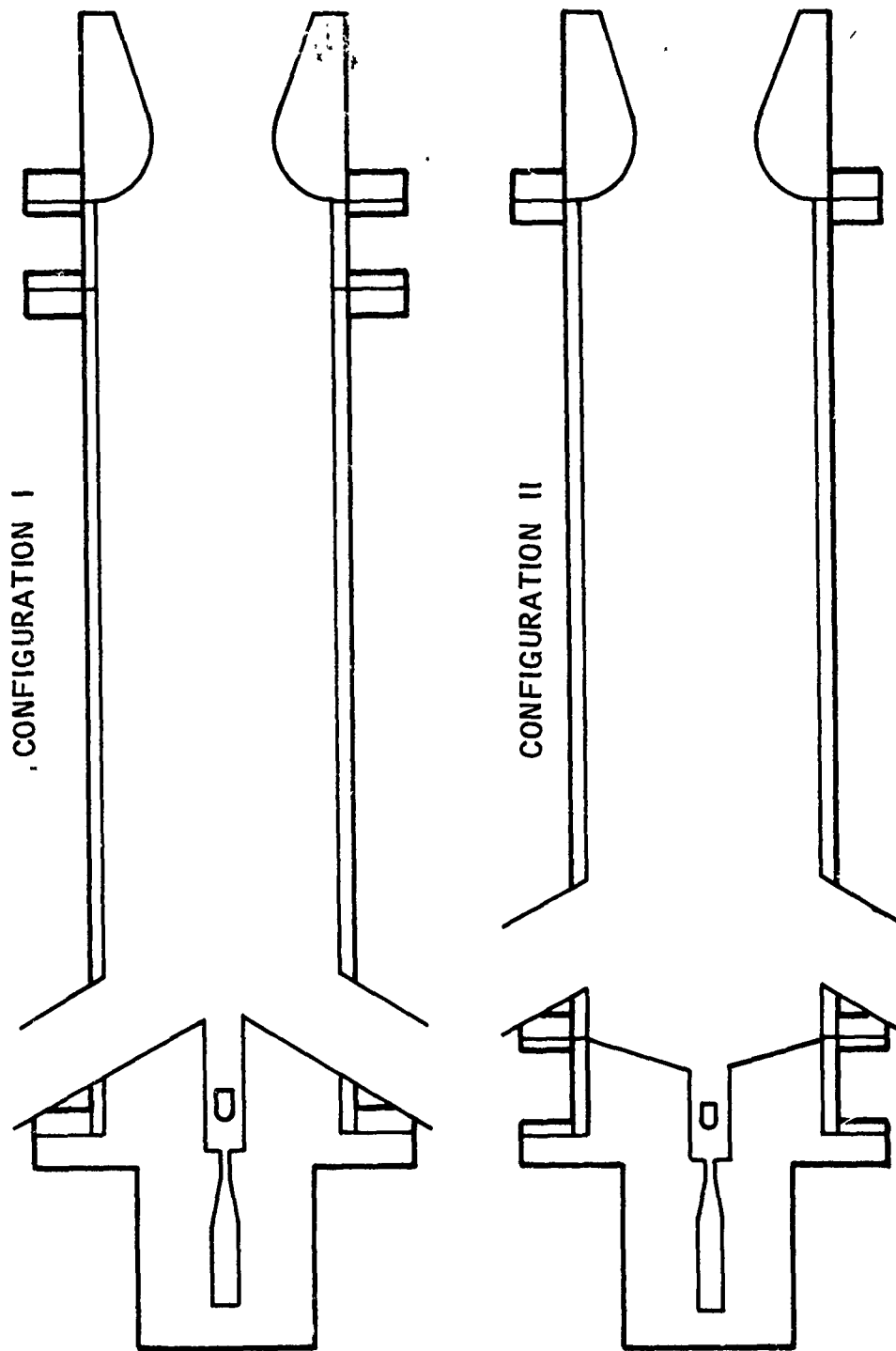


Figure 32
AIR AUGMENTATION CONFIGURATIONS

A404-6

-78-

UNCLASSIFIED

UNCLASSIFIED

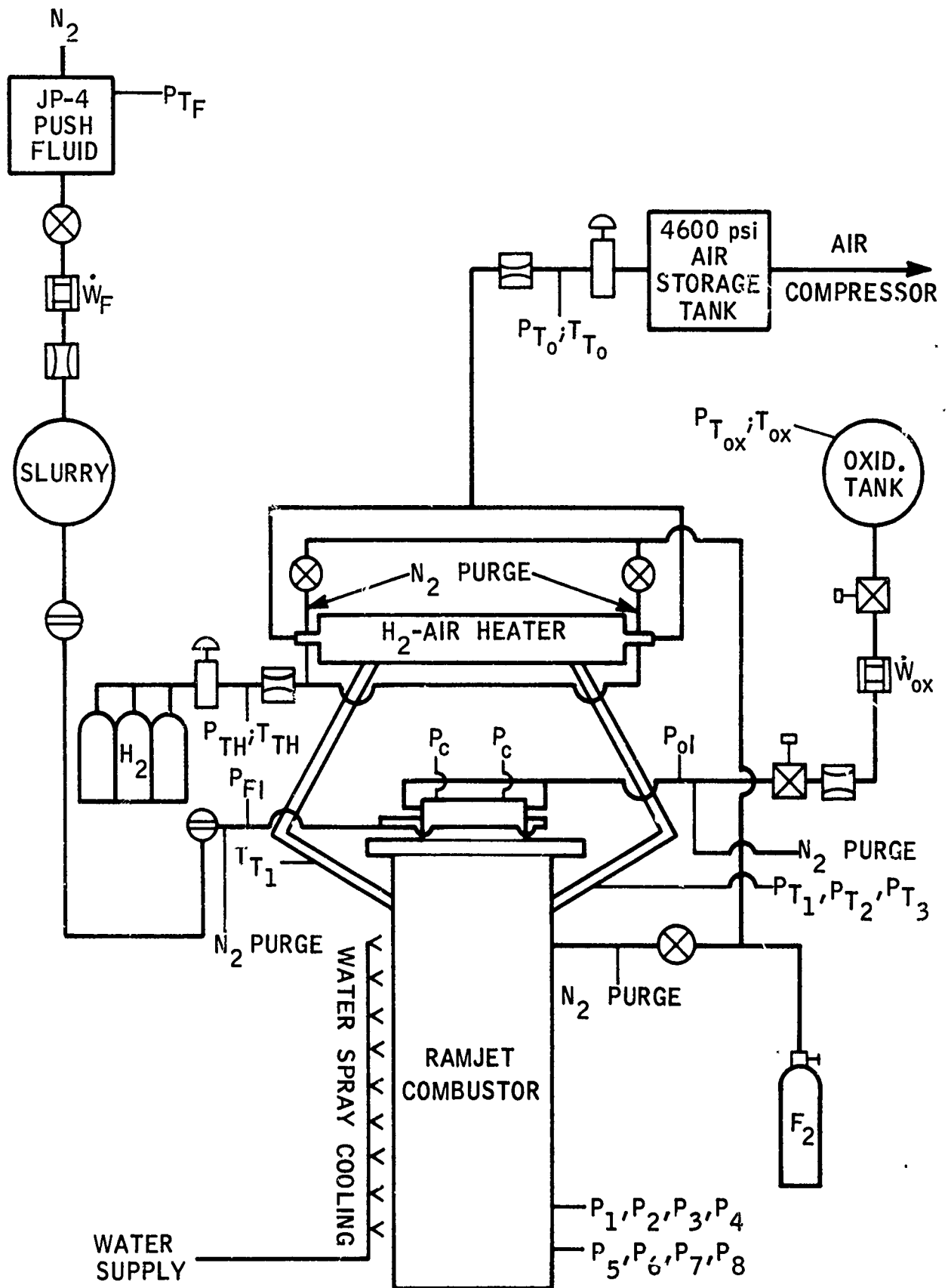


Figure 33
PLUMBING AND INSTRUMENTATION SCHEMATIC
AIR AUGMENTATION PHASE

UNCLASSIFIED

UNCLASSIFIED

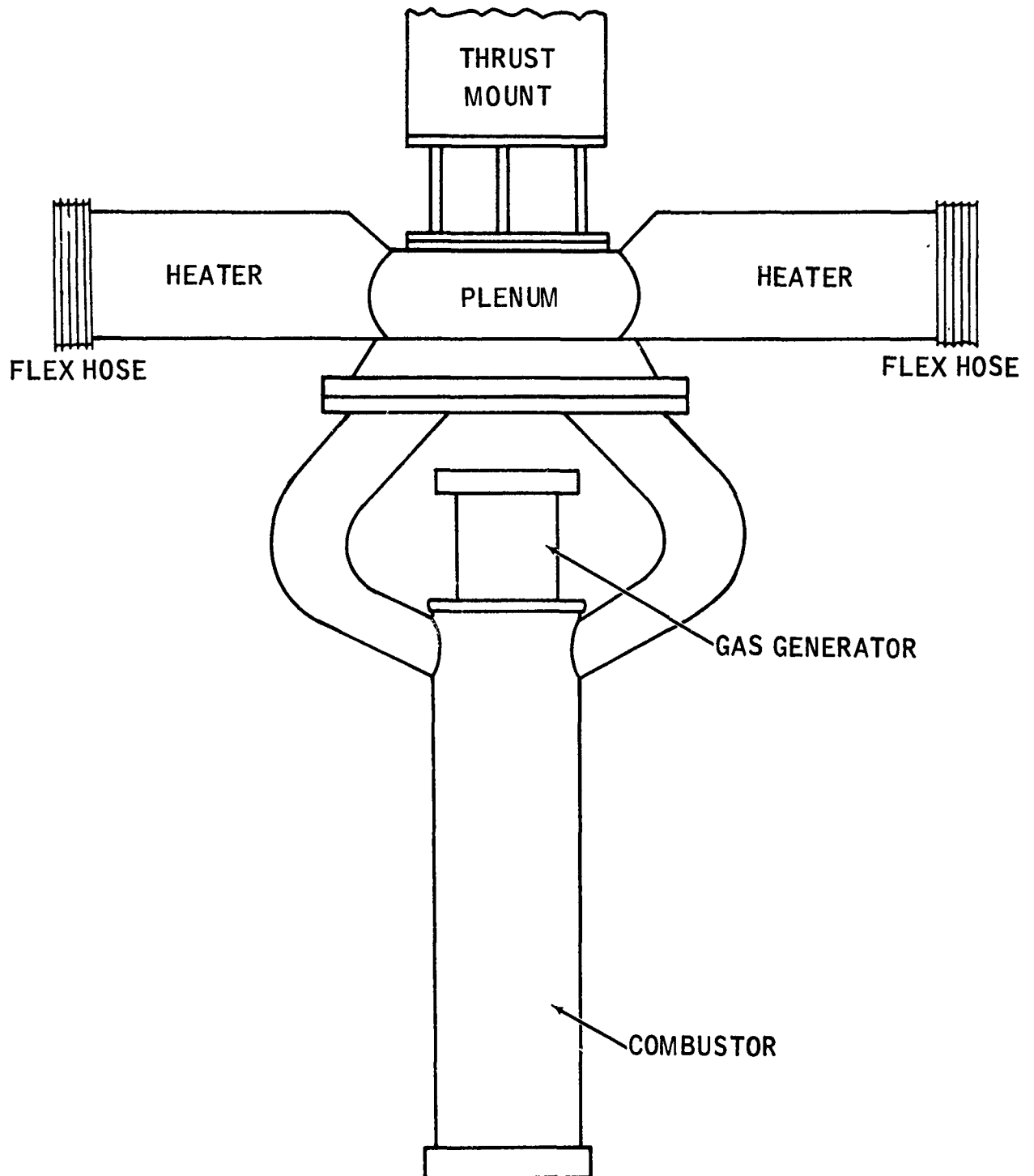


Figure 34
AIR AUGMENTED ROCKET TEST CONFIGURATION

R-25,257

UNCLASSIFIED

UNCLASSIFIED

air heater. Both the air heater and test item were suspended from the thrust mount. Cold facility air was routed through two sections of horizontal flex-hose and into the hydrogen-fueled direct vitiation heater. All other propellant and instrumentation lines were routed in such a manner as to minimize force components when pressurized. To establish any thrust component due to the hardware plumbing, a flat plate was put over the secondary combustor exit and the test item was pressurized. A plot of thrust component versus chamber pressure was then made. At a chamber pressure of 250 psia, a negative force of about 20 pounds was generated. The thrust readings during engine operation were then corrected by the appropriate amount. This arrangement permitted reliable thrust readings during the air augmentation tests.

(U) Performance of the afterburner was determined primarily from flow rate and pressure measurements. Test item instrumentation is shown in Figure 35. Gross thrust readings also provided a check on performance. The following measurements were recorded for determining performance.

- Gross Thrust (thrust transducer)
- Gas Generator Pressure (pressure transducer)
- Oxidizer Flow Rate (turbine flowmeter)
- Oxidizer Injector Pressure (pressure transducer)
- Boron Slurry Flow Rate (turbine flowmeter in push fluid)
- Boron Slurry Injector Pressure (pressure transducer)
- Gas Generator Exhaust Temperature (thermocouple)
- Air Flow Rate (venturi)
- Air Temperature (thermocouple probes before and after heater)
- Air Total Pressure (total pressure rake in one inlet)
- Hydrogen Flow Rate (venturi)
- Static Pressure in Combustor (multiple taps at combustor entrance and nozzle)

(U) The output of the transducers was recorded on oscillograph paper for a rapid estimate of performance and on magnetic tape for subsequent computer analysis and printout.

(U) A photograph of the air augmentation setup installed in the test facility is shown in Figure 36. The afterburner exhaust shoots downward through a hole in the floor and into an elbow that ducts the exhaust products out through the side of the hill. The exhaust is sprayed with water to cool and dilute it before it is exhausted into the atmosphere.

UNCLASSIFIED

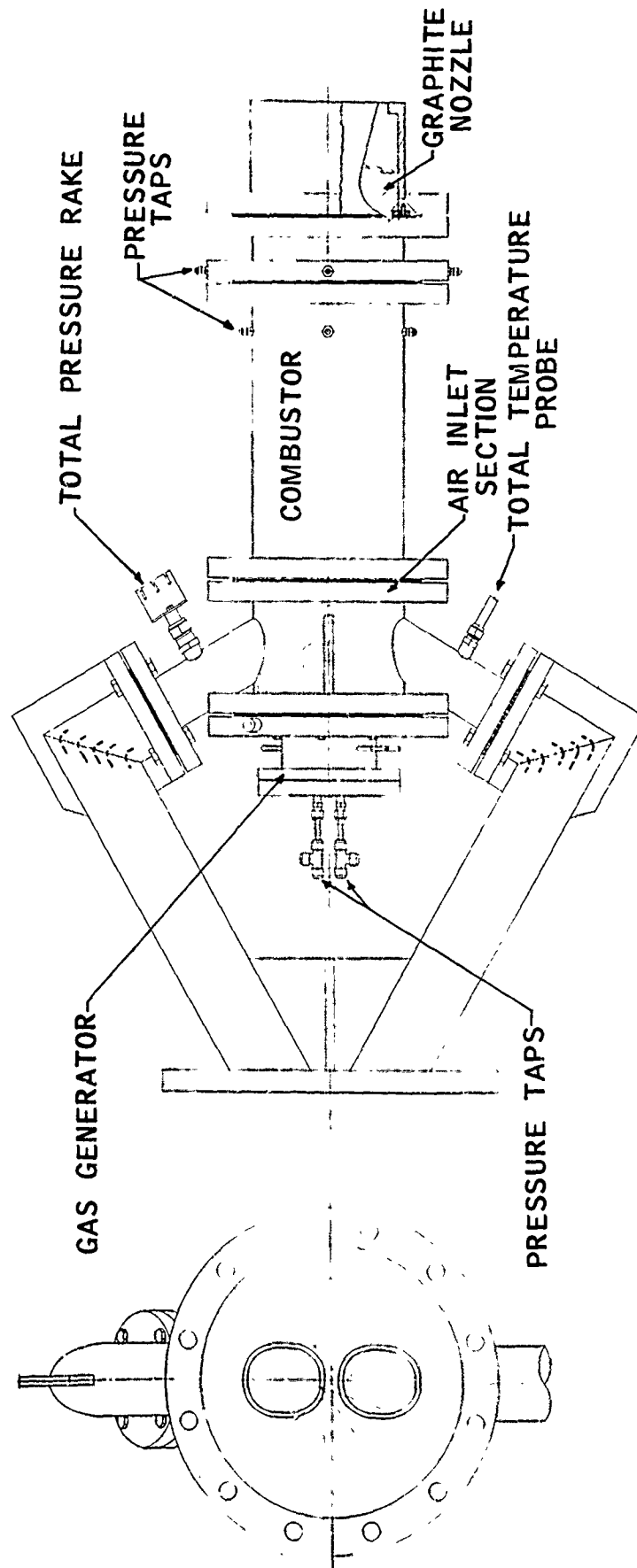


Figure 35
SYSTEM DESIGN FOR DIRECT-CONNECT AIR AUGMENTATION TESTS

R-25,437

-82-

UNCLASSIFIED

CONFIDENTIAL

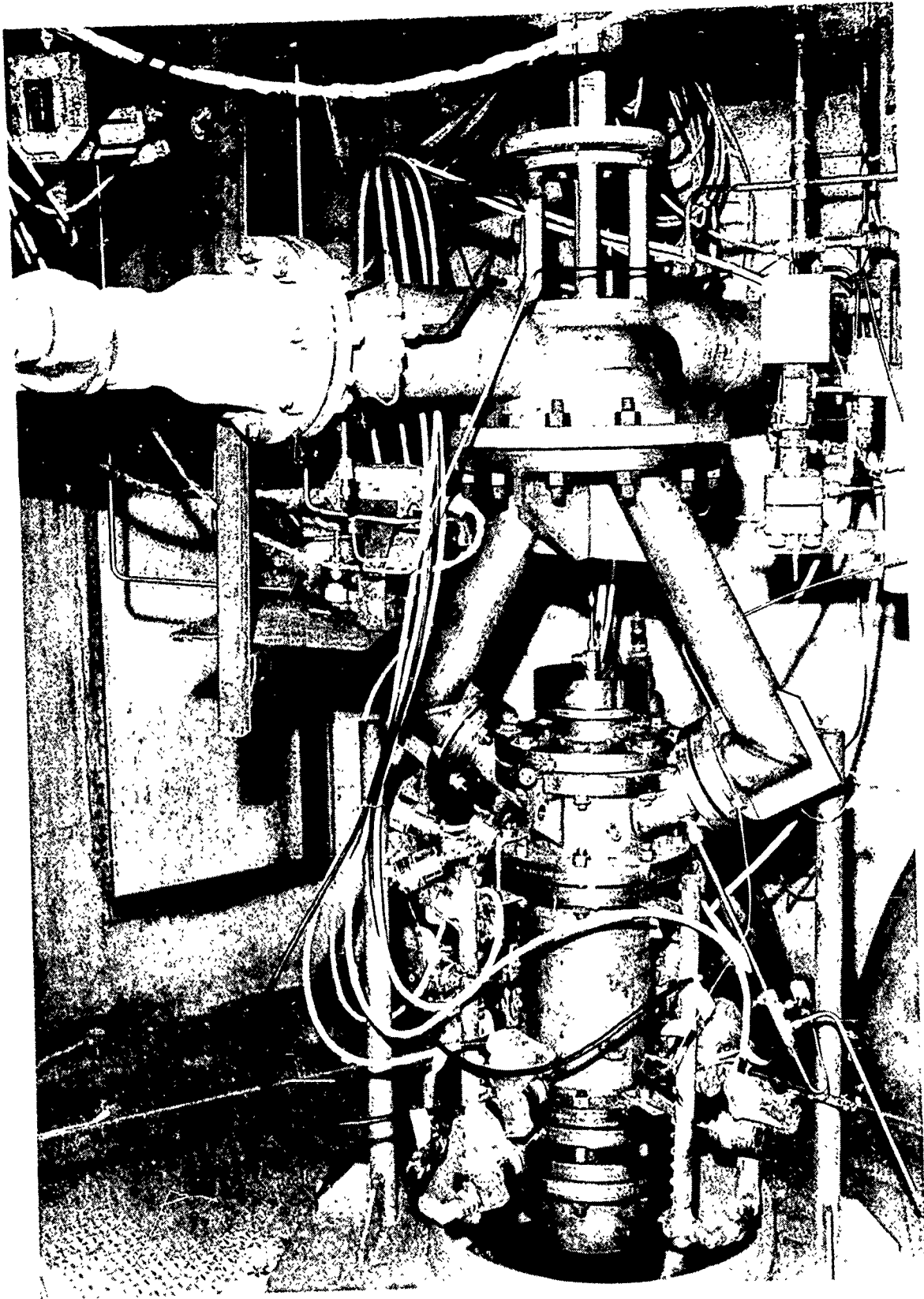


Figure 36
AIR AUGMENTATION HARDWARE INSTALLED

R-25,885
Neg. T6053-2

-83-

CONFIDENTIAL

(This page is Unclassified)

CONFIDENTIAL

C. EXPERIMENTAL TESTING

(C) Following selection of the promising gas generator from Phase I and fabrication of necessary Phase II hardware, air augmentation tests were initiated with the afterburner design shown as Configuration I in Figure 32. With Configuration I, a total of six runs were made using CTF under conditions simulating Mach 2.9 and 500 ft altitude. Of these six runs, five yielded afterburning data. The afterburner did not autoignite during Run 4, precluding the obtaining of data. During each of the first three runs, the CTF injector tip burned off (due to improper propellant sequencing during startup) which resulted in pressure oscillations in the afterburner. Only on Run 3 were the oscillations so great as to preclude use of the data. Modifying the propellant sequencing (increasing the oxidizer lead) on Run 4 and subsequent runs prevented further oxidizer injector tip damage except during Run 13 where the injector tip again burned off later in the run. During Run 6, two separate test points were evaluated to investigate performance variation during the run. Thus a total of five test points covering four test conditions are presented for Configuration I.

(C) Following Run 6, the afterburner configuration was changed to the backup design (Configuration II) and testing was continued. Configuration II demonstrated improved ignition characteristics and higher combustion efficiencies and therefore was used for the remainder of the program. The Phase II test summary is presented as Figure 37 and as is indicated, a total of 14 test points corresponding to 13 distinct test conditions were obtained with Configuration II with CTF. Following the CTF tests, the oxidizer was switched to BPF and data for an additional nine test conditions were obtained. Figure 37 also shows the number of test points obtained at each test condition.

(C) Details of the specific run conditions and resultant combustion efficiency for each test point are presented in Table V for the CTF runs and in Table VI for the BPF runs. As shown, three different combustion efficiencies were computed for each point. The first value listed the efficiency computed on an enthalpy basis. The next efficiency was computed by the temperature rise method using the mix mean temperature of the inlet air and exhaust products from the primary rocket as the starting base. The last method is the temperature rise method using the inlet air temperature as the base. Details of the data reduction procedure are presented in Appendix A. As is evident from Tables V

CONFIDENTIAL

CONFIGURATION	NO. TEST CONDITIONS
I CTF	6 (2 N.G.)
II CTF	13
II BPF	9
	28 (26 USEFUL)

ALTITUDE FEET	MACH NUMBER	NUMBER OF TEST POINTS	
		I (CTF)	II (BPF)
500	2.9	5*	2
8,000	2.9	0	1
40,000	2.8	0	5
MISC.		0	1
		5	14
			9

*INCLUDES ONE ADDITIONAL POINT AT ONE TEST CONDITION

Figure 37
TEST SUMMARY
PHASE II

CONFIDENTIAL

TABLE V
DATA SUMMARY FOR AIR AUGMENTATION RUNS USING CTF

Run No.	Config	Nominal Mach No.	Nominal Alt. (ft)	\dot{W}_a/\dot{W}_p	O/F	\dot{W}_p (pps)	P _{A/B} (psia)	T _{To} (°R)	$\eta_{\Delta H}$	$\eta_{\Delta T_{mix}}$	$\eta_{\Delta T_{air}}$	$F_{exp}/F_{theor.}$
1	I	2.9	500	40.6	0.101	0.489	198.6	1450	-	-	0.712	-
2	I	2.9	500	39.2	0.128	0.498	193.1	1420	-	-	0.785	-
3	I	2.9	500	41.3	0.192	0.490	-200.0	1388	-	-	-	-
4	I	2.9	500	37.9	0.100	0.489	144.0	1415	-	-	-	-
5	I	2.9	500	39.1	0.249	0.485	214.9	1422	0.998	0.999	0.999	0.964
6	I	2.9	500	39.8	0.145	0.492	221.0	1389	0.861	0.876	0.876	0.971
6'	I	2.9	500	39.5	0.146	0.493	213.6	1406	0.852	0.868	0.867	0.967
7	II	2.9	500	40.4	0.145	0.494	222.5	1388	0.986	0.987	0.988	0.969
8	II	2.9	500	37.0	0.100	0.490	212.4	1457	0.922	0.936	0.934	0.985
9A	II	2.9	500	29.2	0.148	0.618	219.3	1415	0.892	0.918	0.918	0.986
9B	II	2.9	8,000	20.6	0.147	0.618	158.4	1390	0.773	0.855	0.856	0.972
9C	II	2.7	5,000	19.7	0.146	0.614	151.6	1231	0.803	0.878	0.872	0.978
10A	II	2.9	500	18.7	0.127	0.847	205.5	1414	0.794	0.888	0.887	0.991
10A'	II	2.9	500	18.1	0.127	0.847	206.1	1420	0.783	0.876	0.875	1.010
10B	II	2.4	-	19.7	0.127	0.846	198.4	1129	0.703	0.782	0.786	1.015
10C	II	2.0	-	18.9	0.127	0.846	195.4	914	0.792	0.868	0.873	1.022
11A	II	2.8	40,000	20.3	0.203	0.187	43.6	1064	0.691	0.793	0.801	-
11B	II	-	-	20.4	0.205	0.187	42.2	644	0.803	0.822	0.832	-
12A	II	2.8	40,000	31.1	0.178	0.135	43.2	1043	0.653	0.691	0.699	-
12B	II	2.6	37,000	29.2	0.174	0.134	43.5	942	0.725	0.741	0.749	-
12C	II	2.4	34,000	31.3	0.174	0.134	44.3	818	0.778	0.788	0.796	-

CONFIDENTIAL

TABLE VI
DATA SUMMARY FOR AIR AUGMENTATION RUNS USING ERF

Run No.	Config.	Nominal Mach No.	Nominal Alt. (ft)	\dot{W}_a/\dot{W}_p	O/F	\dot{W}_p (pps)	P _{A/B} (psia)	T _{T0} (°R)	$\eta \Delta H$	$\eta \Delta T_{mix}$	$\eta \Delta T_{air}$	F _{exp} /F _{theor.}
13A	II	2.8	40,000	22.8	0.158	0.176	46.2	1046	0.730	0.805	0.807	
13B	II	2.8	40,000	22.7	0.174	0.179	46.1	1057			0.794	
13C	II	2.8	40,000	22.5	0.184	0.180	45.5	1057	0.634	0.729	0.733	
13D	II	2.8	40,000	22.0	0.208	0.184	46.8	1056			0.785	
13E	II	2.8	40,000	21.8	0.226	0.186	47.2	1056	0.684	0.771	0.776	
14A	II	2.9	500	42.8	~0.06	0.440	212.7	1529	0.894	0.904	0.906	1.005
14B	II	2.9	500	44.4	~0.005	0.431	204.1	1280	0.829	0.844	0.839	.975
14C	II	2.9	8,000	32.9	~0.002	0.430	163.8	1399	0.797	0.842	0.836	1.010
14D	II	2.4	-	33.0	0.002	0.430	157.2	1108	0.814	0.835	0.832	1.016

CONFIDENTIAL

and VI, the two ΔT methods of computing efficiency give substantially the same result, and these methods compute higher efficiencies than the enthalpy method as the efficiency departs from 100%. This result was not unexpected and is a result of the change in slope of temperature with enthalpy as may be seen from Figure 38.

(U) Also included in Tables V and VI is a ratio of experimental thrust to theoretical thrust. The experimental thrust was that which was measured during the test, and the theoretical was that computed on the basis of the derived combustion efficiencies. The good agreement between the measured and computed value of thrust add further credence to the computed values of combustion efficiency. For the altitude runs where flow in the exhaust nozzle was separated, the measured value of thrust is not valid and therefore no thrust ratios are included in the table. Without detailed nozzle instrumentation, corrections cannot be made for a separated nozzle. All testing was conducted with atmospheric back pressure, so it was expected that the C-D nozzle would separate under simulated altitude conditions.

(U) Significant combustion efficiency data are plotted in curve form and discussed in the next section. For these plots, the ΔT efficiency is used since it is most commonly used within applied combustion work.

(C) In contrast to the Phase I testing, the gas generator deposit problem was very minimal during the air augmentation tests. Deposits were a problem in those runs where the oxidizer injector tip burned off but only during Runs 8 and 9 did any deposit buildup occur and this only became evident at the end of the runs of 12 and 36 seconds respectively.

(U) During Run 14, a malfunction in the oxidizer system (unknown source of restriction) resulted in lower than planned BPF flow, which accounts for the very low O/F ratios. After point 14A, the exit of the primary unchoked and resulted in some pressure oscillations in the remainder of that run.

D. DISCUSSION OF RESULTS

(C) 1. Ignition and Combustion Performance

One of the secondary objectives of the program was to determine the autoignition characteristics of the afterburner. Results from the first six runs made with Configuration I showed that autoignition of the afterburner would occur at lower primary O/F ratios when the oxidizer injector

CONFIDENTIAL

$M_0 = 2.9$, SEA LEVEL, $O/F = 0.127$, $A/P = 18.65$

RUN 10A

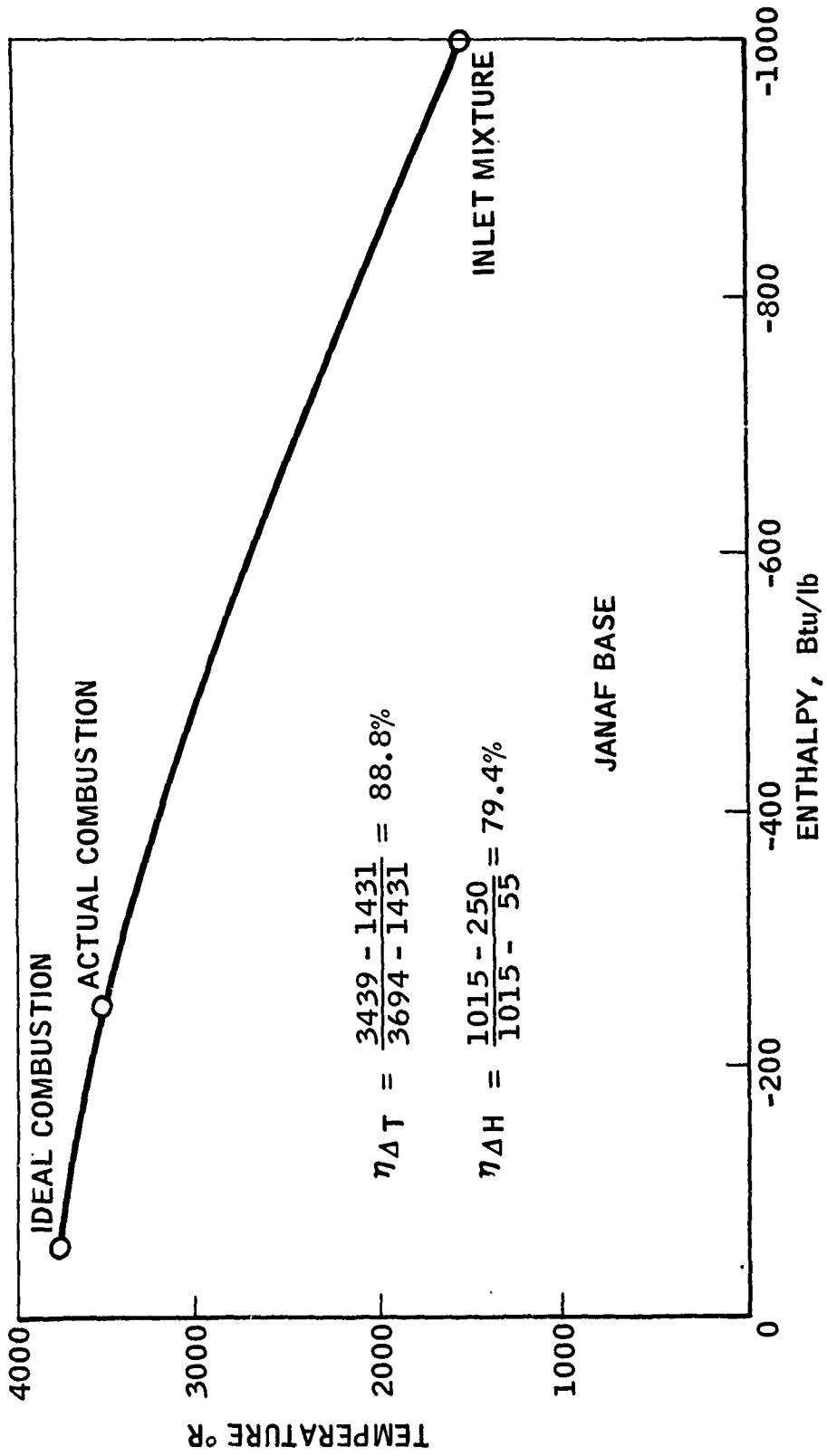


Figure 38

ENTHALPY TEMPERATURE CHARACTERISTICS

A407-26

CONFIDENTIAL

CONFIDENTIAL

tip was burned off than when the gas generator was operating properly. For example, autoignition occurred at an O/F ratio of 0.1 during Run 1 but not at 0.1 during Run 4 nor at 0.145 during Run 6. It is believed that the poor oxidizer/fuel mixing in the gas generator as a result of injector burnout resulted in local regions of high O/F ratios (and high temperatures) which acted as ignition sources in the afterburner. Considering only ignition data obtained with intact hardware, Figure 39 was generated. Spontaneous ignition of the afterburner occurred under most of the conditions tested. In only a few instances at altitude were actual limits established. With Configuration I under sea level conditions, ignition occurred at an O/F ratio of 0.245 but not at an O/F ratio of 0.145. Therefore the limit for that configuration must lie between those two values. With Configuration II under sea level conditions, ignition occurred in an O/F ratio of 0.10 with CTF and at 0.06 with BPF. Ignition may have been possible at lower O/F ratios but no ignition attempts were made. The air-to-propellant ratio for all sea level ignition conditions was 40. Under altitude conditions with Configuration II actual limits were established by gradually increasing the O/F ratio until ignition occurred. At an air-to-propellant ratio of 20, ignition occurred at an O/F ratio of 0.157 with BPF and 0.19 with CTF. At an air-to-propellant ratio of 30, ignition occurred at an O/F ratio of 0.165 with CTF. Although the ignition limits are not precisely established over the range of test conditions, the results indicate that no ignition problems should occur in application.

(C) It was demonstrated during Run 6 that an auxiliary igniter could be used to ignite the afterburner if the primary O/F ratio was too low for spontaneous ignition. During Run 6 and Configuration I, the afterburner did not spontaneously ignite when the primary O/F ratio was 0.145. A slug of fluorine was injected near the forward end of the secondary combustor. This ignited the afterburner and stable burning continued after the fluorine was shut off.

(C) Combustion efficiency data are presented in Figures 40 through 45. Figure 40 shows the performance of the two configurations as a function of O/F ratio for low altitude conditions. At O/F ratios less

CONFIDENTIAL

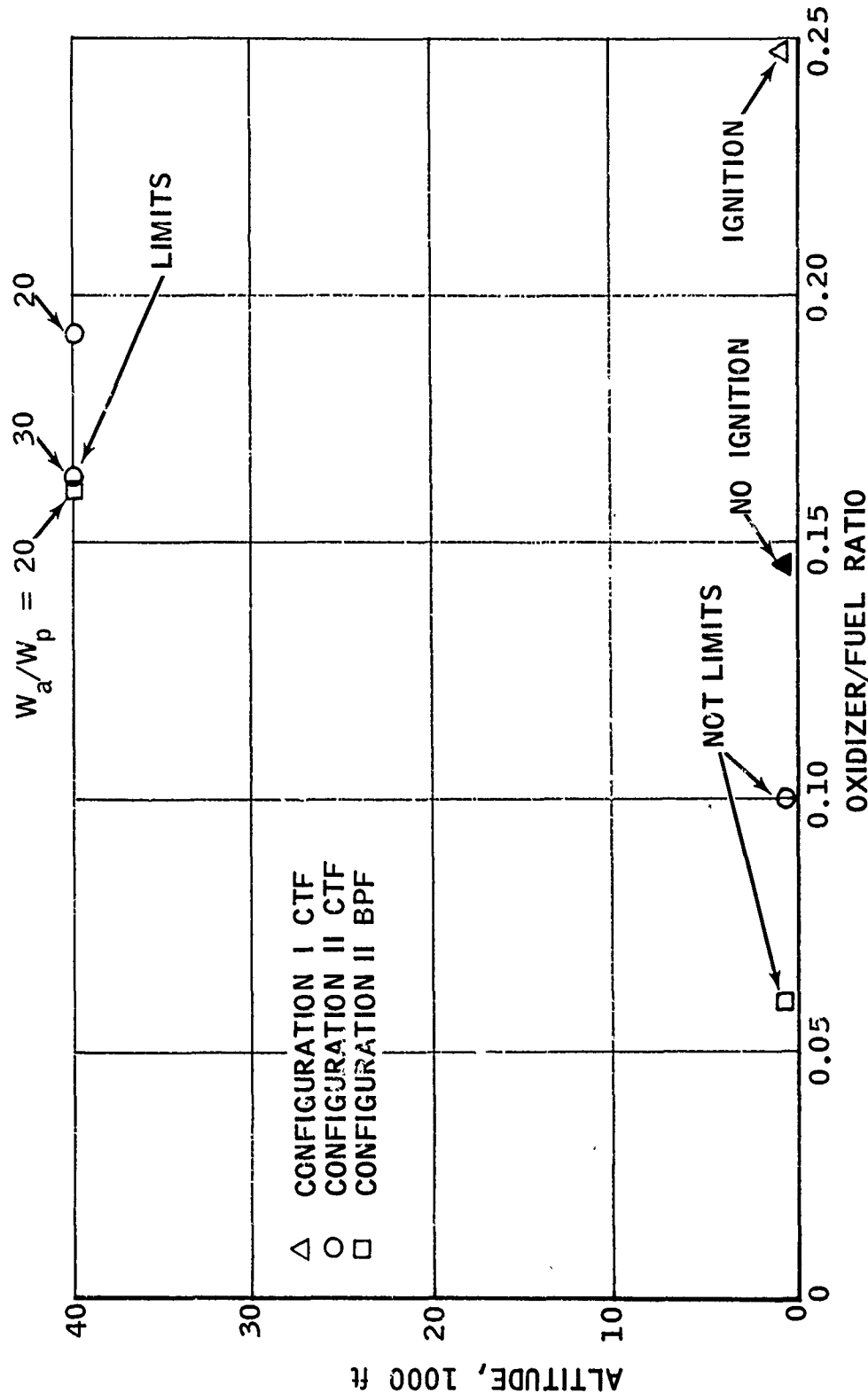


Figure 39
AFTERBURNER AUTOIGNITION RESULTS

R-25,884

CONFIDENTIAL

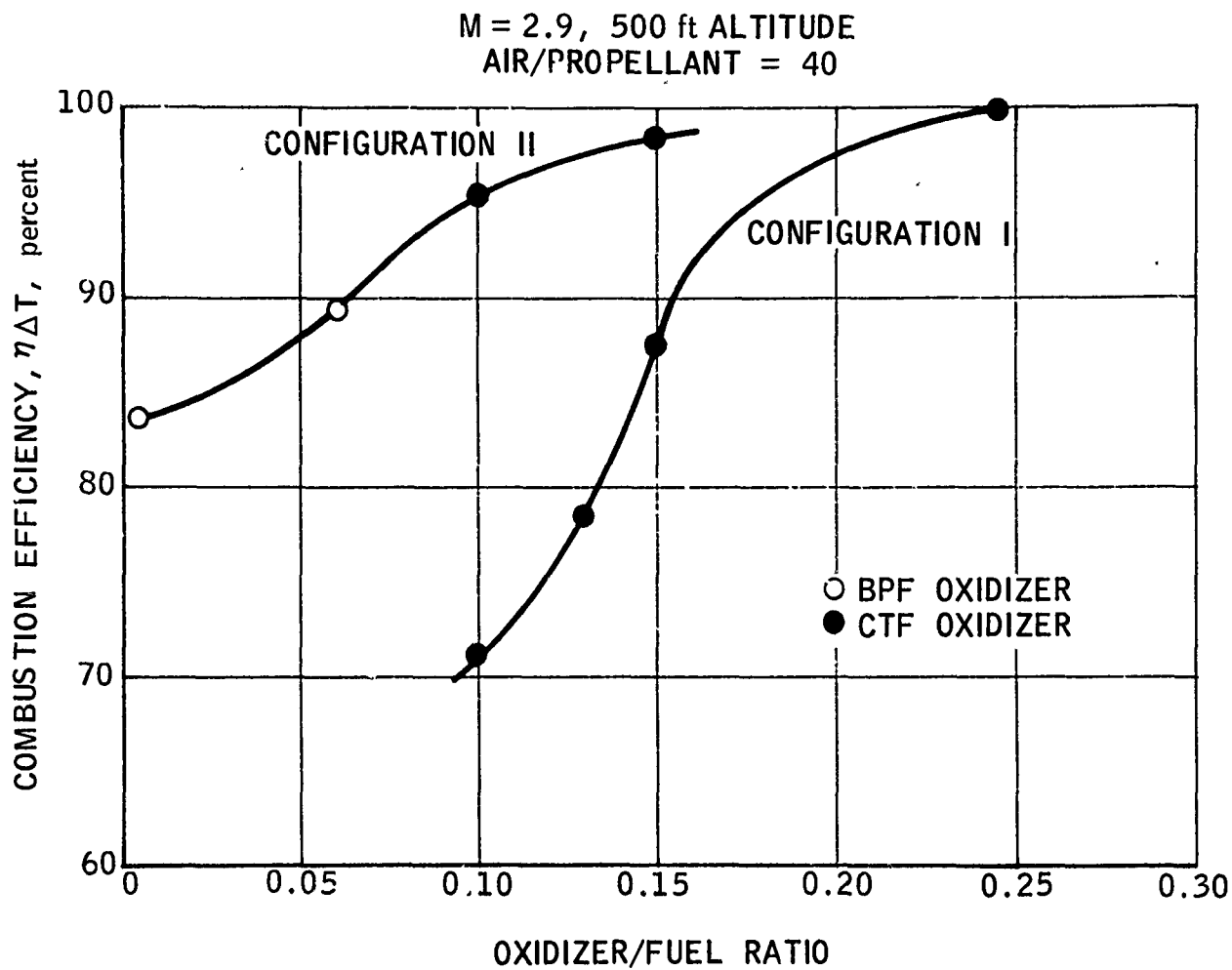


Figure 40
EFFECT OF GAS GENERATOR OXIDIZER/FUEL RATIO UPON AFTERBURNER
COMBUSTION EFFICIENCY

R-25,886

CONFIDENTIAL

CONFIDENTIAL

than 0.2, Configuration II is shown to be capable of providing combustion efficiencies considerably higher than those of Configuration I. The degradation in performance of Configuration I at low O/F ratios is probably attributable to quenching of the oxidation reactions by the very rapid mixing with low temperature air. In contrast, Configuration II provides for a relatively low velocity zone where the initial oxidation reactions can occur to raise the mixture temperature sufficiently to prevent quenching at the region where the mixing becomes vigorous. Spontaneous ignition was always achieved with Configuration II, and, once ignited, the O/F ratio could be reduced to very low values, just sufficient to disperse the slurry, without a radical change in combustion efficiency. This was demonstrated in Run 14.

(C) As is evident from Figure 40, the data for BPF appear to lie on a logical extension of the CTF data, indicating no significant difference between the two oxidizers.

(C) The combustion efficiency as a function of air/propellant ratio at low altitude conditions is presented in Figure 41. At the higher O/F ratios there is a definite tendency for combustion efficiency to increase with air/propellant ratio. This result is in conflict with solid propellant findings from tests in which the geometry of Configuration I was employed. However, it is consistent with some ramjet burner experience. Ramjet burners can be tailored to produce peak efficiency at a given air/propellant ratio within certain limits.

(C) Although the data are limited, the combustion efficiency trend with air/propellant ratio at high altitude conditions appears to be in the opposite direction from the trend at low altitude, as is seen in Figure 42. The reduction in efficiency as air/propellant ratio is increased is somewhat exaggerated by the O/F ratio change noted in the figure (the higher O/F ratio would normally provide the higher efficiency). The bromine pentafluoride data points fall in the same vicinity as the corresponding test points for CTF, but there is moderate data scatter. Whereas one would expect the efficiency to increase with O/F ratio for these points, the opposite trend was observed. This reverse trend and data

CONFIDENTIAL

CONFIDENTIAL

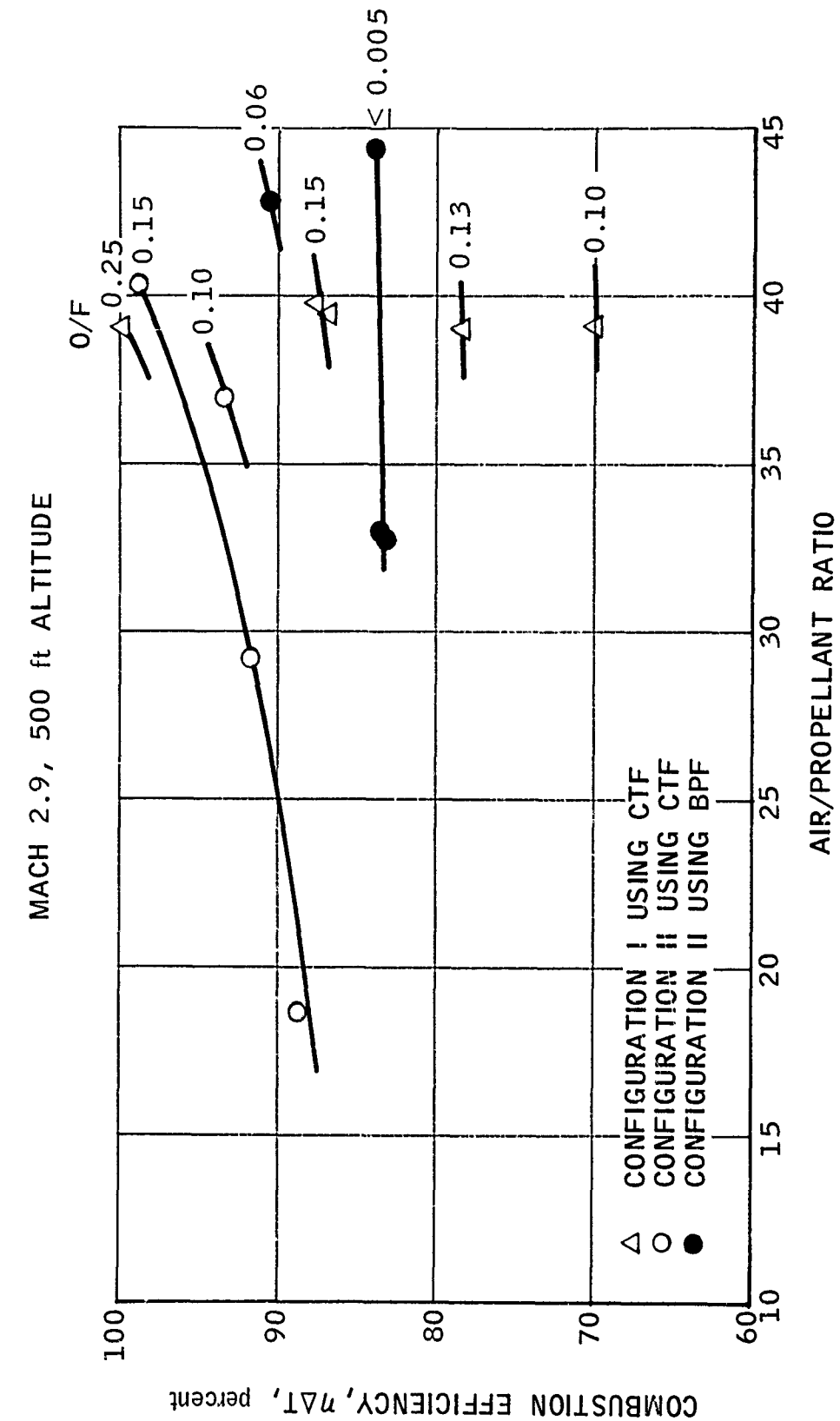


Figure 41
AFTERBURNER COMBUSTION EFFICIENCY

R-25,885

CONFIDENTIAL

R-25,887

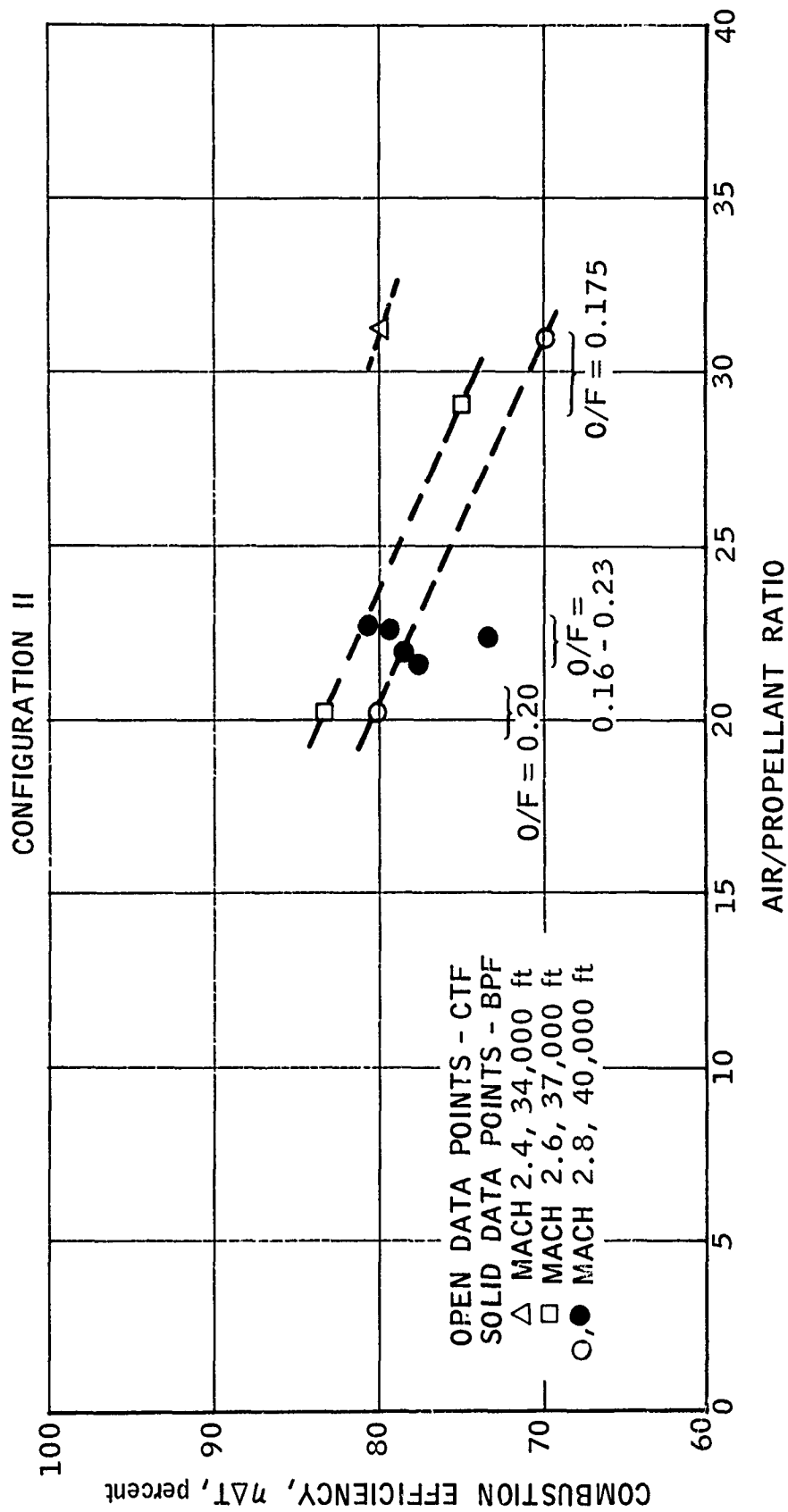


Figure 42
AFTERBURNER COMBUSTION EFFICIENCY
HIGH ALTITUDE CONDITIONS

CONFIDENTIAL

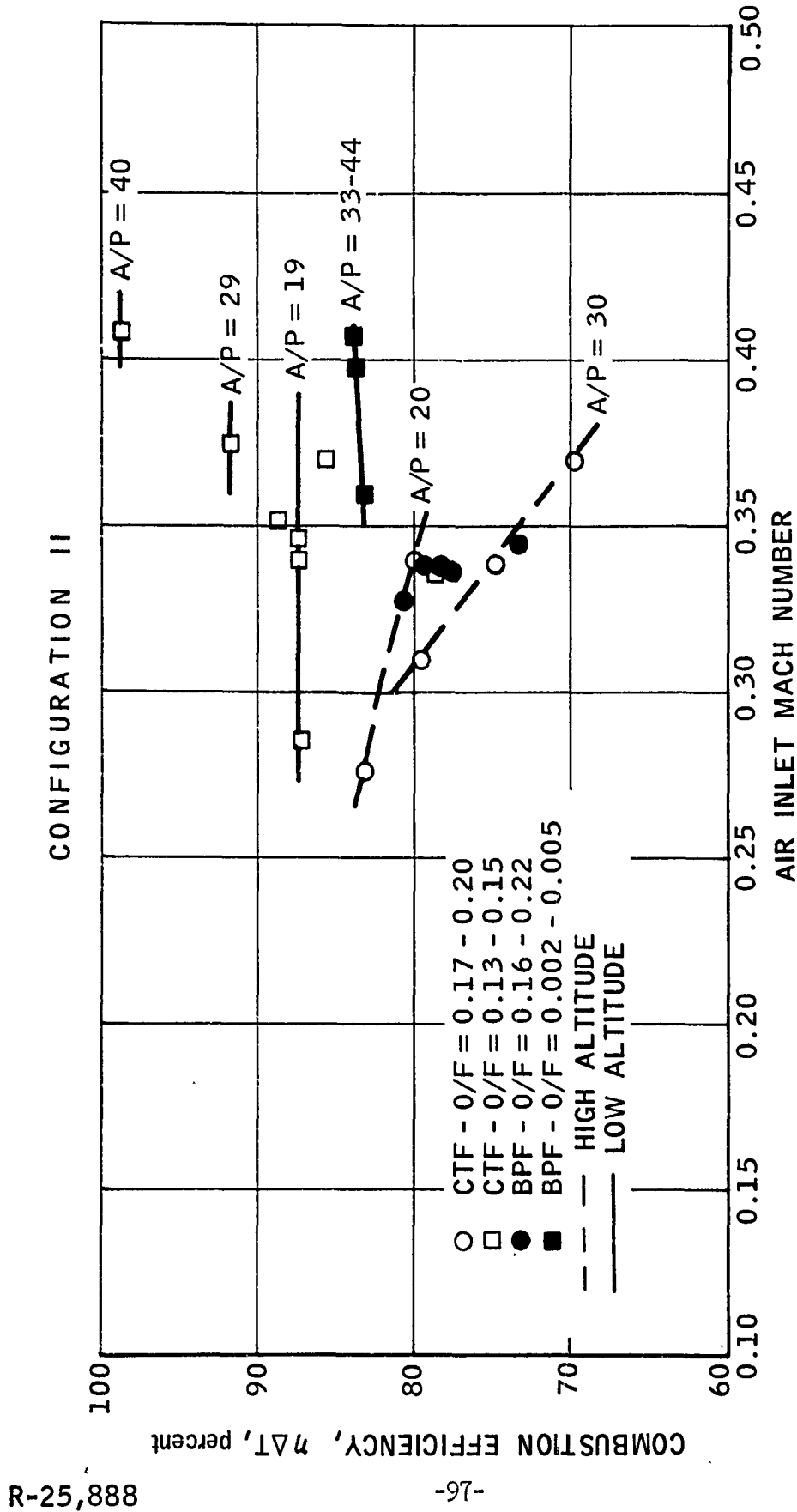
scatter for the BPF data probably are the result of the oxidizer injector damage that occurred during Run 13.

(C) Figure 43 shows the effect of the air inlet dump Mach number on combustion performance. At low altitude conditions, corresponding to afterburner pressures ranging from 150 psia to 225 psia, the combustion efficiency is seen to be independent of dump Mach numbers of air entering the afterburner. However, at altitude conditions, corresponding to the pressure level of 40 psia to 50 psia, the efficiency is seen to decrease as air inlet Mach number is increased. The Mach number sensitivity is greater at the higher air/propellant ratio presented. The BPF data points, corresponding to $A/P = 22$, are approximately in the proper position, with the exception of the one point at $\eta_{\Delta T} = 73.4\%$ corresponding to Run 13C. The CTF data are consistent with the exception of one point (square symbol at $\eta_{\Delta T} = 79\%$ corresponding to Run 10B). The general conclusions to be drawn from Figure 43 are that combustion efficiency is insensitive to the air/exhaust product mixing characteristics at higher afterburner pressures, but becomes quite sensitive at low afterburner pressures.

(C) If inlet air temperature were to have a significant effect on combustion efficiency, the trend would be to increase efficiency with increasing temperature. This trend with temperature is quite pronounced in ramjet burners where cold fuel is injected and the air temperature aids in vaporizing the hydrocarbon carrier. The results presented in Figure 44 do not follow this trend but in some cases show the reverse. Consequently, it is safe to conclude that the observed trends are not a temperature effect but rather the result of changes in some other parameter which significantly affects combustion efficiency. The decrease in efficiency with inlet air temperature for the low pressure data is found to correspond to the decrease in efficiency with inlet air Mach number, as presented in Figure 43. The conclusion that the mixing process strongly affects efficiency at low combustion pressure is therefore reinforced. Any temperature effect, if it exists, must be small compared to other influences upon combustion.

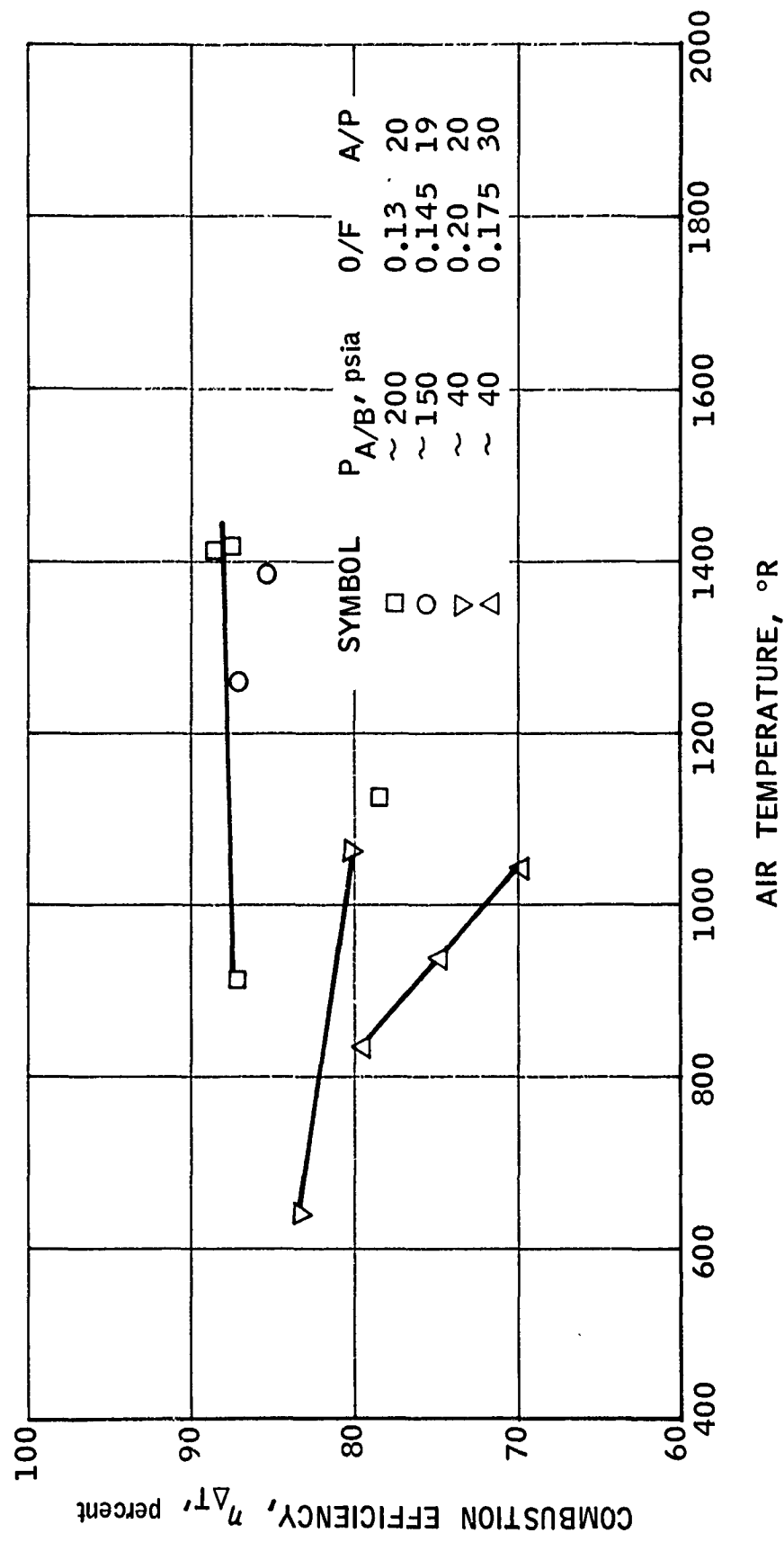
(C) It may be significant that during Runs 11 and 12, where these

CONFIDENTIAL



CONFIDENTIAL

Figure 43
EFFECT OF INLET AIR MACH NUMBER UPON AFTERBURNER COMBUSTION EFFICIENCY



RELATIONSHIP BETWEEN COMBUSTION EFFICIENCY AND INLET AIR TEMPERATURE
FOR CONFIGURATION II

Figure 44

CONFIDENTIAL

data were obtained, the run sequence was from the high temperature condition to the low temperature condition without shutting off the afterburner. It is believed that the run durations were long enough to reach steady state, but the high temperature of the hardware may have contributed to better burning at the lower inlet temperatures. These run durations may be seen from Figure A-1 in Appendix A.

(C) Figure 45 presents the effect of afterburner pressure upon combustion efficiency. Although these data cover a range of inlet air temperatures, it was concluded from Figure 44 that efficiency is probably insensitive to air temperature. Since the other significant parameters, with the exception of O/F ratio, were well controlled. The data plot substantiates the direct effect of afterburner pressure upon combustion efficiency. In this plot O/F ratio decreases from low pressure to high pressure, so in accordance with the trends of Figure 40, any O/F ratio effect which exists would be expected to increase the slope of a curve plotted at a fixed O/F ratio. The effect of pressure upon combustion efficiency is thus established and appears significant. This trend is consistent with the combustion of boron slurry in ramjet engines.

(C) From Table V, it is evident that the fixed geometry gas generator used possessed considerable throttling capability. Between Runs 10 and 12, the total propellant flow rate varied over a range slightly greater than 6:1. Intermediate flow rates were obtained during Runs 7 and 9. This throttling capability was demonstrated at a primary O/F ratio less than 0.2. Although the O/F ratio varied slightly, from about 0.13 to 0.17, it could have been held constant. From Figure 28, it is evident that the primary chamber pressure during Run 12 was on the order of 100-120 psia and during Run 10 was about 800 psia. This approximately 7:1 pressure variation could be used to advantage for control purposes if desired. Demonstration of this throttling capability provides further evidence of the applicability of the Bipropellant Gas Generator Concept for air augmentation applications where both low and high altitude operation are required.

(C) In Figure 46 is plotted the total pressure recovery achieved in dumping the supply air from the inlet ducts into the afterburner as a function of the inlet air Mach number. The total pressure of the supply air (P_{T_1}) was taken to be the average of three total pressure probes spanning one inlet air duct. The afterburner total pressure was derived

CONFIDENTIAL

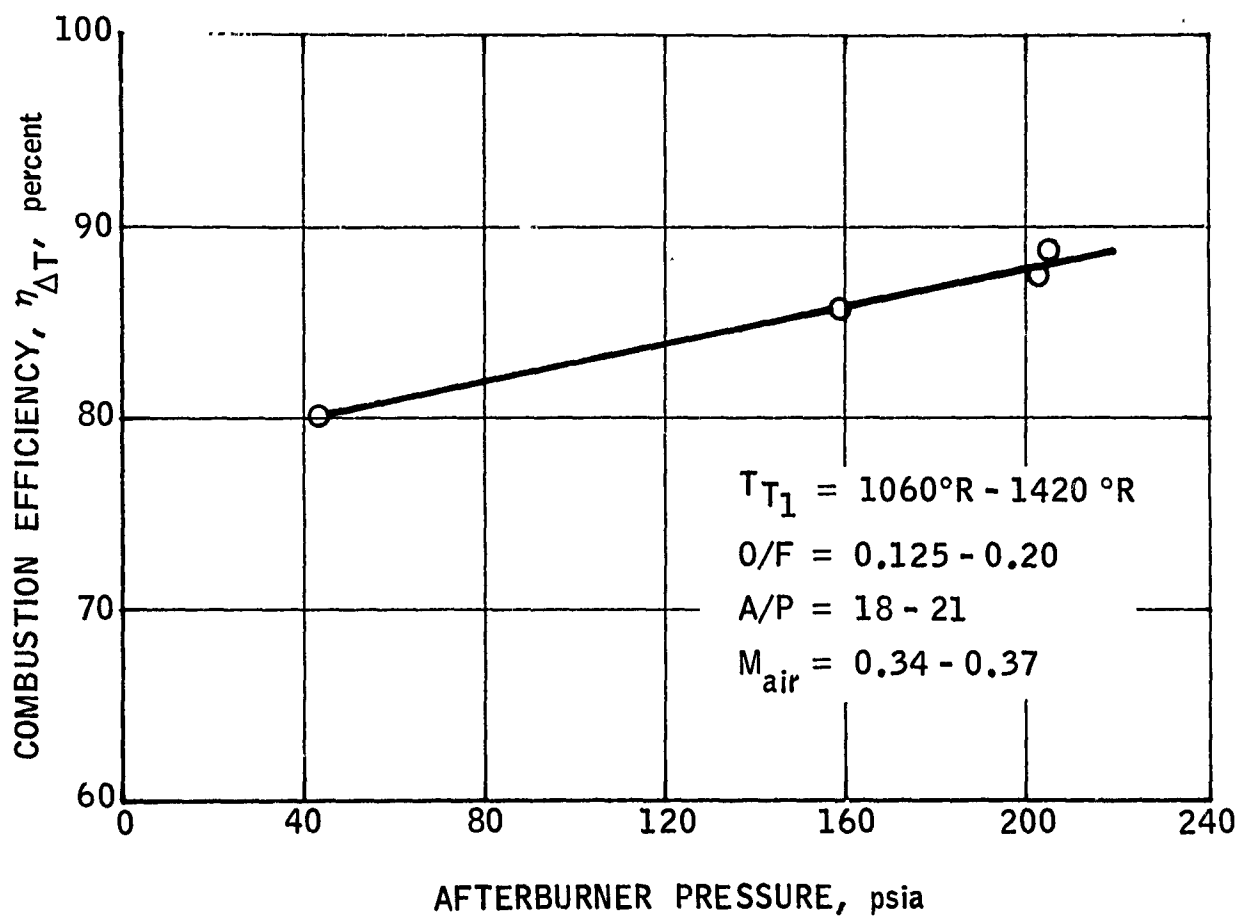


Figure 45
EFFECT OF AFTERBURNER PRESSURE UPON COMBUSTION EFFICIENCY

CONFIDENTIAL

CONFIDENTIAL

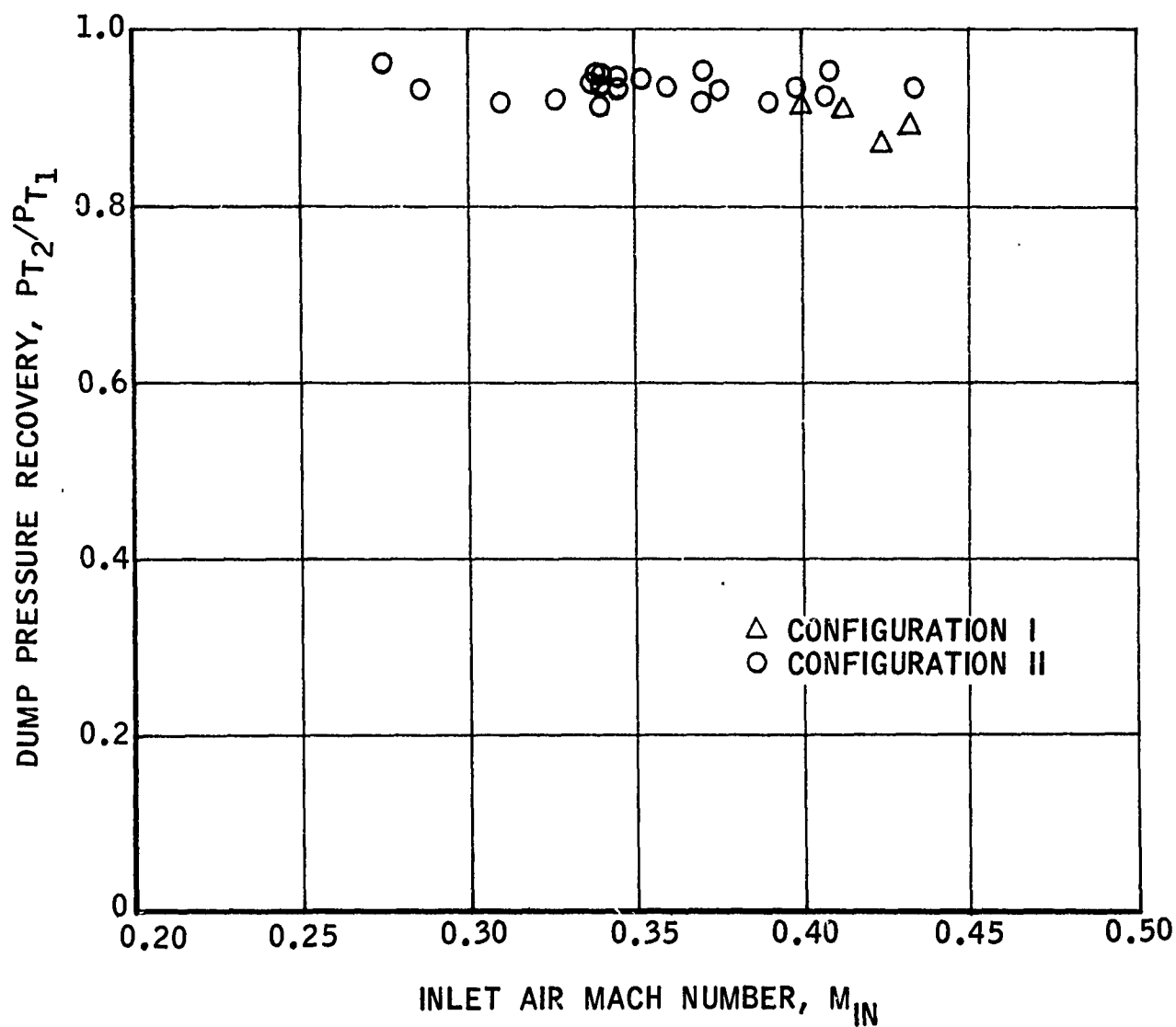


Figure 46
DUMP PRESSURE RECOVERY OF AIR AUGMENTATION COMBUSTOR

CONFIDENTIAL

CONFIDENTIAL

from static pressure measurements in the afterburner. The pressure recoveries achieved with Configuration II exceed 0.90 in all cases. Configuration I appears to exhibit a slightly lower pressure recovery.

2. Hardware Durability

(C) Four gas generator chambers were required for the air augmentation test series. Their utilization is presented in Table VII together with the nozzle throat erosion experienced by each. Figure 47 shows Primary Chamber No. II after the 160 second duration firing (Run 12). Although the graphite had cracked, it was still in good operating condition and was used again for Run 14.

(C) The silver infiltrated tungsten target, against which the sonic efflux of the gas generator impinged, experienced no appreciable deterioration in the 399 seconds of run time accumulated on it. Originally the tungsten target had a flat face, but after Run 3, the leading edge was rounded to prevent deposit buildup on it. After it was rounded, the accumulated run time was 370 seconds. Figure 48 is a postrun photograph showing the leading edge of the target mounted in the gas generator exhaust tube.

(C) The post run condition of the afterburner combustor hardware after nearly 400 seconds of run time is evident from the photographs of Figures 49, 50 and 51. The air inlet section, shown in Figure 49, experienced considerable erosion of the $\frac{1}{2}$ inch thick P-150 ceramic coating just downstream of the inlet ducts. The upstream portion of the air inlet section was in excellent condition. The front end insulator was unaffected around the periphery, but was badly eroded in the region surrounding the gas generator exhaust injection port. Figure 50 shows that the main portion of the combustor survived in excellent condition, except for some erosion adjacent to the air inlet section. Figure 51 shows the nozzle entrance section as it appeared after Run 14. This nozzle was employed throughout the test series. The 0.010-inch thick RM-005 silicon carbide coating on the graphite nozzle was completely satisfactory, withstanding the combustion conditions as well as the mechanical cleaning of deposits from the nozzle throat between runs. The overall durability of the air augmentation hardware was excellent.

CONFIDENTIAL

from static pressure measurements in the afterburner. The pressure recoveries achieved with Configuration II exceed 0.90 in all cases. Configuration I appears to exhibit a slightly lower pressure recovery.

2. Hardware Durability

(C) Four gas generator chambers were required for the air augmentation test series. Their utilization is presented in Table VII together with the nozzle throat erosion experienced by each. Figure 47 shows Primary Chamber No. II after the 160 second duration firing (Run 12). Although the graphite had cracked, it was still in good operating condition and was used again for Run 14.

(C) The silver infiltrated tungsten target, against which the sonic efflux of the gas generator impinged, experienced no appreciable deterioration in the 399 seconds of run time accumulated on it. Originally the tungsten target had a flat face, but after Run 3, the leading edge was rounded to prevent deposit buildup on it. After it was rounded, the accumulated run time was 370 seconds. Figure 48 is a postrun photograph showing the leading edge of the target mounted in the gas generator exhaust tube.

(C) The post run condition of the afterburner combustor hardware after nearly 400 seconds of run time is evident from the photographs of Figures 49, 50 and 51. The air inlet section, shown in Figure 49, experienced considerable erosion of the $\frac{1}{2}$ inch thick P-150 ceramic coating just downstream of the inlet ducts. The upstream portion of the air inlet section was in excellent condition. The front end insulator was unaffected around the periphery, but was badly eroded in the region surrounding the gas generator exhaust injection port. Figure 50 shows that the main portion of the combustor survived in excellent condition, except for some erosion adjacent to the air inlet section. Figure 51 shows the nozzle entrance section as it appeared after Run 14. This nozzle was employed throughout the test series. The 0.010-inch thick RM-005 silicon carbide coating on the graphite nozzle was completely satisfactory, withstanding the combustion conditions as well as the mechanical cleaning of deposits from the nozzle throat between runs. The overall durability of the air augmentation hardware was excellent.

CONFIDENTIAL

TABLE VII

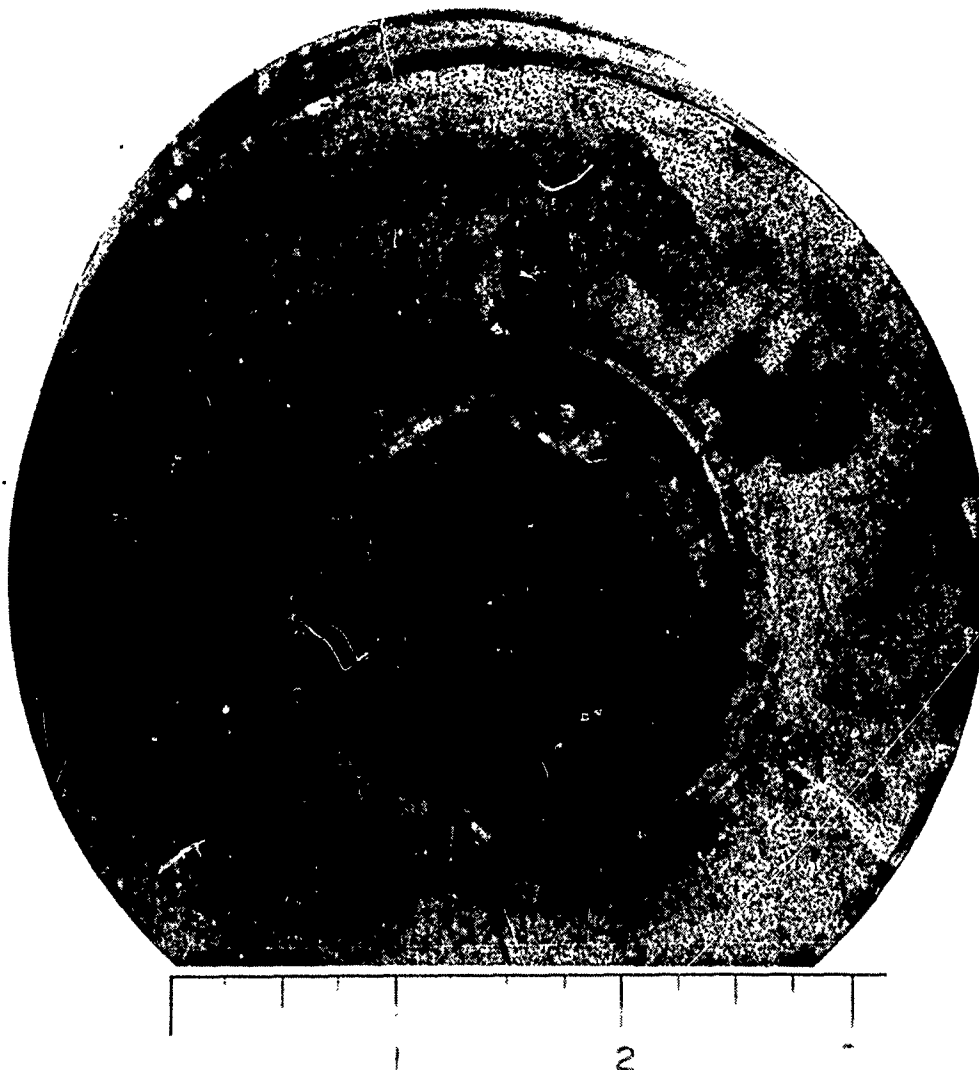
Throat Erosion in Gas Generator Chambers

Primary Chamber	Runs	Run Duration (sec.)	Total Propellant Flow (lb)	Final Throat Area/ Initial Throat Area
I	1 to 3	29	14.4	1.2
II	4 to 9	94	50.7	1.54
III	10 to 12	190	55.4	1.12
	14	36	15.5	1.11
IV	13	50	9.0	1.13
		<u>399</u>		

CONFIDENTIAL

(This page is Unclassified)

CONFIDENTIAL



R-25,904
Neg. T6053-7

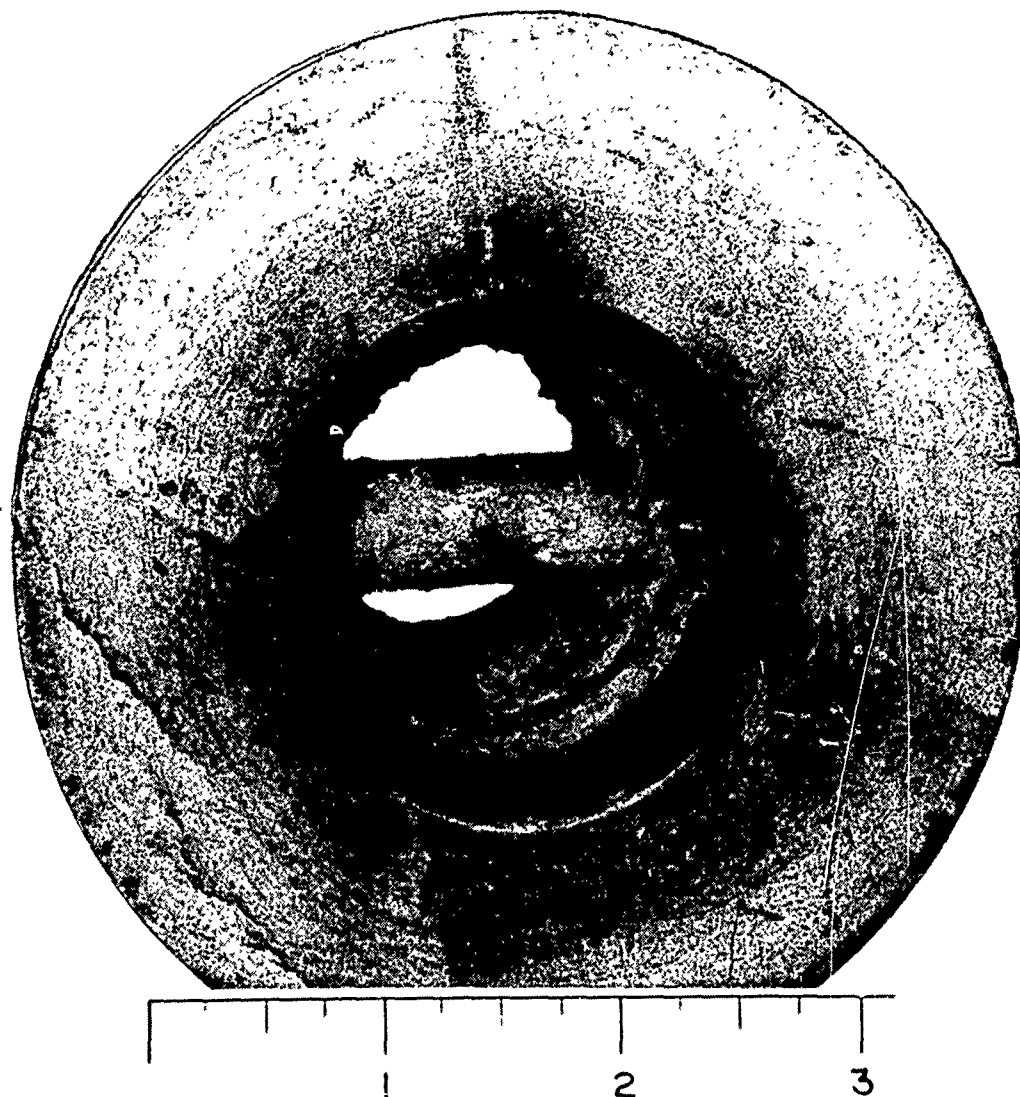
Figure 47
GAS GENERATOR EXIT AFTER LONG DURATION RUN

-104-

CONFIDENTIAL

(This page is Unclassified)

UNCLASSIFIED



R-25,905
Neg. T6053-6

Figure 48
GAS GENERATOR HARDWARE - EXHAUST TUBE AND TARGET

-105-
UNCLASSIFIED

UNCLASSIFIED

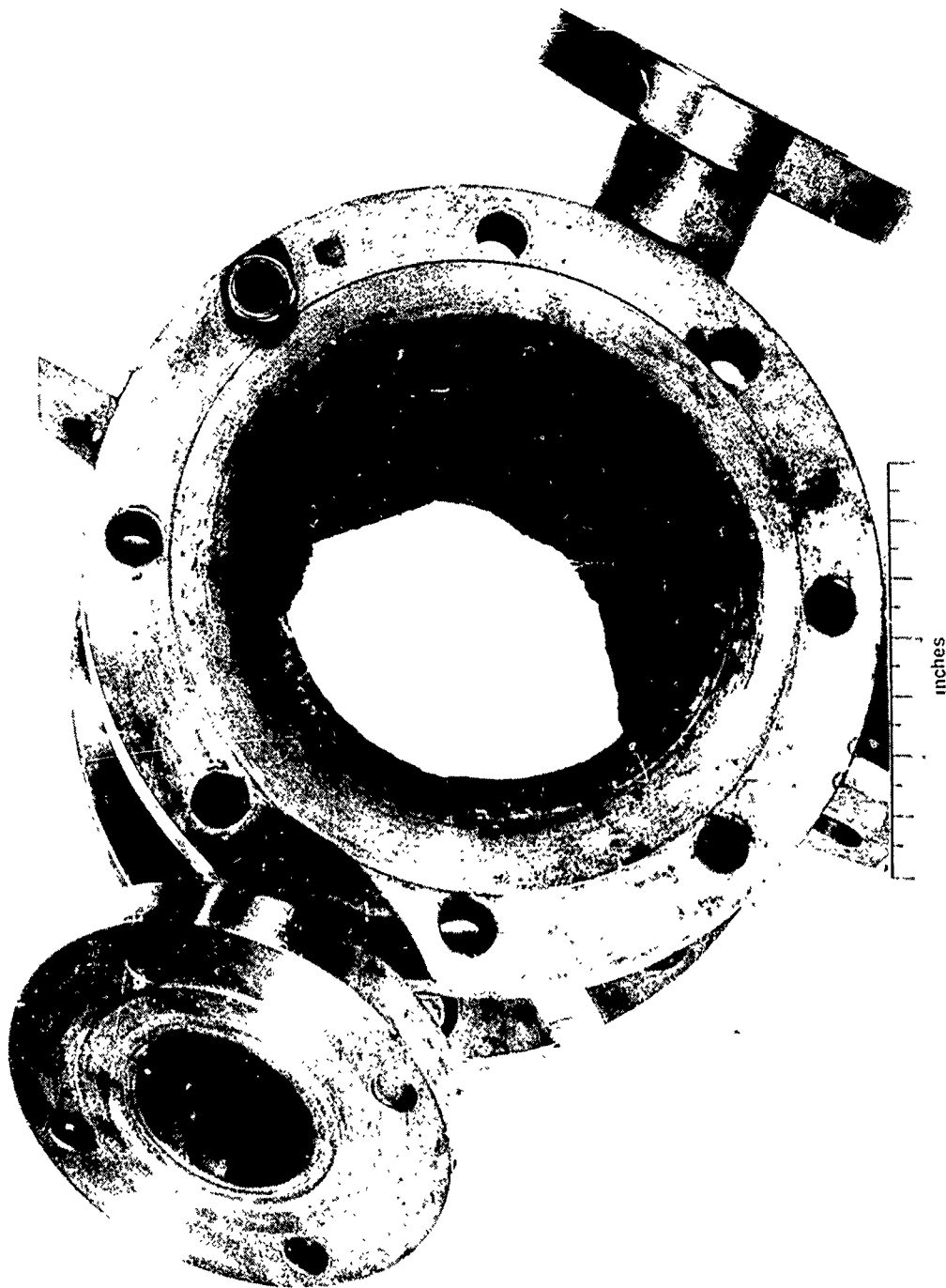


Figure 49

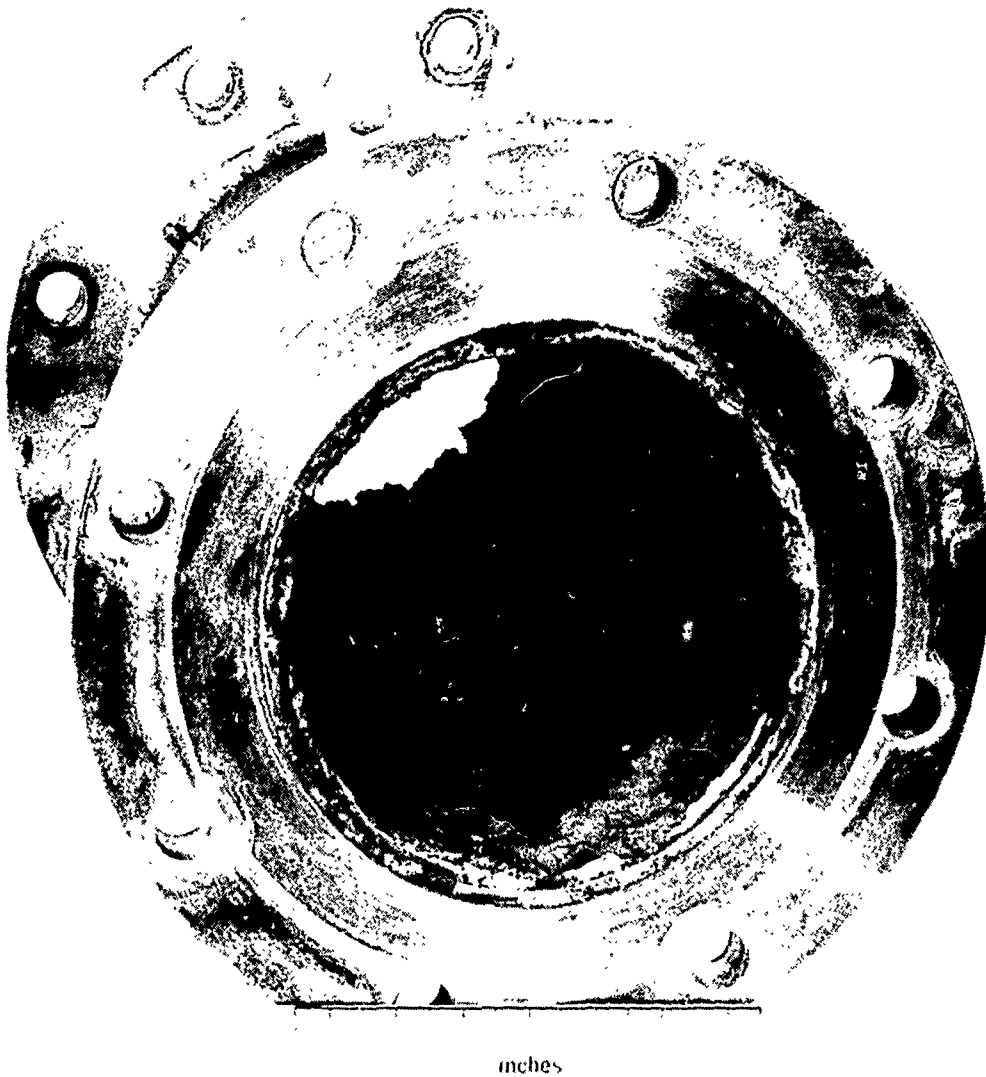
AIR AUGMENTATION TEST HARDWARE - AIR INLET SECTION

R-25,886
Neg. T6053-3

-106-

UNCLASSIFIED

UNCLASSIFIED



R-25,888
Neg. T6053-4

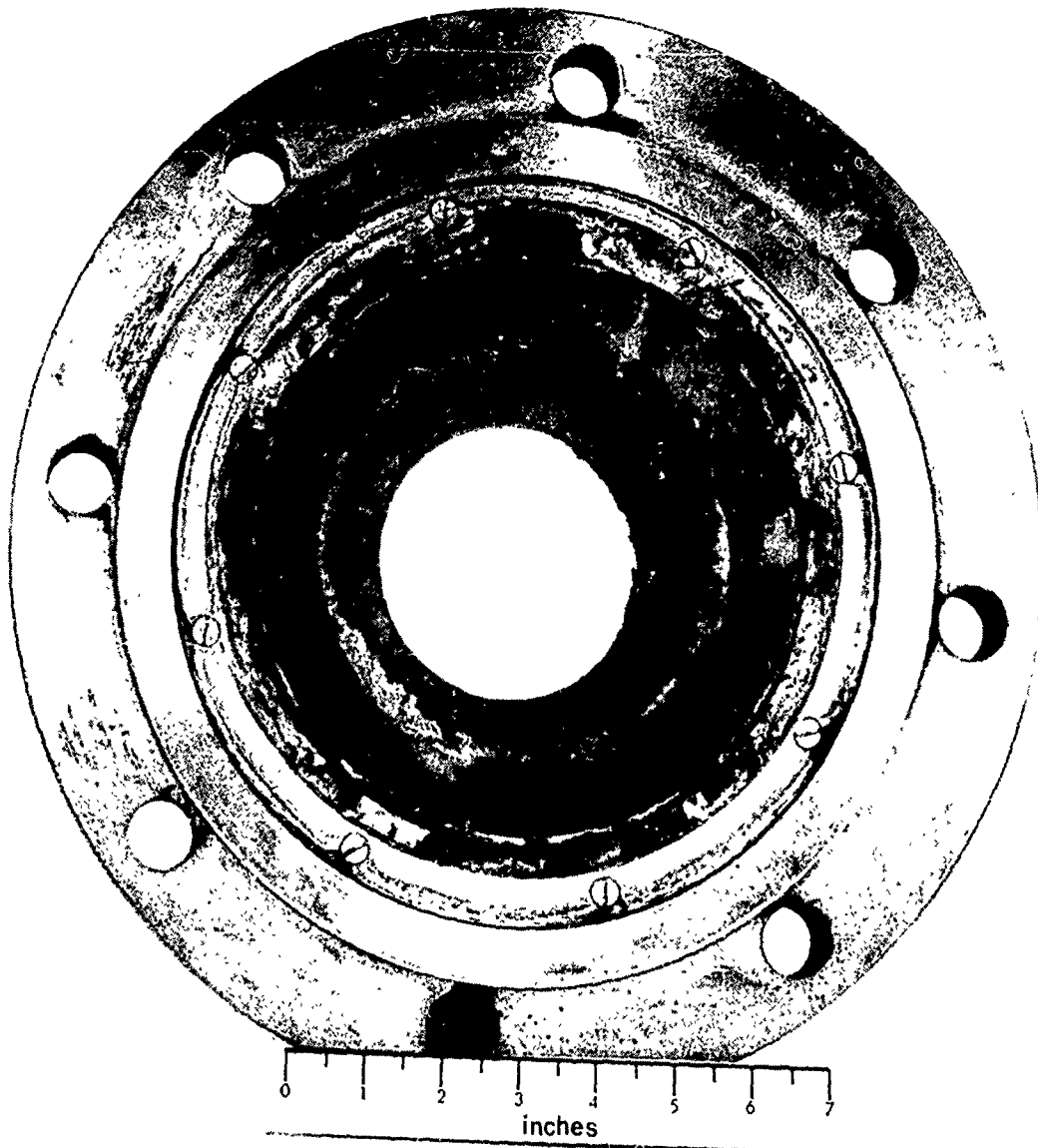
Figure 50

AIR AUGMENTATION TEST HARDWARE - COMBUSTOR

-107-

UNCLASSIFIED

UNCLASSIFIED



R-25,887
Neg. T6053-5

Figure 51

AIR AUGMENTATION TEST HARDWARE - THROAT SECTION

-108-

UNCLASSIFIED

CONFIDENTIAL

VI

CONCLUSIONS

A. GAS GENERATOR

(C) As a result of both Phase I and Phase II testing, the following conclusions can be drawn:

(1) The internal geometry of a primary gas generator for air augmentation applications is critical, when using boron slurry fuels and interhalogen oxidizers, and significantly affects deposit buildup and erosion characteristics. Complicated flow passages, corners and sudden changes in flow area should be avoided. A simple straight-through passage is best when used in conjunction with the proper propellant injector design.

(2) Deposit buildup within the gas generator must be a major consideration and becomes worse with increasing O/F ratio (in the range from 0.1 to 0.5) and/or increasing chamber pressure.

(3) Analyses of deposits in the gas generator show that the deposit is a mixture of B_4C , subcarbides of boron, sintered boron and unburned boron.

(4) Propellant injector design also is critical for the proper operation of a gas generator and designs that produce large areas of contact between the fuel and oxidizer work better and produce more uniform conditions within the gas generator than impinging streams which depend upon particle kinetics for mixing.

(5) Erosion of graphite parts in the primary gas generator can be a problem but a thin coating of silicon carbide can effectively minimize or eliminate this problem.

(6) MARNAF 731 was hypergolic with either CTF or BPF under all conditions, even at O/F ratios as low as 0.06.

CONFIDENTIAL

(7) The propellant starting sequence was fairly critical in the final gas generator design. Any delay between fuel injection and oxidizer injection would result in damage to the oxidizer injector tip.

(8) A slight oxidizer lead in the starting sequence, allows the gas generator to operate effectively over a wide O/F ratio range. Under the subject program, the O/F ratio tested with the final design ranged from 0.002 to 0.25. (On a TMC in-house program, the same design was operated at O/F ratios up to 1.0.)

(9) If multiple gas generators are used, provisions must be made in the propellant feed system to prevent feedback between gas generators.

(10) Use of a target is an effective method of reducing the sonic exhaust stream from the primary to subsonic velocities. Impingement on the target may also help break up large particles and disperse the gas generator exhaust products.

(11) Silver impregnated tungsten is an excellent target material and readily withstands gas generator exhaust temperature and erosive properties.

(12) Gas generator test results indicate that at low O/F ratios the combustion process in the primary more closely follows a nonequilibrium kinetics model and indicates significant evaporation of the hydrocarbon carrier in the boron slurry fuel.

(13) Gas sampling data indicated that significant amounts of hydrogen and methane were formed in the primary and that these species along with the vaporized trimethylhexane should readily burn in the secondary combustor and raise the local temperature sufficiently high to ignite the boron particles.

(14) Experimental results indicate that a throttling capability of at least 6:1 can readily be achieved with a fixed geometry bipropellant gas generator.

B. AIR AUGMENTATION

(C) As a result of the Phase II tests, the following conclusions can be drawn:

CONFIDENTIAL

(1) A piloting and recirculation zone in the forward end of the secondary combustor promotes ignition and permits very high afterburner combustion efficiencies at low primary O/F ratios.

(2) Based upon oscillograph traces, it appears that ignition in Configuration I takes place near the aft end of the combustor, and a finite time was required for the chamber pressure to rise after the primary exhaust products were introduced into the chamber. Ignition occurs in the recirculation zone of Configuration II and the pressure rises immediately upon propellant introduction.

(3) Chlorine trifluoride and bromine pentafluoride produce essentially the same general combustion characteristics, and limited data indicate that BPF promotes autoignition in the afterburner at slightly lower O/F ratios.

(4) Afterburner autoignition could readily be achieved with Configuration II and CTF at O/F ratios as low as 0.10 at low altitudes and above 0.18 at 40,000 feet altitude. Slightly less BPF was required for the same conditions.

(5) With both afterburner geometries, combustion could be maintained at lower O/F ratios than were required for autoignition. With Configuration II and BPF, 83% η_c was achieved at low altitude with an O/F ratio as low as 0.002.

(6) Under low altitude conditions, combustion efficiencies above 90% were demonstrated at O/F ratios as low as 0.07 at an air-to-propellant ratio of 40 with Configuration II and efficiencies above 85% were demonstrated at O/F ratios above 0.15 with Configuration I.

(7) With both configurations, afterburner combustion efficiency increased with increasing O/F ratios.

CONFIDENTIAL

(8) As anticipated, combustion efficiency decreased with increasing altitude. At 40,000 feet simulated altitude, a combustion efficiency of 80% was achieved at an O/F ratio of 0.20 and an air-to-propellant ratio of 20.

(9) Although not fully understood, combustion efficiency increased with increasing air-to-propellant ratio at low altitudes but decreased with increasing air-to-propellant ratio at altitude.

(10) Inlet air temperature appeared to have less effect upon combustion efficiency than did air inlet Mach number or chamber pressure.

(11) Combustor dump pressure recovery above 90% can be achieved.

(12) Excellent hardware durability was demonstrated with the air augmentation hardware. Some erosion of the aluminum oxide insulator occurred in localized areas, but this did not delay testing or require repairing.

(13) The advantages of MARNAF 731 and CTF (or BPF) have been demonstrated for air augmentation applications. The potential mission flexibility offered by this propellant combination should make it a leading contender for ducted rocket applications.

(14) Based upon the work accomplished under this program, design criteria for the bipropellant gas generator - air augmented combustor has been established and sufficient data exist to permit realistic application studies of this concept for Air Force missile applications.

UNCLASSIFIED

VII

RECOMMENDATIONS

(U) As a result of the performance demonstrated on this program and because of the potential of this bipropellant liquid system, it is recommended that additional work be conducted to:

- (1) Explore and determine combustion performance at higher altitudes for various O/F ratios.
- (2) Better establish and document ignition limits both at sea level and altitude conditions.
- (3) Develop full scale flight weight hardware.
- (4) Conduct full scale air augmentation tests to further the technology of the system.

(U) Because of the performance and flexibility offered by this system, it is recommended that the bipropellant system for ducted rockets be considered for future Air Force missile applications.

THIS REPORT HAS BEEN DELIMITED
AND CLEARED FOR PUBLIC RELEASE
UNDER DOD DIRECTIVE 5200.20 AND
NO RESTRICTIONS ARE IMPOSED UPON
ITS USE AND DISCLOSURE.

DISTRIBUTION STATEMENT A

APPROVED FOR PUBLIC RELEASE,
DISTRIBUTION UNLIMITED.

UNCLASSIFIED

VIII

REFERENCES

1. Phillips, D. G., "Demand Mode Integral Rocket-Ramjet"(U), TMC Report 25,217, dated 30 March 1967 - CONFIDENTIAL
2. Samsonov, G. V., "Boron-Carbon" in Chap. VI of "Boron, It's Compounds and Alloys", G. V. Samsonov, Ed., Academy of Sciences, Ukranian SSR, Kiev 1960 - Unclassified
3. Glaser, F. W., Moskowitz, D., and Post, B. J., Appl. Phys. 24, 731-3, 1953 - Unclassified
4. Sanderson, R. T., "Vacuum Manipulation of Volatile Compounds", John Wiley & Sons, Inc., New York, 1948, page 147 - Unclassified
5. AFRPL-TR-66-236, MHD Research, Inc., September 1966, page 79 - Unclassified
6. Phillips, D. G. "Demand Mode Integral Rocket-Ramjet" (U), TMC Report 25,256, dated 26 April 1968. CONFIDENTIAL

UNCLASSIFIED

APPENDIX A

DATA REDUCTION TECHNIQUE

(U) Afterburning runs ranged in length from 7 seconds to 160 seconds. During a number of runs several test conditions were achieved by changing air flow, air temperature or oxidizer flow. In order to avoid any arbitrariness in selection of those portions of the run which were to be utilized in performance evaluation, wherever possible, steady data at the end of each test condition were selected. The selected data reduction regions, as a function of run time, are shown in Figure 52 for all runs that yielded good data.

(U) The selected intervals ranged from 0.8 to 1.3 seconds in width except for Runs 1 and 2 which were 0.64. The intervals correspond in general to steady conditions of afterburner pressure, inlet air temperature, O/F ratio, propellant flow rate, air flow rate and thrust. In instances where one or more of the aforementioned quantities were varying, the interval was selected as close to the end of the run condition as feasible. Such applies to Runs 8, 13B and 13E. In Run 8 pressure was varying at the end of the run; in Run 13B O/F ratio was increasing; and in Run 13E there was an unexplainable drop in thrust near the end.

(U) The vacant intervals between test conditions within a given run correspond to the transition period. The total run durations may exceed the maximum time indicated in Figure 11. Run 12, for example, was continued for an additional 126 seconds.

(U) The pressure, temperature and flow rate data, as provided by the digital printout at approximately four data points per second, were averaged over the selected interval to provide the input for computer evaluation of performance. The reference afterburner throat area for a given set of input data corresponded to that represented by a linear growth of nozzle throat deposits with time, as determined by throat measurements before and after the runs.

(U) Following selection of the desired data, performance calculations were made on the IBM 360/40 computer. An effective temperature is defined as that which will pass the measured weight flow per unit area through the nozzle throat with isentropic expansion from the measured chamber pressure to the throat. At a temperature less than ideal, the density will be greater than ideal, and the throat mass velocity will be greater than ideal. The Marquardt rocket performance

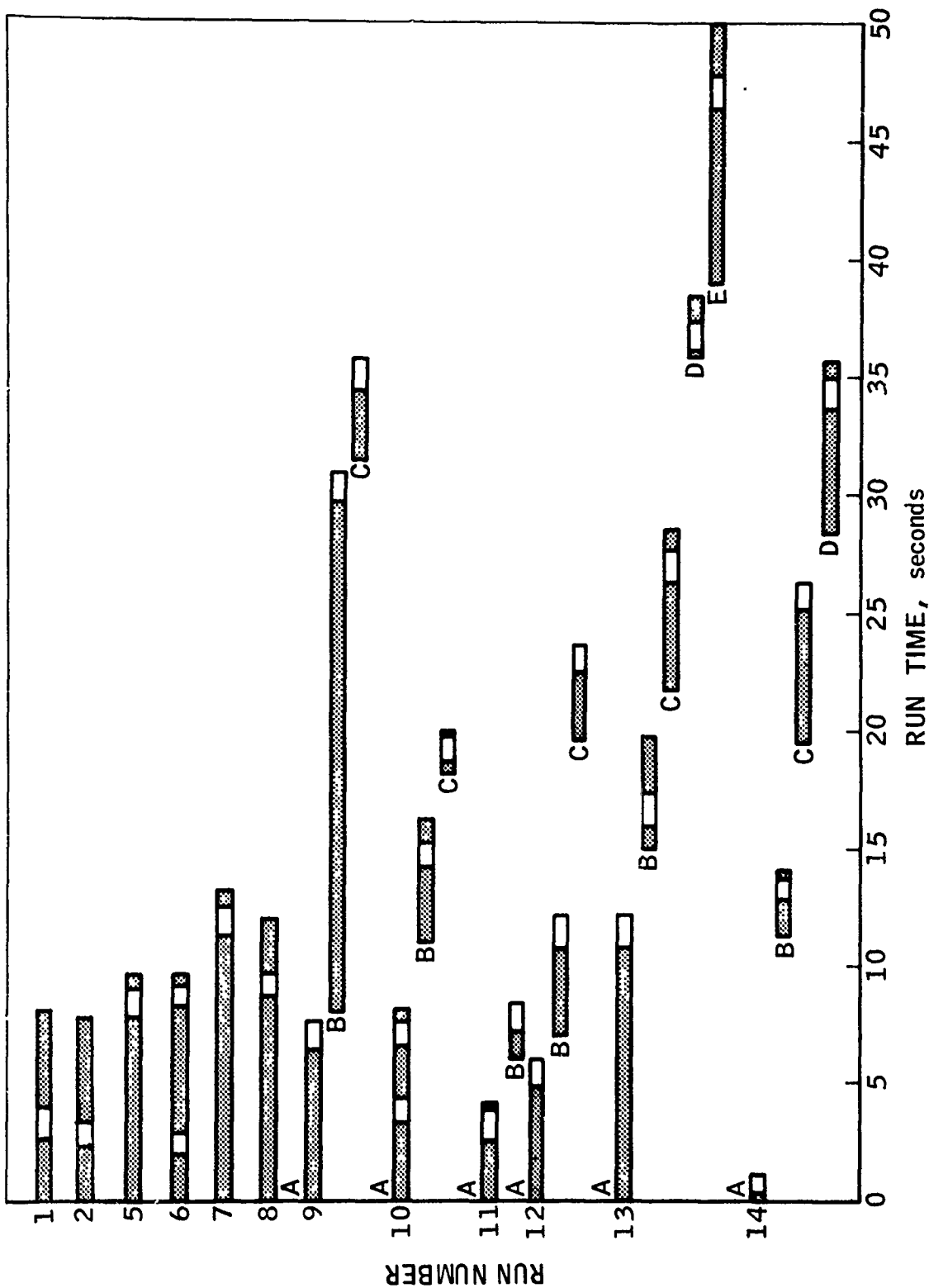


Figure 52

DATA SAMPLING INTERVALS IN AIR AUGMENTATION RUNS

UNCLASSIFIED

program has an input option to reduce the assigned chamber temperature below the ideal value until the computed throat mass velocity equals the measured quantity. The corresponding enthalpy (at chemical equilibrium) is taken as the effective enthalpy in the chamber. Since all component weight flows and also the chamber pressure are measured quantities, the "rocket performance" program applies in this context for ramjet combustor performance.

(U) The most significant measure of combustion efficiency is the enthalpy difference ratio, because one is basically interested in interpreting what effective loss of heat corresponds to the effective suppression of combustor temperature below the ideal value. To compute this combustion efficiency, an ideal enthalpy of fully reacted material is required, as well as the enthalpy of unreacted material. This calls for computation of an equivalent mixing temperature of "unreacted" material. In the afterburning sense, "unreacted" material means gas generator products unreacted with the air stream into which they are being mixed. The enthalpy difference ratio is then the difference between the effective enthalpy (at the effective chamber temperature) and the enthalpy of equilibrium products at the mixing temperature divided by the difference between the ideal enthalpy and the same enthalpy of equilibrium products at the mixing temperature (see Equation 1 below).

(U) The equivalent mixing temperature is computed on a semi-equilibrium basis. Those chemical species are precluded which represent interaction between streams, while those are allowed which represent dissociative equilibrium within a stream. The situation is made more complex by vitiation preheating of the air flow, or by the presence of oxide impurity in the fuel. However, the difficulties can be surmounted by the use of close approximations.

UNCLASSIFIED

(U) The first step was the computation of preheater performance. This was assumed to be ideal on the basis of 95% of the measured hydrogen fuel flow. Since the outlet temperature was below the dissociation regime, performance was computed on the basis of stoichiometric conversion of H_2 to H_2O , and the preheater outlet temperature was determined from an enthalpy balance. The preheater efflux was next taken as pure air at this temperature, for the mixing temperature calculation. The gas generator fuel was taken as without oxide impurity (with due regard for the influence of this assumption on the equivalent heat of formation) for the mixing temperature calculation. Thus, there were no necessary oxidation species in the mixing temperature calculation, only B/C/H/Cl/F or B/C/H/Br/F species and pure air species. Based on the enthalpies of the preheater equivalent air, the gas generator fuel (without oxide impurity), and the oxidizer, an enthalpy balance with semi-equilibrium yielded the equivalent mixing temperature. (For the test data reduced, this generally fell within about $100^\circ R$ of the measured preheater outlet temperature.)

(U) After the equivalent mixing temperature was thus established, the enthalpy of fully reacted products was computed from a complete equilibrium calculation at this temperature. For this, the various flows were exactly described chemically, i.e., with oxide impurity in the slurry fuel accounted for, and with vitiation in the preheater accounted for.

(U) Also required was the ideal enthalpy of the weighted flows as exactly described chemically. This was computed as the sum of the products of the weight fraction times the assigned enthalpy of the component. For the slurry fuel ingredients and the oxidizer, these assigned enthalpies were simple tabular values; for air and hydrogen they were functions of temperature.

UNCLASSIFIED

UNCLASSIFIED

(U) The enthalpy difference ratio was calculated as:

$$\eta_{\Delta H} = \frac{H_{\text{effective}} - H_{\text{prod, Tmix}}}{H_{\text{ideal}} - H_{\text{prod, Tmix}}} \quad (1)$$

(U) At the ideal enthalpy an ideal equilibrium temperature was calculated, providing the basis for calculation of the temperature difference ratio:

$$\eta_{\Delta T} = \frac{T_{\text{effective}} - T_{\text{mix}}}{T_{\text{ideal}} - T_{\text{mix}}} \quad (2)$$

(U) An air temperature rise ratio was also calculated:

$$\frac{\Delta T_{\text{eff}}}{\Delta T_i} = \frac{T_{\text{effective}} - T_{\text{mix}}}{T_{\text{ideal}} - T_{\text{mix}}} \quad (3)$$

(U) For a small perturbation of operating conditions, corresponding to a small perturbation of effective chamber temperature, the thermodynamic properties of the fluid between chamber and exhaust nozzle throat can be considered nearly constant. Thus, with a solution which matches chamber and throat, one can extract an effective Mach number/specific heat ratio function as an operator between chamber temperature and flow parameters. Then this function can be employed to estimate the change in effective chamber temperature associated with a given net change in the combination of flow parameters. By solving for equilibrium enthalpy at this displaced temperature, the effect upon $\eta_{\Delta H}$ of an assigned net error in the flow parameters can be established. This is a simple first approximation, since the matching of chamber temperature to throat conditions is not iterated for a second time. For a net error of -2% in C^* , equivalent to -4% at T , trial values of $\eta_{\Delta H}$ were computed. Grossly speaking, a net error of +2% in C^* resulted in an error of about +8% in $\eta_{\Delta H}$ at high $\eta_{\Delta H}$ and +5% at low $\eta_{\Delta H}$. The accuracy of the experimental data was judged to be approximately +2% at a level of confidence of three standard deviations.

UNCLASSIFIED

(U) On the attached flow diagram, Figure 53, output values A, B, and C are required for Equation (1), D, E, and F for Equation (2), and D, E, and G for Equation (3); G is used for T_{air} .

UNCLASSIFIED

UNCLASSIFIED

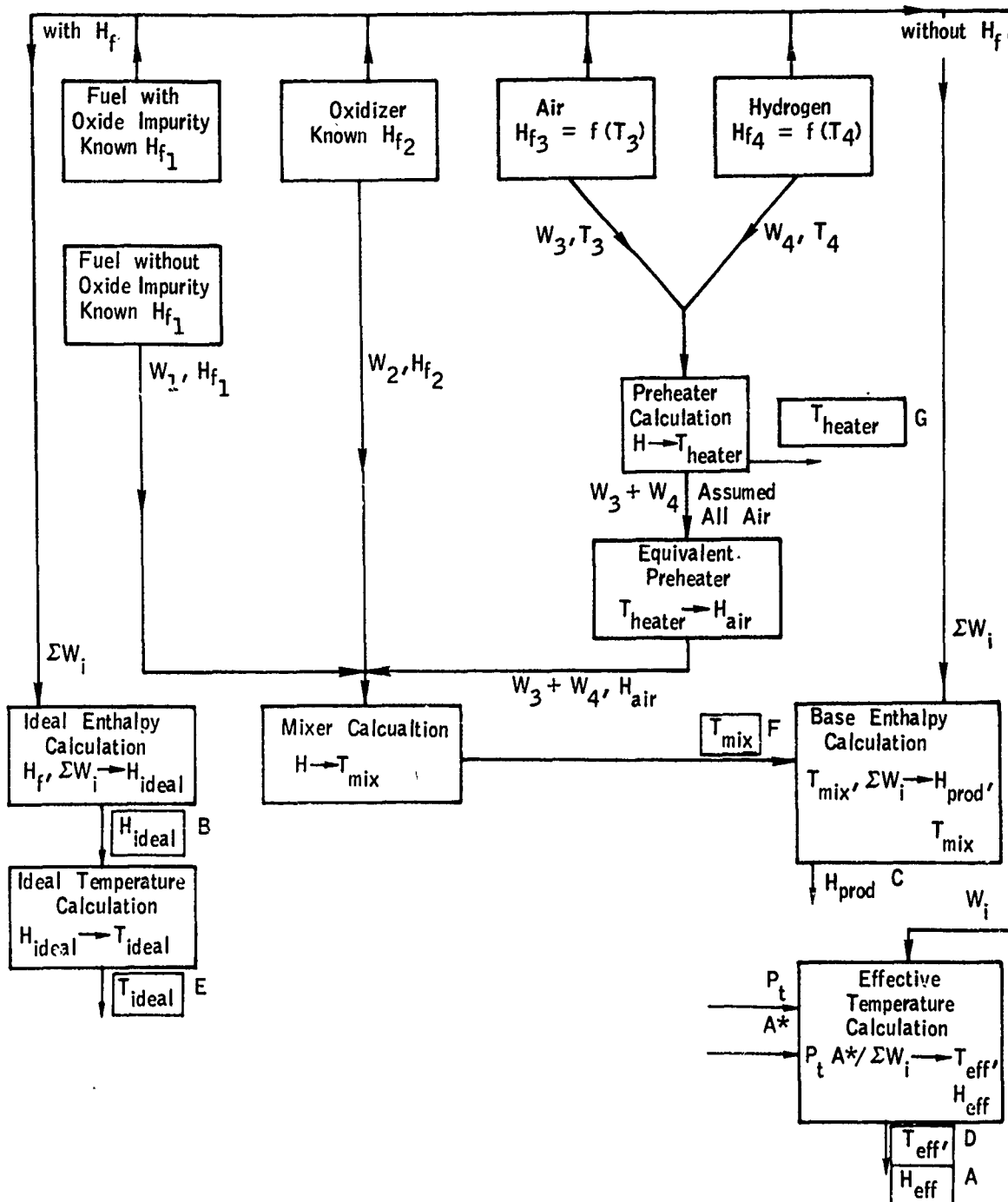


Figure 53
COMPUTATION FLOW DIAGRAM

UNCLASSIFIED

CONFIDENTIAL

APPENDIX B

DESCRIPTION AND PROPERTIES OF MARNAF 731

I. Fuel Description

(C) MARNAF 731 is a high concentration boron slurry fuel that is well suited for volume-limited, airbreathing propulsion system applications. The fuel is manufactured by The Marquardt Corporation*. The composition of MARNAF 731 is as follows:

<u>Component</u>	<u>Percentage (by weight)</u>
90-92% purity amorphous boron	73.0
2,2,5 trimethylhexane	22.75
Gellant	3.65
Processing inerts**	0.6

The boron used in the production of MARNAF 731 is the 90-92% pure commercial grade amorphous boron supplied by American Potash and Chemical Company (Trona). The carrier fluid, 2,2,5 trimethylhexane (TMH), is 95% pure, technical grade. The TMH used is purchased from Phillips Petroleum Company. The gellant used serves both as a wetting and a gelling agent. It is classified as an ash-less organic gellant.

(C) The heating value is computed herein for a 73% boron (2,2,5 trimethylhexane) slurry fuel in which the commercial boron is assumed to contain 91% of elemental boron. The following table gives both the basis and the results of the computation:

* MARNAF 731 is no longer in production. It has been replaced by MARNAF 732 which is a very similar product that has improved low temperature flow properties.

** Extrinsically introduced during blending.

CONFIDENTIAL

Gravimetric Heating Value		Heat of	Heating	Heat
		Formation	Value	Contribution
Slurry Fuel Component	Concentration	Btu/lb	Btu/lb	Btu/lb
(1) 90-92% amorphous boron (taken as 91% elemental boron and 9% crystalline B_2O_3 , or B_6O_3).	73.00%	-707	22981	16776
(2) 2,2,5 trimethylhexane	22.65	-1000	18991	4301
(3) Gelling agent	3.65		15750	575
(4) Processing inerts	0.60		- 0 -	- 0 -
		TOTAL	21652* Btu/lb	

*Neglects contribution due to magnesium impurity.

(C) The density of the 73% boron (TMH) slurry fuel is taken as 92.08 lbs/cu ft at 25°C. Hence the volumetric heating value equals

$$21,652 \text{ Btu/lb} \times 92.08 \text{ lbs/cu ft} = 1.994 \times 10^6 \text{ Btu/cu ft}$$

(C) The above volumetric heating value is considered to be minimal, for it neglects any contribution from magnesium (total magnesium being present as 4 to 5% of the 90-92% amorphous boron). A large portion of this total magnesium may be present as magnesium borides or as elemental magnesium in the commercial boron product; and therefore, the magnesium can be expected to make a minor contribution to the heating value.

(C) In the instance of the above boron (TMH) slurry fuel, an undoubtedly maximal heating value should result from the assumption that 4% of elemental magnesium is present in the boron (i.e., the assumption that the 90-92% amorphous boron contains 91% elemental boron plus 4% elemental magnesium, plus 5% crystalline B_2O_3). On this basis, the assigned heating value of the commercial boron becomes 23,409 Btu/lb; and accordingly, the volumetric heating value of the boron (TMH) slurry fuel becomes 2.023×10^6 Btu/cu ft for purposes of evaluation of engine performance.

CONFIDENTIAL

CONFIDENTIAL

(C) On the basis of the above high and low estimates, a "best estimate" volumetric heating value for the fuel is suggested as 2.01×10^6 Btu/cu ft for purposes of evaluation of engine performance.

II. Fuel Properties

(C) For convenience, important properties of MARNAF 731 are tabulated below:

Heating value (Best Estimates)

Gravimetric - 21,800 Btu/lb

Volumetric - 2.01×10^6 Btu/ft³

Density - 1.475 g/cm³

Viscosity (see Figure 54)

Vapor pressure* - The vapor pressure is essentially identical to that of the carrier 2,2,5 trimethylhexane. Intrapped air may cause the pressure in a sealed container to rise a few psi above the normal vapor pressure of the carrier but there is no danger of pressure buildup due to gas evolution.

Stability* - MARNAF 731 has been subjected to prolonged storage, temperature cycling and vibration tests and the results indicate a very stable product.

Safety* - MARNAF fuels will not detonate and toxicity is equivalent to TMH.

*Reference 6 contains results of qualification tests on MARNAF fuels.

CONFIDENTIAL

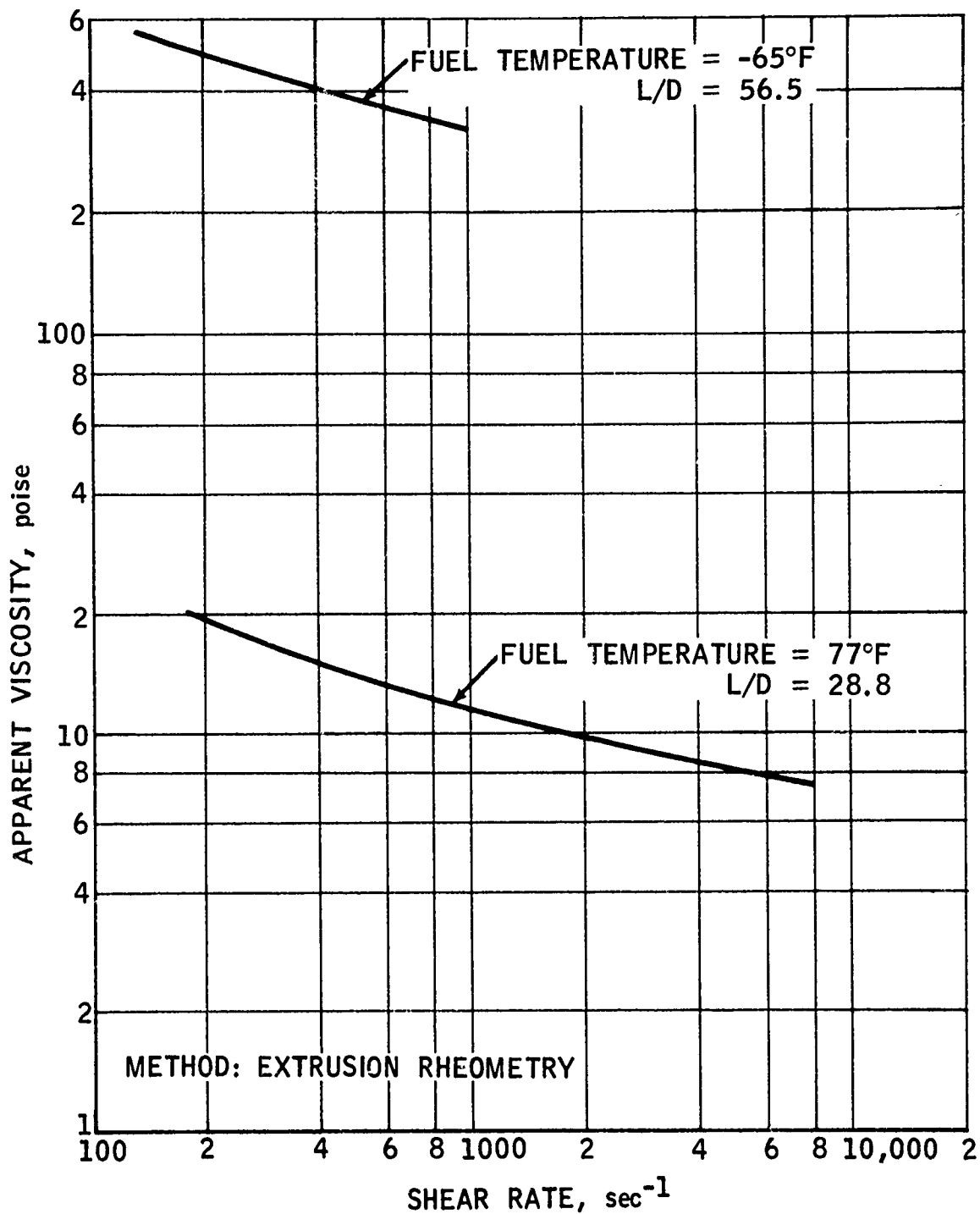


Figure 54
VISCOSITY-TEMPERATURE CHARACTERISTICS OF MARNAP 731

R-25,438A

-128-

CONFIDENTIAL

(This page is Unclassified)

UNCLASSIFIED

III. Handling Characteristics

(U) Because MARNAF 731 is a high concentration slurry fuel, any significant carrier evaporation will affect flow properties. Reasonable care must be exercised to prevent carrier evaporation during loading and transfer operations, especially on a very hot day. Exposure to air for more than a few seconds will cause a skin to form which could result in plugging of small injector orifices.

(U) During storage, precautions must be taken to ensure that the storage container is sealed to prevent evaporation of carrier.

PRECEDING PAGE BLANK NOT FILLED

UNCLASSIFIED

Security Classification

DOCUMENT CONTROL DATA - R & D

(Security classification of title, body of abstract and indexing annotation must be entered when the overall report is classified)

1. ORIGINATING ACTIVITY (Corporate author) The Marquardt Corporation 16555 Saticoy St. Van Nuys, California		2a. REPORT SECURITY CLASSIFICATION Confidential	
		2b. GROUP IV	
3. REPORT TITLE Demonstration of Bipropellant Gas Generator Technology for Air Augmentation Applications			
4. DESCRIPTIVE NOTES (Type of report and inclusive dates) Rough Draft of Final Report - 15 June 1967 to 1 July 1968			
5. AUTHOR(S) (First name, middle initial, last name) Donald G. Phillips William F. Hassel			
6. REPORT DATE August 1968		7a. TOTAL NO. OF PAGES 130	7b. NO. OF REFS 5
8a. CONTRACT OR GRANT NO. FO4611-67-c-0110		9a. ORIGINATOR'S REPORT NUMBER(S) The Marquardt Corporation Report No. 25,265	
b. PROJECT NO. c. 5730 d.		9b. OTHER REPORT NO(S) (Any other numbers that may be assigned this report)	
10. DISTRIBUTION STATEMENT In addition to security requirements which must be met, this document is subject to special export controls and each transmittal to foreign governments or foreign nationals may be made only with prior approval of the AFRPL (RPPR-STINFO) Edwards, Calif.			
11. SUPPLEMENTARY NOTES None		12. SPONSORING MILITARY ACTIVITY Department of the Air Force Air Force Rocket Propulsion Laboratory Edwards Air Force Base, California 93523	
13. ABSTRACT (U) During the period from 15 June 1967 to 1 July 1968, The Marquardt Corporation conducted an experimental program to demonstrate the feasibility of a bipropellant gas generator for air augmentation applications. Efforts concerned both development of the gas generator and its evaluation during air augmentation tests. The propellants used were MARNAF 731, a boron slurry manufactured by The Marquardt Corporation, and chlorine trifluoride. Testing with bromine pentafluoride also was conducted. The final gas generator design permitted operation over the desired O/F range, demonstrated throttling capability and permitted the attainment of high afterburner combustion efficiencies with small scale hardware. This report describes the development of a gas generator, presents an evaluation of a number of variables affecting secondary combustor performance and presents results that demonstrate that the bipropellant gas generator concept, when using MARNAF 731 and CTF (or BFF), is a very promising system for future ducted rocket applications.			

DD FORM 1 NOV 65 1473

UNCLASSIFIED

Security Classification

UNCLASSIFIED

Security Classification

14. KEY WORDS	LINK A		LINK B		LINK C	
	ROLE	WT	ROLE	WT	ROLE	WT
Air Augmentation Bipropellant Gas Generator Ducted Rocket Boron Slurry Afterburner						

UNCLASSIFIED

Security Classification